THE IMPACTS OF ANTHROPOGENIC GLOBAL CHANGE AND LOCAL HUMAN ACTIVITIES ON REEF-BUILDING CORALS ON THE BELIZE MESOAMERICAN BARRIER REEF SYSTEM

Justin H. Baumann

A dissertation submitted to the faculty at the University of North Carolina at Chapel Hill in partial fulfillment of the requirements for the degree of Doctorate of Philosophy in the Marine Sciences Department in the School of Natural Sciences and Mathematics.

Chapel Hill
2018

Approved by:

Karl D. Castillo

Justin B. Ries

John M. Bane

John F. Bruno

Christopher S Martens

ABSTRACT

Justin H. Baumann: THE IMPACTS OF ANTHROPOGENIC GLOBAL CHANGE AND LOCAL HUMAN IMPACTS ON REEF-BUILDING CORALS ON THE BELIZE MESOAMERICAN BARRIER REEF SYSTEM
(Under the direction of Karl D. Castillo)

Coral reefs are some of the most diverse and important ecosystems on earth, yet they are experiencing global scale declines in coral cover, diversity, and ecosystem health due to the impacts of climate change, ocean acidification, and local human impacts such as land-use change, overfishing, and pollution. This dissertation explores the impacts of thermal history on coral community composition (Chp 1), coral-associated *Symbiodinium* community structure (Chp 2), coral growth rates (Chp 3), and the acclimatization and/or local adaptation capacity of *Sidereastrea siderea* and *Pseudodiploria strigosa* corals (Chp 4) on the Belize Mesoamerican Barrier Reef System (MBRS). The Belize MBRS can be subdivided into three distinct thermal regimes following a nearshore-offshore gradient of warmer and more thermally variable to cooler and less thermally variable seawaters. Nearshore reefs (warmer and more thermally variable) experienced lower coral cover and diversity and that weedy and stress-tolerant coral species persisted on these reefs (Chp 1). Coral-associated *Symbiodinium* communities varied by thermal regime in one of the three study species, and that thermally tolerant *Symbiodinium* did not dominate in warmer nearshore reefs (Chp 2). This finding suggested that *Symbiodinium* likely did not play a large role in providing some corals with the capacity to sustain themselves in the warmest and most thermally variable thermal regimes. Nearshore corals grew faster than offshore

conspecifics, yet suffered declining growth rates, while growth rates of offshore corals remained stable (Chp 3) suggesting that historically there has been a growth advantage to living nearshore. However, recent declines suggest that compounding negative impacts outweigh this growth advantage, leading to declining growth. In a follow-up reciprocal transplant experiment, native and transplant *S. siderea* and *P. strigosa* corals preferred the nearshore, indicating that nearshore species may not exhibit greater acclimatization ability when transplanted (Chp 4). Overall, low diversity nearshore reefs appear especially threatened by continued ocean warming, as corals on these reefs exhibit declining growth rates and are not better equipped to acclimatize to new conditions than do offshore corals. A swift and significant reduction in emissions combined with continued local scale mitigation would provide hope for the future survival of these corals.

To my wife, Casey, whose constant support and understanding made this journey possible

ACKNOWLEDGEMENTS

I acknowledge Travis Courtney, Joseph Townsend, Hannah Aichelman, JP Rippe, Colleen Bove, Kathryn Cobleigh, Samir Patel, Lauren Speare, Joyah Watkins, Meg Van Horn, and Catherine Trusky for their assistance in the lab and the field. Thanks also to my research partners in Belize: Lisa Carne and Fragments of Hope, Mariko Wallen, Dale Godfrey, Victor Fox, The Belize Fisheries Department, SEA, and TIDE. Thanks also to my committee, Dr. Karl Castillo, Dr. John Bruno, Dr. John Bane, Dr. Justin Ries, and Dr. Christopher Martens for years of guidance and feedback. Lastly, thanks to my mentors including Dr. Karl Castillo and Dr. Sarah Davies for encouraging me and providing expert guidance over the course of this dissertation.

TABLE OF CONTENTS

LIST OF TABLES

LIST OF FIGURES

LIST OF ABBREVIATIONS

ABR- Atoll Backreef

AFR- Atoll Forereef

ANOVA- Analysis of variance

BR- Backreef

FR- Forereef

GIS- Geographic Information System

MBRS- Mesoamerican Barrier Reef System

MUR- Multi-scale Ultra-high Resolution

NASA JPL- National Aeronautics and Space Administration Jet Propulsion Laboratory

NS- Nearshore

NMDS- Non-metric multidimensional scaling

NOAA- National Oceanic and Atmospheric Administration

NSF- National Science Foundation

PCA- Principal component analysis

PSTR- *Pseudodiploria strigosa*

SSID- *Siderastrea siderea*

SST- Sea-surface temperature

CHAPTER 1: INTRODUCTION

Coral reefs are threatened globally due to a combination of direct and indirect anthropogenic impacts such as increasing greenhouse gas emission, excessive agricultural runoff, overfishing, and habitat destruction (Hughes et al. 2003; Hoegh-Guldberg et al. 2007; Veron et al. 2009; Frieler et al. 2013b). Of particular concern are greenhouse gas emissions which are causing climate change resulting in significant warming of the tropical oceans (Hoegh-Guldberg 1999; Hughes et al. 2003; Donner et al. 2005a). This ocean warming trend is especially troubling in the Caribbean, where rates of warming are higher than in many other tropical basins globally (Chollett et al. 2012b), and where corals have declined up to 80% in recent decades (Gardner et al. 2003). Elevated sea-surface temperature is the primary cause of mass coral bleaching, a phenomenon during which communities of corals loose a significant amount of their vital endosymbionts (*Symbiodinium*) and/or their algal photosynthetic pigments (Jokiel and Coles 1990; Glynn 1996; Hoegh-Guldberg 1999; D'Croz et al. 2001a). Bleaching events are predicted to increase in frequency and severity as the climate continues to warm (Wilkinson 2000; Buddemeier et al. 2004; Donner et al. 2005a; Wooldridge et al. 2005). Combining global-scale stressors such as rising seawater temperatures and ocean acidification (Hoegh-Guldberg et al. 2007; Veron et al. 2009) with local-scale stressors such as increased sedimentation, overfishing, unsustainable tourism practices, and high ultraviolet radiation exposure (Carilli et al. 2009b) has emplaced corals under tremendous duress.

Although the future seems rather bleak for corals during this ocean warming interval, there are indications that some corals may have developed the capacity to survive in this changing climate. Reef-building corals are able to survive in a variety of habitats and, in some cases, become resilient to environmental stress due to phenotypic plasticity, morphological differences, genetic diversity, switching and/or shuffling of endosymbiotic *Symbiodinium spp.*, species specific adaptation, and acclimatization resulting from short- or long-term local environmental conditions (Stone et al. 1999; D'Croz et al. 2001a; Loya et al. 2001; Grottoli et al. 2006; Jones et al. 2008; Sampayo et al. 2008; Armoza-Zvuloni et al. 2011; Fine et al. 2013).

Here, a holistic approach was used to examine the influence of thermal environment on coral holobiont (coral host + *Symbiodinium* + symbiotic bacterial communities) physiology and stress tolerance along the Belize Mesoamerican Barrier Reef System (MBRS). First, the Belize MBRS was characterized into three thermal regimes based on summer temperatures and annual temperature variability. 3-5 reefs were surveyed within each thermal regime to identify how thermal history and reef environment impacted coral species diversity and community structure. Next, *Symbiodinium* DNA was extracted from representatives of 3 coral species across the 3 thermal regimes to determine the potential impacts of thermal history and reef environment on the distribution and diversity of *Symbiodinium* communities both within and between coral species across thermal regimes and reef environments. Third, 134 coral cores of the species *Sidereastrea siderea* and *Pseudodiploria strigosa* were collected from reefs throughout the Belize MBRS, Coral growth rates were compared between species and reef environments, in order to characterize century-scale growth trends within and between reef environments. Lastly, a reciprocal transplant experiment was used

to assess if thermal history or environmental conditions may provide a boost to the acclimatization and/or local adaptation capacity of a coral. Fragments of *S. siderea* and *P. strigosa* were collected from warmer and more thermally variable nearshore reefs and cooler and less thermally variable offshore reefs. Half of these corals were placed back into their native reef habitat and half were transplanted to a new habitat (either offshore or nearshore). Measurements of coral calcification, protein content, *Symbiodinium* density, and *Symbiodinium* chlorophyll-*a* were taken after 3 months to assess the impacts of the transplant treatments on each coral fragment. Overall, this research seeks to investigate the role of thermal and environmental history on the growth and survival potential of Caribbean corals, and to the physiological underpinnings of differential thermal tolerance, acclimatization, and adaptation between coral species during this interval of rapid climate and environmental change. Such information will aide in the continued management of tropical reef ecosystems in order to preserve and protect the vital biodiversity and resources they provide.

CHAPTER 2: TEMPERATURE REGIMES IMPACT CORAL ASSEMBLAGES ALONG ENVIRONMENTAL GRADIENTS ON LAGOONAL REEFS IN BELIZE[1]

Introduction

Coral reefs are threatened locally and globally by anthropogenic stressors such as warming induced by increasing greenhouse gas emissions, excessive nutrients from runoff and sewage effluent, overfishing, and habitat destruction (Hughes et al. 2003; Hoegh-Guldberg et al. 2007; Frieler et al. 2013b). Of particular concern are increasing greenhouse gas emissions that continue to cause warming of the global oceans (Hughes et al. 2003; Donner et al. 2005a). This warming trend is especially troubling in the Caribbean Sea, where rates of warming are higher than in many other tropical basins (Chollett et al. 2012b), and where coral cover has declined by up to 80% in recent decades (Gardner et al. 2003). Elevated sea surface temperature (SST) is the major cause of the breakdown of the essential coral-algal symbiosis, which if widespread results in mass coral bleaching (Jokiel and Coles 1990; D'Croz et al. 2001a). In Belize, the 1998 El Niño bleaching event was the most significant bleaching induced mass coral mortality event on lagoonal reefs over the last 3000 years (Aronson et al. 2002a). These large-scale coral bleaching events are projected to increase in frequency and severity as the climate continues to warm (Donner et al. 2005a; Wooldridge et al. 2005). In fact, if ocean warming persists, corals in the Caribbean Sea are predicted to bleach biannually within th

[1] This chapter previously appeared as an article in the journal PLOS ONE. The original citation is as follows: Baumann JH, Townsend JE, Courtney TA, Aichelman HE, Davies SW, Lima FP, Castillo KD. "Temperature regimes impact coral assemblages along environmental gradients on lagoonal reefs in Belize." *PLOS ONE*, 2016.

next 20-30 years (Donner et al. 2007b), with annual bleaching events occurring as soon as 2040 (van Hooidonk et al. 2015a). Caribbean-wide and global-scale bleaching events are predicted to continue unless corals can increase their thermal tolerance at a rate of 0.2-1.0°C per decade (Donner et al. 2005a). Annual and daily thermal variability have recently been identified as important factors influencing coral thermal tolerance (Oliver and Palumbi 2011b; Soto et al. 2011a; Barshis et al. 2013). Indeed, previous exposure to thermally variable environments increases a coral's tolerance to future temperature stress (Oliver and Palumbi 2011b; Carilli et al. 2012; Castillo et al. 2012; Pineda et al. 2013b), and research suggests that Pacific and Red Sea corals living in areas with high summer maximum SST are less susceptible to bleaching (van Woesik et al. 2012; Fine et al. 2013). Along the Belize Mesoamerican Barrier Reef System (MBRS) and on Pacific Atolls, corals historically exposed to less thermal variability exhibited slower growth rates and/or greater susceptibility to bleaching in response to SST increases (Carilli et al. 2012; Castillo et al. 2012). In the Florida Keys, coral growth rates and coral cover were higher in nearshore environments exposed to more variable seawater temperatures than on deeper reefs experiencing more stable temperatures (Lirman and Fong 2007). In contrast, while many studies suggest that high temperature variability leads to higher coral resilience (Oliver and Palumbi 2011b; Barshis et al. 2013; Pineda et al. 2013b), there is also evidence that corals experiencing moderate long term temperature variability (either annual or daily variation) are better able to cope with stress (Soto et al. 2011a). Collectively, these studies emphasize the importance of thermal variability on the response of corals to environmental stress, and highlight its capacity to shape coral community composition across a reef system.

Multi-species coral assemblages have recently been proposed to comprise four major life history guilds: competitive (large, fast growing, broadcast spawning, e.g., Caribbean *Acropora spp.*), weedy (small, opportunistic colonizers of recently disturbed habitat, e.g., Caribbean *Porites spp.*), stress-tolerant (massive, slow growing, broadcast spawning, e.g., *Siderastrea siderea*), and generalist (share traits characteristic of all three other groups, e.g., *Orbicella spp.*) (Darling et al. 2012). Grouping species by life history strategy allows for prediction of responses to disturbance (e.g., temperature stress) as life history strategies are trait based (Grime and Pierce 2012). Additionally, each guild is expected to be differentially impacted by stressors and life histories predict coral community response to multiple stressors (Darling et al. 2013). Therefore, life history strategies offer a more elegant and predictive alternative to traditional genus or species level analysis.

Competitive corals are by definition not very stress tolerant (Darling et al. 2012). As such, region-wide decline of these species would be expected as the impact of anthropogenic stressors increase (including coral disease). This decline has already occurred in the Caribbean (Gardner et al. 2003). Generalist corals became dominant on Caribbean reefs in the late 1970s following mass die off of competitive corals. Generalists are more stress tolerant than competitive species but bleaching and other stressors have led to high mortality of *Orbicella spp.* in the Caribbean (Alvarez-Filip et al. 2011) and continued decline is expected as temperature stress increases (Greenstein et al. 1998; Gardner et al. 2003; Buglass et al. 2016), leading to a decline in reef complexity (Alvarez-Filip et al. 2009)

Weedy and stress tolerant corals have been shown to be more resilient than competitive and generalist species (Darling et al. 2012; Darling et al. 2013), and are hypothesized to dominate warmer and more impacted reefs (e.g., reefs closer to the shore). A shift from

dominance of competitive and generalist species to weedy and stress tolerant species occurred on Okinawan reefs following the 1998 El Niño bleaching event (Loya et al. 2001; Van Woesik et al. 2011) and an overall decline in coral cover and abundance currently occurring in the Caribbean has been coupled with an increase in abundance of weedy species (Green et al. 2008; Buglass et al. 2016). Interestingly, fossil assemblages from excavated pits on reefs in Panama reveal that mortality and changes in reef communities caused by anthropogenic impact (such as land clearing and overfishing) predate mass bleaching events, indicating that other sub-lethal stressors can impact coral community structure (Cramer 2010; Cramer et al. 2012; Cramer et al. 2015). Collectively, evidence suggests that differential responses between coral species to increasing anthropogenic stressors may lead to community scale shifts in reef composition from dominance of competitive and generalist species to dominance of stress tolerant and weedy species.

The purpose of the current study was to investigate the impact of thermal regimes on present day coral community composition (coral abundance, species richness, diversity, percent cover, density, and life history strategies) of lagoonal reefs (i.e., region extending from the barrier reef's crest to the mainland) across the Belize MBRS. A novel GIS-based metric was developed to characterize lagoonal reefs across this reef system into three thermally distinct regimes. Within these three regimes, thirteen reef sites were identified and benthic surveys were conducted to quantify coral community composition. These thermal regimes exist along a nearshore-offshore productivity gradient, which may also influence coral community structure. Quantifying coral community differences among these thermally distinct reefs will help us better predict how coral community structure may be impacted by climate change. Identifying which areas and species are best able to cope with environmental stress

(and which are least able) may allow for more targeted management strategies, as it is important to protect both high-risk and low-risk reef sites to improve our chances of conservation success (Game et al. 2008).

Materials and Methods

Site identification

SST estimate assembly

Daily 1-km horizontal resolution SST estimates were acquired from the Jet Propulsion Laboratory's Multi-Scale High Resolution SST (JPL MUR SST) records via the Physical Oceanography Distributed Active Archive Center (PO.DAAC) at the NASA JPL, Pasadena, CA (http://podaac.jpl.nasa.gov). Conventional 1-km resolution satellite-derived SST measurements (infrared, IR) are contaminated by clouds, creating data-void areas. Microwave (MW) data sets can penetrate clouds to gain better temporal coverage, but with a much coarser spatial resolution (25 km) (Chin et al. 2013). MUR combines these two datasets to present a more comprehensive and complete SST product. It employs multi-resolution variational analysis (MRBA) as an interpolation method to combine high resolution datasets with more conventional datasets, generating a product that contains no cloud contamination (Chin et al. 2013). MUR reports estimates of foundation SST, or SST at the base of the diurnal thermocline (~5-10m depth). Comparison of in-situ temperature (recorded by HOBO® v2 data loggers), MUR, and other SST products revealed that MUR outperforms other products in estimating in-situ temperature, although it also underestimates the temperature corals experience at depth (Fig S1). However, due to its temporal coverage and temporal resolution, high spatial resolution, lack of cloud contamination, and smaller method error compared to similar products

such as Group for High Resolution SST (GHRSST), MUR was determined to be the ideal SST product for use in the current study.

Site classification

Multiple thermal parameters were calculated at different temporal resolutions and examined across thirteen lagoonal reef sites (Table S1). Lagoonal reefs are located between the barrier reef's crest and the mainland, and therefore do not include the seaward facing fore-reef. Instead, lagoonal reefs include nearshore reefs, patch reefs, and the back reef. Four thermal parameters produced distinct environments for the reef sites across the Belize MBRS: average annual maximum temperature (S2A Fig), average annual temperature range (S2B Fig), average annual number of days above the regional bleaching threshold of 29.7°C (Aronson et al. 2002a) (S2C Fig), and average annual consecutive days above the regional bleaching threshold (i.e., longest potential thermal stress events) (S2D Fig). A metric that combined all four thermal parameters was generated using ArcGIS© in order to assess thermal environments across the Belize MBRS. Data from each of the four parameters in the metric (Table 1) were divided into 8-10 bins (0.5 standard deviations (SD) of the mean) and overlaid on a map of the Belize MBRS. Reefs were not present in areas where the value of any single variable was <1 SD below or >2 SD above the mean (across the entire data set from 2003-2012). For all four parameters, areas that were classified in bins ≥1 SD above the mean were designated high temperature parameter ($high_{TP}$) sites (Fig 1). Moderate temperature parameter (mod_{TP}) sites were classified as areas where all values were 0.5 to 1 SD above the average annual temperature range and the average annual maximum temperature, and within 1 SD of the average annual consecutive

days and the average annual number of days above the regional bleaching threshold (Fig 1). Low temperature parameter (low_{TP}) sites were classified as bins that were 0.5 SD above the average to 2 SD below the average for annual temperature range and annual maximum temperature, and below the average for consecutive and annual days above the regional bleaching threshold (Fig 1). Using the metric presented in Fig 1, fifteen sites were identified, thirteen of which were visited and surveyed in November 2014 (the two northernmost $high_{TP}$ sites were not surveyed as corals were not located within the marked geographic area) (Table 1, Fig 1).

Benthic surveys

In November 2014, benthic surveys were performed at the thirteen reef sites. Depth of each reef site was standardized to 3-5m. Reef types surveyed included back reefs, patch reefs, and nearshore reefs. A team of three divers surveyed six belt transects (dimension 6 x 10 m) at each site following Atlantic and Gulf Rapid Reef Assessment (AGRRA) methodology (Ginsburg and Lang 2003). Briefly, a diver classified the genus and species of every coral >6cm^2 within 1m of the transect line along a 10m transect. The number and size (length, width, and height) of individual colonies of each coral species were recorded on underwater data sheets. The collected data were used to calculate coral species diversity, abundance, richness, and coral life history (following Darling *et al.* (Darling et al. 2012)) for each site.

Additionally, six video belt transects (1 x 20m) were also performed at each site using GoPro® cameras attached to PVC stabilizing apparatuses allowing each diver to stabilize the camera while surveying transects. Video transects were analyzed at the University of North Carolina at Chapel Hill (UNC-Chapel Hill) in a manner similar to the AGRRA method used in the field, except two additional parameters (percent coral cover and coral density) were

calculated. Results of the diver and video transect surveys were not significantly different (p=0.300). As a result diver and video survey data were pooled at each site when possible. Full details and a comparison of the methods employed are available in S1 Appendix.

Coral life history

Coral species were grouped into four life history strategies as previously described by Darling *et al.* 2012 (Darling et al. 2012). In their study, Darling *et al*. 2012 identified four life history guilds for corals based on multivariate trait analysis: competitive, weedy, stress-tolerant, and generalist (Darling et al. 2012). The four guilds are primarily separated by colony morphology, growth rate, and reproductive rate. The classification was based on a thorough sampling of global Scleractinian coral diversity. Each coral that is included in a guild in Darling *et al.* 2012 (Darling et al. 2012) was classified into the appropriate guild for this study and comparisons of life history strategies between sites and site types were made.

Chlorophyll-a

Eight-day composite 4-km horizontal resolution *chlorophyll-a* (*chl-a*) estimates over the interval 2003-2015 were obtained from NASA's Moderate Resolution Imaging Spectroradiometer (AQUA MODIS) via NOAA's Environmental Research Division's Data Access Program (ERDDAP) (Simons 2011a). Eight-day composite data were selected in order to minimize gaps in data from cloud cover. Unlike the MUR SST data used for temperature calculations, there is no integrated, high-resolution product for *chl-a*. Similar to temperature calculations, monthly and yearly average *chl-a* values were calculated for each survey site (S2E Fig). *Chl-a* is a widely used proxy for primary productivity and nutrient delivery in seawater (Bell 1992; Bell et al. 2014), as it is the main photosynthetic pigment present in phytoplankton which can often quickly deplete nutrient concentrations below detectable limits.

It has been shown that remotely sensed data, such as *chl-a* concentration, yields better metrics for water quality than traditional measures such as distance from shore and distance from the nearest river (Polónia et al. 2015). Here, *chl-a* data are used as a proxy for primary production across the Belize MBRS.

Statistical analysis

Standard deviations used for temperature bins and site classification were calculated in ArcGIS©. All other statistical analysis were carried out in R 3.2.2 (2014). Transect averaged survey data for species richness, abundance, Shannon diversity, coral cover, coral density, and log-transformed *chl-a* data were analyzed using analyses of variance (ANOVA). Three fixed factors were included in the ANOVA (survey method, site, and site type) for species richness, abundance, and Shannon diversity. Only two fixed factors (site and site type) were included in the ANOVA for coral cover and coral density, since only data from video surveys were used to calculate these averages. Two fixed factors (site and site type) were included in the ANOVA for *chl-a* concentrations since they were calculated using satellite estimates and survey type was not a factor.

If factors were significant ($p<0.050$), a post-hoc Tukey's HSD test was used to evaluate the significance of each pair-wise comparison. Spatial autocorrelation was evaluated using Moran's I (Gittleman and Kot 1990). Significant *p-values* for Moran's I ($p<0.050$) indicate an effect of spatial autocorrelation. Spatial autocorrelation was only a factor for coral cover ($p=0.040$). To correct for the effect of spatial autocorrelation, the cut-off value for significance within the ANOVA for coral cover was decreased to $p<0.010$, following Dale and Fortin (Dale and Fortin 2002).

To visualize coral community differences between site types, non-metric multidimensional scaling (NMDS) ordination was implemented using Bray-Curtis similarity coefficients in the vegan package in R (Oksanen et al. 2013). An optimal stress test was performed to determine the optimal k value (k=20). Resulting NMDS scores were visualized in two-dimensional ordination space. A PERMANOVA test was performed to analyze the site type differences using the *adonis* function in the vegan package in R (Oksanen et al. 2013).

Linear models tested for the influence of temperature parameters and *chl-a* on the variation observed along NMDS1 and NMDS2 (within and between site type community variations). Linear models were run using the *lm* function in R (R Core Team, 2014). R^2 and *p*-values were calculated for each parameter based on each linear model (Table S2). For NMDS1, data were also divided by site type in order to assess within site type variation (Table S3).

Ethics statement

All research related to this projected was completed under official permit from the Belize Fisheries Department (#000045-14).

Results

Coral community composition

Combined results of AGRRA diver surveys and GoPro® video surveys for all thirteen sites revealed that coral species richness varied as a function of site location ($p<0.001$) as well as site type ($p=0.002$). Coral abundance was significantly lower at $high_{TP}$ sites compared to low_{TP} ($p=0.005$) and mod_{TP} ($p=0.020$) sites, but was not significantly different between low_{TP} and mod_{TP} sites (Fig 2A). Coral cover, Shannon diversity, coral density, and species richness also

followed these same patterns ($p \leq 0.020$; Fig 2B-E). NMDS analysis of the ecological parameters showed that community structure was significantly different (stress=0.018, adonis test p=0.006) between $high_{TP}$ sites and low_{TP}/mod_{TP} sites along the NMDS2 axis, but was not different between low_{TP} and mod_{TP} sites (p>0.050) (Fig 3). The most dominant taxa at low_{TP} and mod_{TP} sites were *Orbicella spp*., *Porites spp*., *Undaria spp*., *S. siderea*, and *Pseudodiploria spp*, while at $high_{TP}$ sites they were *Siderastrea spp*., *P. astreiodes*, and *Pseudodiploria spp*. Variation along the NMDS1 axis represents within site type differences while variation along the NMDS2 axis represent between site type differences (Fig 3).

Linear modeling of temperature and productivity parameters against NMDS1 and NMDS2 revealed that average annual maximum temperature, average annual temperature range, average annual days above the bleaching threshold, and average annual consecutive days above the bleaching threshold all had significant effects on the NMDS1 variation. All four temperature parameters, as well as *chl-a*, also had significant effects on NMDS2 variation (Table S2; Fig S3). Average annual consecutive days above the bleaching threshold explained the most variation for NMDS1 and NMDS2 (R^2=0.1026, 0.604 respectively; p <0.001 for both; Table S2; Fig S3).

Linear regressions of temperature parameters and *chl-a* within site types along NMDS1 revealed significant effects (p<0.050) of average annual maximum temperature, average annual days above the bleaching threshold, and average annual consecutive days above the bleaching threshold for all site types, average annual temperature range for mod_{TP} and $high_{TP}$ sites, and *chl-a* for $high_{TP}$ sites only (Table S3; Fig S3). Average annual days above the bleaching threshold yielded the highest R^2 for low_{TP} and mod_{TP} sites, while average annual temperature range yielded the highest R^2 for $high_{TP}$ sites (Table S3; Fig S3).

Coral life history

Site exhibited a significant effect on the number of corals in each of the four coral life history guilds (Darling et al. 2012) (p<0.001). The distribution of coral life history strategies differed significantly between low_{TP} and $high_{TP}$ site types (p=0.049; Fig 4), while mod_{TP} sites did not differ from low_{TP} or $high_{TP}$ sites (Fig 4). Overall, there appears to be a pattern of lower abundances of all life history guilds at $high_{TP}$ sites compared to low_{TP} sites. Competitive species were not present and generalist species were only present in very small number at $high_{TP}$ sites.

Chlorophyll-a

Annual average *chl-a* concentrations varied over time and differed by site type (p<0.001), but were consistently lowest at low_{TP} sites and highest at $high_{TP}$ sites regardless of year (Fig 5A). *Chl-a* concentrations averaged over 2003-2015 were significantly different across all three site types (p<0.001 in all cases). Low_{TP} sites exhibited the lowest average 13-year *chl-a* concentrations. Mod_{TP} sites exhibited average 13-year *chl-a* concentrations that were significantly higher than low_{TP} sites, but significantly lower than $high_{TP}$ sites. $High_{TP}$ sites exhibited significantly higher average 13-year *chl-a* values than both low_{TP} and mod_{TP} sites (p<0.001 in all cases, Fig 5B). The pattern seen in *chl-a* concentrations is positively correlated with the patterns seen in all temperature parameters (*chl-a* and temperature parameters are lowest at low_{TP} sites and highest at $high_{TP}$ sites) (Fig 1, Fig S2).

Discussion

Coral community composition

Coral species richness, abundance, diversity, density, and percent cover were all lower at $high_{TP}$ sites compared to low_{TP} and mod_{TP} sites (Fig 2). Differences in coral community composition between $high_{TP}$ sites and low_{TP}/mod_{TP} sites are historically explained by more stressful conditions nearshore and less stressful conditions offshore (Done 1982; Cortés 1990). These nearshore stressors include, but are not limited to temperature, eutrophication, sedimentation, and wave energy (Done 1982; Cortés 1990). Our findings suggest that lower coral species richness, diversity, abundance, percent cover, and density at $high_{TP}$ sites may be driven by high thermal variability, elevated maximum temperatures, and prolonged duration of exposure to temperatures above the bleaching threshold; three variables that have been shown to cause coral community decline (Loya et al. 2001; McClanahan and Maina 2003; McClanahan et al. 2008; Thompson and Van Woesik 2009; Soto et al. 2011a). These temperature parameters were more strongly correlated with changes in coral community composition between site types than with *chl-a* (Fig S3), indicating that they likely play a greater role in determining coral community composition than productivity. High weekly thermal variability has also been shown to correlate with low coral cover on nearshore reefs in the Florida Keys (Soto et al. 2011a). Therefore, differences in thermal variability observed across site types may have influenced coral community composition in Belize.

Our findings are contrary to the results of Soto *et al*. (2011) (Soto et al. 2011a), which showed that reef sites with moderate temperature variability (equivalent to mod_{TP} sites in the current study) in Florida had higher coral cover than sites exposed to low (offshore deep

reefs) or high temperature variability. Soto *et al.* (2011) (Soto et al. 2011a) suggests that corals exposed to moderate weekly thermal variation are able acclimatize to a wide range of environmental conditions, making them more resilient than corals that experience less variation. At the same time, corals exposed to extremely high thermal variation generally do not survive(Soto et al. 2011a). Our results may contrast with that of Soto et al. (2011) because fore reef locations were not included in the present study (i.e., low_{TP} sites are located in the back reef). Our $high_{TP}$ sites follow the same pattern seen in Soto *et al.* (2011) (Soto et al. 2011a) as they have lower coral cover than mod_{TP} sites (Fig 2).

Our results also contrast those of Lirman and Fong (2007) (Lirman and Fong 2007), which showed that nearshore reefs (equivalent to our $high_{TP}$ sites) exhibited higher coral cover and growth rates than offshore reefs (equivalent to our low_{TP} sites) in the Florida Keys. Interestingly, these nearshore Florida reefs also experienced lower water quality than the offshore reefs (Lirman and Fong 2007). The authors hypothesized that higher coral cover and growth rates on nearshore reefs were due to the ability of some corals to switch trophic mode under adverse conditions (Lirman and Fong 2007), a pattern that has been observed in previous studies, but was not quantified in the current study (Anthony 1999; Grottoli et al. 2006). Differences in coral community composition between the Florida Reef tract and the Belize MBRS may explain our contrasting results in coral cover as nearshore patch reefs in Florida appear to have relatively high numbers of *Orbicella spp*. (Lirman and Fong 2007), whereas $high_{TP}$ sites in Belize were almost void of this species.

Life history strategies

In the current study, high$_{TP}$ sites contained no competitive species, few generalists, and were dominated by stress-tolerant and weedy genera, while both low$_{TP}$ sites and mod$_{TP}$ sites contained all 4 life history types (Fig 4). Low$_{TP}$ sites contained all four life history strategies in roughly equal proportions. Mod$_{TP}$ sites were similar but with fewer competitive species than low$_{TP}$ sites, and high$_{TP}$ sites had comparatively fewer of all four life histories, but were dominated by weedy and stress tolerant genera. Shifts toward weedy and stress tolerant genera under climate change conditions were predicted by Darling *et al*. (2012) (Darling et al. 2012), and have been recorded in many areas of the world (Loya et al. 2001; McClanahan et al. 2014), including the Caribbean (Aronson et al. 2004; Green et al. 2008; Alvarez-Filip et al. 2011). Even in the face of region-wide decline in coral cover and decrease in abundance of competitively dominant species (Gardner et al. 2003), some weedy species, such as *Porites astreoides*, are actually increasing in prevalence within the Caribbean (Green et al. 2008). This weedy coral species is likely able to succeed in high stress environments due to its ability to brood and mature quickly, which allows it to rapidly colonize a recently disturbed area (Green et al. 2008; Darling et al. 2012).

In contrast, a stress-tolerant species such as *S. siderea* is likely able to survive in high$_{TP}$ environments due to its massive size and long life span, which allows it to sustain a population in the absence of successful recruitment. This can increase the long-term survival potential of this species in harsh conditions (Hughes and Tanner 2000). These two contrasting strategies seem most effective in high$_{TP}$ environments (Fig 4), and are likely to be most effective in future conditions as the oceans continue to warm. This prediction is corroborated by Loya *et al.* (2001) (Loya et al. 2001), who showed that mounding (e.g., *S. siderea*) and encrusting (e.g.,

P. astreoides) species survived a mass bleaching event in 1997-1998 better than corals of other morphologies (e.g., branching). Ten years after the bleaching event these same types of coral continued to dominate. However, some branching species recovered and increased in abundance (Wild et al. 2011). In the current study, branching species were almost non-existent in $high_{TP}$ sites, which indicates that these sites have experienced a recent thermal stress event or are exposed to chronic stress (e.g., temperature, eutrophication) that prevents such species from succeeding in these environments. It is also possible that $high_{TP}$ sites are more frequently disturbed than both low_{TP} and mod_{TP} sites. Disturbances such as bleaching events, eutrophication, sedimentation, and overfishing are known to cause declines in coral cover, species richness, and diversity (Loya et al. 2001; Van Woesik et al. 2011). These more disturbed or impacted reefs can then become dominated by stress-tolerant corals and corals that quickly colonize areas after a perturbation (i.e., weedy corals) (Loya et al. 2001; Soto et al. 2011a; Van Woesik et al. 2011; Alvarez-Filip et al. 2013), as observed in the current study (Fig 4). Historical and/or geological investigation of reef assemblages (i.e., through pit excavating or coring of reef framework (Aronson et al. 2002a; Cramer et al. 2012; Cramer et al. 2015)) would be a useful next step, as it would allow insight into how reef communities within the three thermal regimes have changed after disturbances and over long periods of time.

Influence of primary productivity on coral community composition

Cross-reef *chl-a* concentrations follow the same patterns as temperature (elevated nearshore and decreasing with increasing distance from the Belize coast) (Fig 1, Fig S2). This means that reefs with higher *chl-a* concentrations have lower coral species richness, abundance, diversity, density, and percent cover. This supports a previous finding that shows

a strong negative relationship between *chl-a* and coral cover, species richness, and abundance at nearshore reefs on the Great Barrier Reef (GBR) (Van Woesik et al. 1999). However, our results reveal that *chl-a* concentrations are not strongly correlated (R^2=0.040) with changes in coral community structure (e.g., percent cover, abundance, diversity, species richness, and density) across site types (S5H Fig), suggesting that *chl-a* concentrations may not best explain differences in community composition between site types in Belize. This may be due to spatial scale (e.g., we focused on nearshore, patch reef, and back reef sites as opposed to exclusively nearshore sites) (Van Woesik et al. 1999), or the coarse scale of the *chl-a* dataset (4 km x 4 km grid; each survey site is <1 km). Focusing on variation within nearshore ($high_{TP}$) sites, we do see a correlation between *chl-a* and changes in coral community structure (S4H Fig), which supports results from previous work (Van Woesik et al. 1999; West and Van Woesik 2001).

Other potential factors influencing coral community structure across reef types

Eutrophication

Eutrophication has led to local degradation of reefs (Marubini and Atkinson 1999; Fabricius 2005; Wooldridge 2009a). However, larger scale (regional) reef degradation due to nutrients alone has not been quantitatively shown (Szmant 2002). Wooldridge (2009) (Wooldridge 2009b) demonstrates that lower water quality (e.g., higher nutrient concentrations) are linked to lower bleaching thresholds on nearshore reefs in Australia. If bleaching thresholds are depressed at $high_{TP}$ sites for some species, it may help explain lower diversity measured at these sites, as they experience warmer temperatures and spend more time above the regional bleaching threshold than do mod_{TP} and low_{TP} sites (Fig S2). While *chl-a* does not correlate well with changes in coral community structure in this study (Fig

S3), it should be noted that *chl-a* is an estimate of nutrient delivery and primary productivity, not a measurement of the concentration of any one nutrient pool. Due to this limitation, manipulative field experiments such as Vega-Thurber et al. (2014)(Vega Thurber et al. 2014) and Zaneveld et al. (2016)(Zaneveld et al. 2016) are needed to understand the influence of nutrients on coral community structure and bleaching thresholds at local scales.

Sedimentation

Coastal (nearshore) reefs throughout Belize are influenced by runoff from smaller local rivers, and reefs in southern Belize experience additional runoff and river plumes originating from larger watersheds in Honduras and Guatemala (Paris and Cherubin 2008; Carilli et al. 2009a). It has been previously shown that *Orbicella faveolata* corals on reefs with higher sedimentation rates exhibited suppressed skeletal extension rates for a longer duration than corals on reefs with lower sedimentation rates following the 1998 bleaching event in Belize (Carilli et al. 2009c). In contrast, increased sedimentation did not affect skeletal extension of *S. siderea* or *P. astreoides* corals in Puerto Rico (Torres and Morelock 2002). The results of these two studies suggest that there may be species-specific responses to increased sedimentation rates. In Barbados, reefs with high sedimentation rates were dominated by coral species with high recruitment and high natural mortality (e.g., *P. astreoides*) and reefs with lower sedimentation rates were dominated by coral species with lower recruitment and low natural mortality (e.g., boulder corals) (Hunte and Wittenberg 1992). As sedimentation rate was not quantified in this study, the impacts of sedimentation on coral community structure are not clear.

Circulation and wave energy

The Belize MBRS lies west of the Honduras Gyre, a hydraulic feature that recirculates water inside the Cayman basin (Carrillo et al. 2015). The coastal waters of northern Belize are influenced by the Cayman and Yucatan currents, which move water northwest up the coastline toward Mexico (Sheng and Tang 2003,2004; Tang et al. 2006; Carrillo et al. 2015). In central and southern Belize, current velocities are lower and dominant circulation patterns are less consistent throughout the year (Tang et al. 2006). However, currents appear to bring water and potentially pollution, nutrients, or sediment plumes from coastal Honduras and Guatemala west to southern Belize where they recirculate before slowly moving northward (Andrefouet et al. 2002; Sheng and Tang 2004; Tang et al. 2006; Paris et al. 2007; Paris and Cherubin 2008; Prouty et al. 2008; Carilli et al. 2009a). These circulation patterns have the potential to influence the stress tolerance of corals across sites and latitude in the current study. Our results reveal no spatial autocorrelation between sites for any of our measured variables with the exception of *chl-a* suggesting that the influence of these currents may be minimal. Additionally, wave energy may play a role in shaping coral communities. Wave energy may be elevated at low_{TP} sites as they are located near channels in the fore reef and may not be as sheltered by the reef crest as other mod_{TP}. Similarly, wave energy may be elevated at $high_{TP}$ sites due to the large fetch between the reef crest and nearshore reefs and the prevailing wind direction from offshore to inshore.

Light

Irradiance (light intensity) has been shown to decrease along an offshore-nearshore gradient on the GBR as *chl a* concentrations increase (Cooper et al. 2007). *Chlorophyll-a* concentrations increase with proximity to shore in Belize (Fig 1), so this pattern of decreasing light intensity towards the nearshore likely holds for Belize as well. However, in southern Belize offshore reefs (and nearshore reefs) are subject to seasonal sedimentation and runoff from larger rivers in Honduras and Guatemala (Andrefouet et al. 2002; Prouty et al. 2008). Irradiance is a known stressor, proven to cause coral bleaching alone or in consort with elevated temperatures (Brown 1997). Although depth was held constant in the present study, it is possible that differing light levels both between site types and between individual sites may influence coral community composition across the site types investigated in the current study.

Proximity to human populations

Declining health of coral reefs worldwide has been linked to land-based stressors including nutrients and human use and exploitation (e.g., overfishing) (Brown 1997; Jackson et al. 2001; Fabricius 2005) as well as proximity to sources of these stressors (e.g., major human population centers) (Burke et al. 2004). However, not all reefs that are near to or influenced by land-based stressors are unhealthy (Perry and Larcombe 2003; Lirman and Fong 2007). Some of the study sites were within close proximity to a major human population center, particularly the high$_{TP}$ sites (populations of major towns and cities in Belize can be seen in Table S4). Analysis of spatial autocorrelation revealed no significant differences between high$_{TP}$ sites or between high$_{TP}$ sites and sites that were further offshore,

suggesting that proximity to human population centers did not have a major impact on coral community composition.

Conclusions

$High_{TP}$ reefs exhibit lower coral diversity, abundance, species richness, and cover than do low_{TP} and mod_{TP} reefs in Belize. These $high_{TP}$ reefs are exposed to higher annual temperatures, greater temperature variability, more time above the regional bleaching threshold, elevated *chl-a* concentrations, and likely increased sedimentation rates and lower flow than low_{TP} and mod_{TP} reefs. Temperature parameters, most notably time spent above the bleaching threshold, correlate best with differences in coral community structure. In addition, stress-tolerant and weedy coral life history strategies dominate at $high_{TP}$ reefs. Due to exposure to generally more stressful environmental conditions, $high_{TP}$ reefs may offer a snapshot into the projected future of coral reefs as they become increasingly exposed to local (pollution, runoff, land-use change, and overpopulation) and global (warming and acidification) stressors. Previously, such reefs have been suggested as possible refugia against climate change (Woesik et al. 2012). Globally, this would mean a shift towards dominance of stress-tolerant and weedy corals (McClanahan et al. 2014). Such a shift would dramatically impact the structure and function of reefs, essentially creating novel ecosystems (Graham et al. 2014). $High_{TP}$ reefs should be protected in addition to more pristine reefs in order to improve conservation success (Game et al. 2008). More pristine reefs should be protected as they contain more diversity and provide more ecosystem services than do $high_{TP}$ reefs (Moberg and Folke 1999). However, $high_{TP}$ reefs host coral holobionts that may be best suited to survive in future ocean conditions. To ensure survival and future success of reefs while maintain current diversity both heavily impacted and pristine ecosystems must be

protected. The results of the current study highlight the need to better protect and understand impacted nearshore reef systems, including investigations into what conditions allow more sensitive species (e.g., competitive and generalist) to survive and persist on nearshore reefs.

Data Accessibility

All data are archived on PANGAEA at the following DOI:
doi.pangaea.de/10.1594/PANGAEA.859972

Tables

Factor	Min	Mean	Max	SD	low$_{TP}$ Sites	mod$_{TP}$ Sites	high$_{TP}$ Sites
Mean Annual Max Temp	30.2°C	30.6°C	31.3°C	0.27°C	30.2-30.8°C	30.8-30.9°C	30.9-31.3°C
Mean Annual Temp Range	4.4°C	5.2°C	7.1°C	0.69°C	4.4-5.5°C	5.5-5.9°C	5.9-7.1°C
Mean Annual Days Above Bleaching Threshold	20.0 days	40.1 days	78.4 days	14.3 days	20.0-40.1 days	40.1-54.4 days	54.4-78.4 days
Mean Consecutive Days Above Bleaching Threshold	3.0 days	4.8 days	7.5 days	0.92 days	3.0-4.8 days	4.8-5.7 days	5.7-7.5 days

Table 1: Thermal Parameters Used For Site Classification: Values for the four thermal parameters included in site selection metrics. Values are all averages from 2003-2012 and include measurements for minimum, mean, maximum, and standard deviation (SD) for each thermal parameter. The range at which each factor was classified as low$_{TP}$, mod$_{TP}$, or high$_{TP}$ site is also shown.

Figures

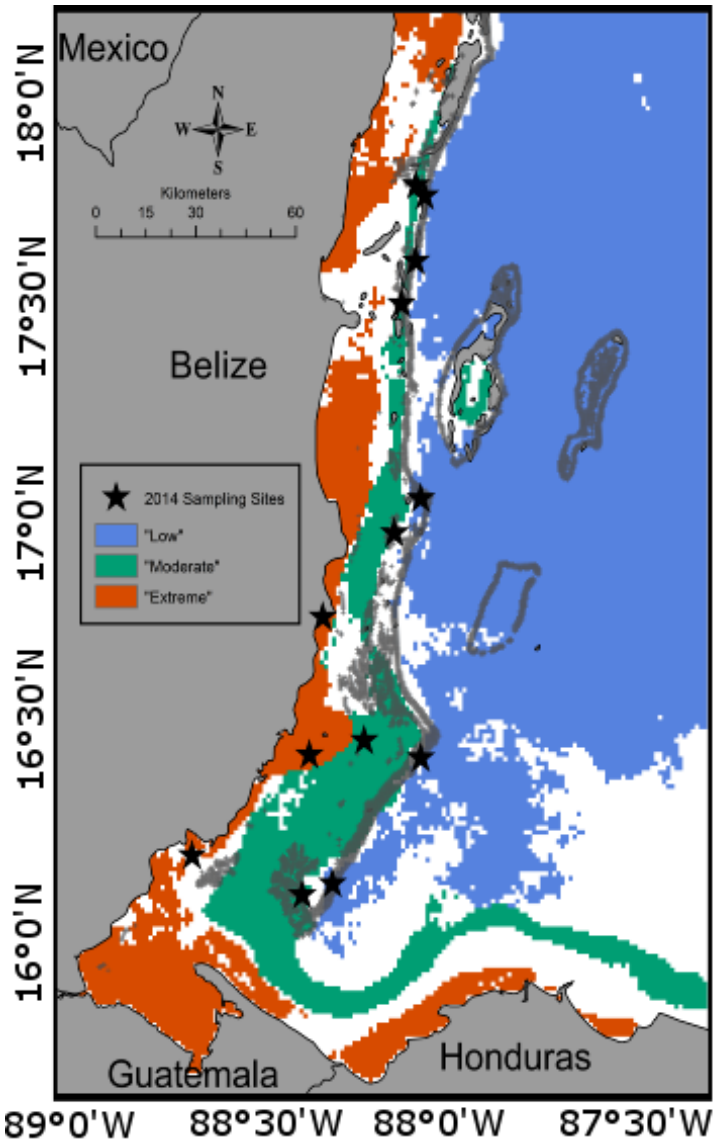

Figure 1: Thermal Regimes and Site Locations: The Belize Mesoamerican Barrier Reef System (MBRS) classified by site type based on four thermal parameters. Blue, green and red regions represent low_{TP}, mod_{TP}, and $high_{TP}$ areas across the reef system. Stars indicate surveyed sampling sites.

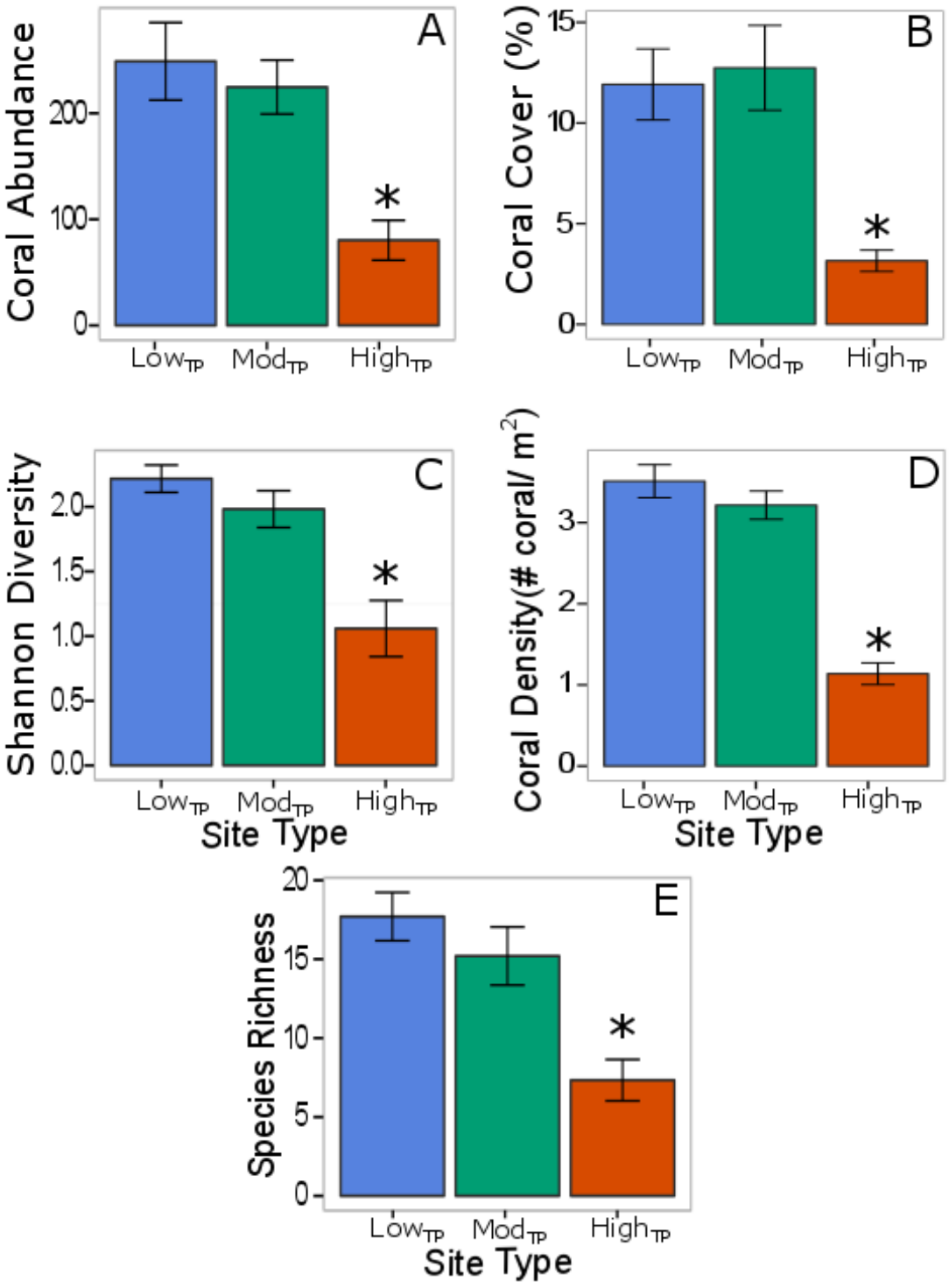

Figure 2: Differences in coral community structure across site type: Average coral abundance (A), percent coral cover (B), coral species diversity (C), coral density (D), and coral species richness (E) at each site type. Statistically significant differences ($p<0.05$) are marked with an *. Blue, green, and red bars (± 1 SE) represent low_{TP}, mod_{TP}, and $high_{TP}$, respectively.

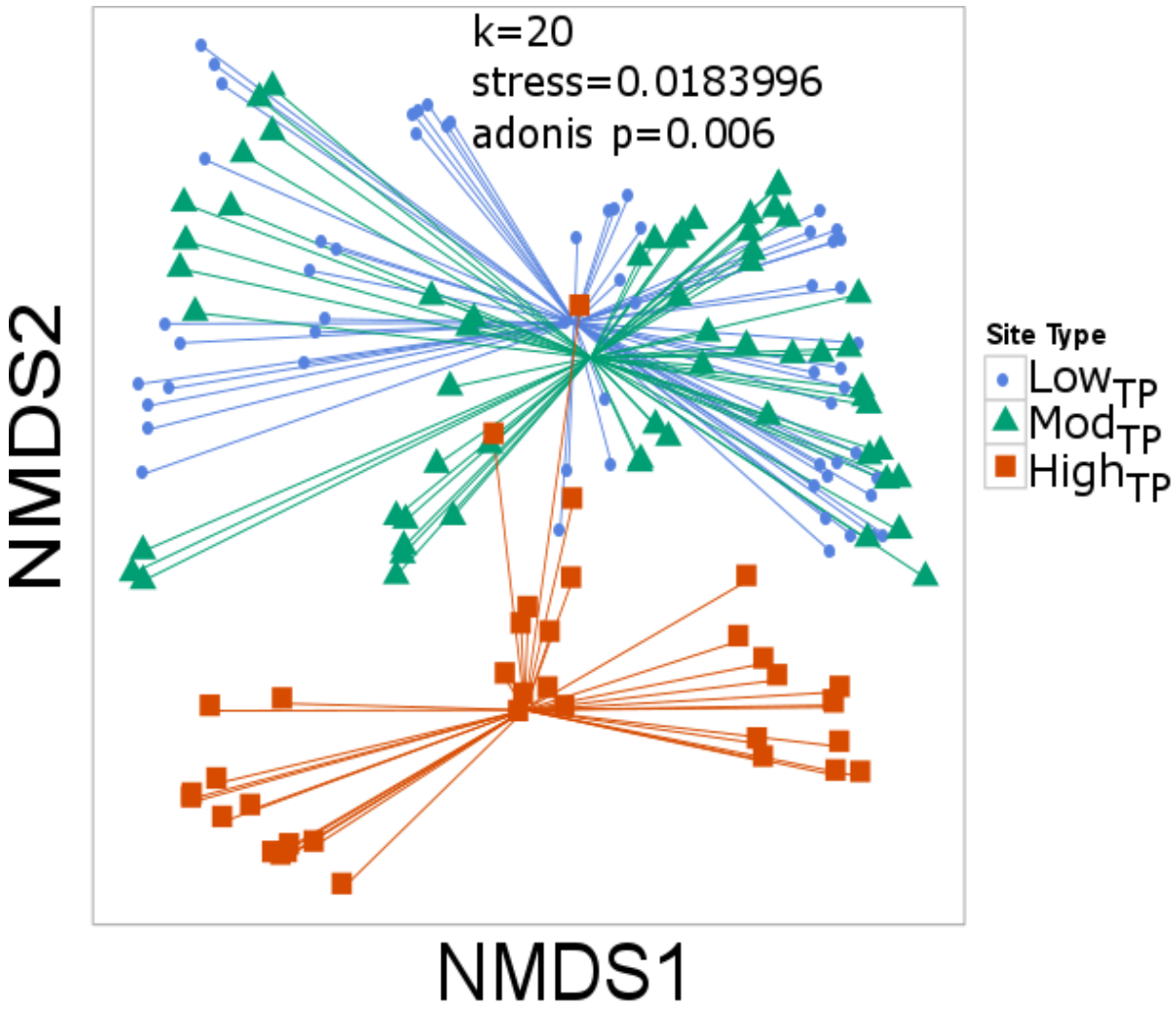

Figure 3: NMDS of coral community variables by site type: Nonmetric multidimensional scaling (NMDS) plot of coral community differences clustered by site type. Blue circles, green triangles, and red squares represent low_{TP}, mod_{TP}, and $high_{TP}$ site types, respectively.

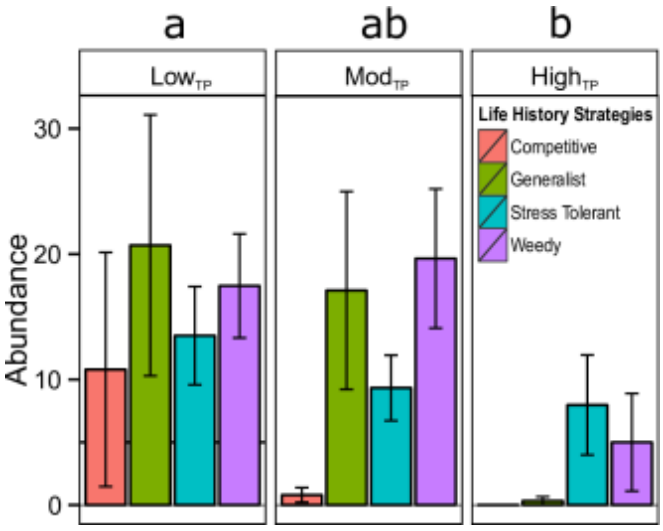

Figure 4: Coral life history strategy by site type: Abundance (count) of corals (±1 SE) grouped by life history (from Darling et al. 2012). Letters 'a' and 'b' show significant differences between site types ($p<0.050$) acquired from post hoc Tukey tests.

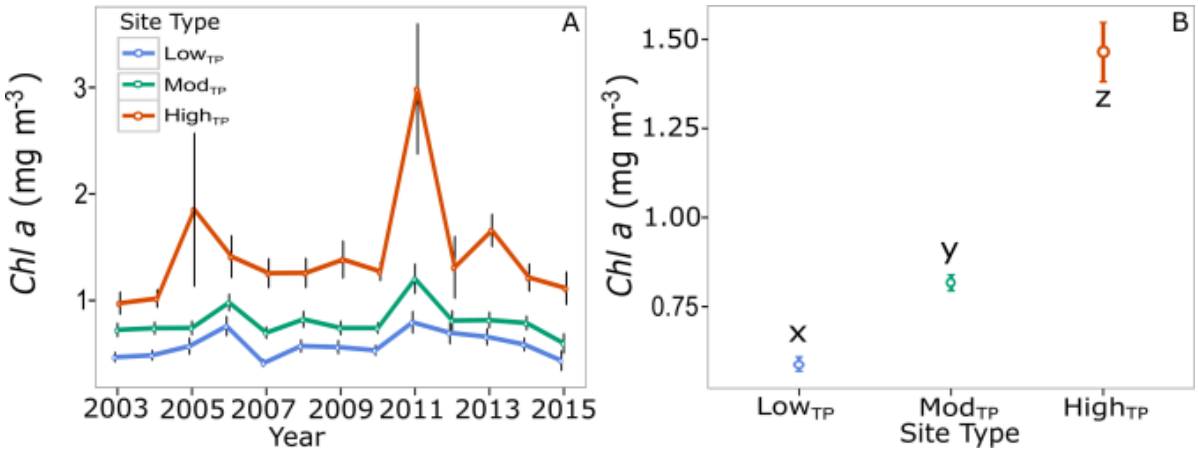

Figure 5: Average chl-a by site type: Chl-a concentration by site type (±SE) Annual average chl-a for low$_{TP}$ (blue), mod$_{TP}$ (green), high$_{TP}$ (red) site types over the interval 2003-2013 (A). Chl-a concentrations averaged over the 13-year interval (B). Letters x, y, and z indicate results of post hoc Tukey tests showing significant differences in 13-year chl-a concentrations across site types ($p<0.050$)

CHAPTER 3: CORAL SYMBIODINIUM COMMUNITY COMPOSITION ACROSS THE BELIZE MESOAMERICAN BARRIER REEF SYSTEM IS INFLUENCED BY HOST SPECIES AND THERMAL VARIABILITY

Introduction

Obligate symbioses, relationships in which two or more organisms depend on one another for nutrition and survival, occur globally. Such symbioses are ubiquitous in plants and algae, i.e., Mycorrhiza (Meyer 1966), lichens (Honegger 1991), or insects, i.e., ants and bacteria (Degnan et al. 2004). The effects of climate change are expected to disrupt proper functioning of many symbioses, including that of reef-building corals (Coles and Brown 2003; Hoegh-Guldberg et al. 2007; Brosi et al. 2011), who's success depends on the symbiosis between the coral host and photosynthetic algae of the genus *Symbiodinium* (Muscatine 1990; Warner et al. 1996; DeSalvo et al. 2010). Under stressful conditions this coral-*Symbiodinium* relationship breaks down, resulting in the loss of endosymbiont cells and/or photosynthetic pigments from the coral tissue in a process known as 'coral bleaching' (Glynn 1993). Coral bleaching is most commonly associated with thermal stress (Hoegh-Guldberg 1999; Hughes et al. 2003; Wild et al. 2011; Heron et al. 2016; Hughes et al. 2017a) and is predicted to increase in frequency and severity as the world's climate continues to change (Jokiel and Coles 1990; D'Croz et al. 2001b; Coles and Brown 2003; Donner et al. 2005b; McWilliams et al. 2005; Wooldridge et al. 2005; Donner et al. 2007c). Increased thermal stress resulting from climate

[2]This chapter previously appeared as an article in the journal *Microbial Ecology*. The original citation is as follows: Baumann JH, Davies SW, Aichelman HE, Castillo KD. "Coral *Symbiodinium* community compositions across the Belize Mesoamerican Barrier Reef System is influenced by host species and thermal variability." *Microbial Ecology*, 2018.

change combined with other local stressors such as eutrophication, habitat destruction, and overfishing has created an uncertain future for coral reefs (Hughes et al. 2003; Hoegh-Guldberg et al. 2007; Frieler et al. 2013a). In the Caribbean Sea, warming rates are higher than in any other tropical basin (Belkin 2009; Chollett et al. 2012c) and coral cover has declined by as much as 80% in recent decades (Gardner et al. 2003). It has been predicted that Caribbean coral reefs may suffer biannual bleaching events within the next 20-30 years (Donner et al. 2007c) and annual bleaching by 2040 (Van Hooidonk et al. 2015b).

In the face of a changing climate and widespread reef declines, corals will need to rapidly increase their thermal tolerance in order to persist in their current form (Donner et al. 2005b; Barshis 2015). Coral thermal tolerance has been shown to be influenced by a coral's thermal history, which among other factors includes average environmental temperature and extent of thermal variability (Castillo and Helmuth 2005; Middlebrook et al. 2008). On average, corals previously exposed to warmer temperatures show decreased mortality during bleaching events (Pineda et al. 2013a) and more stable growth patterns (Castillo et al. 2012) compared with corals exposed to cooler temperatures, which exhibit greater mortality during heat stress and declining growth rates with increased temperatures (Castillo et al. 2012; Pineda et al. 2013a). Exposure to greater daily thermal variation has also been shown to increase coral thermal tolerance (Oliver and Palumbi 2011a) and has been associated with higher coral cover and slower mortality rates when compared to reefs exposed to less thermal variation (Soto et al. 2011b). Coral thermal tolerance is also heritable with larvae from parent colonies on lower-latitude (warmer) reefs showing a 10-fold increase in survival under heat stress when compared to larvae from cooler reefs locations (Dixon et al. 2015). A growing body of evidence suggests that the coral host plays a significant role in thermal tolerance (Baird et al. 2009; Barshis et al.

2013; Kenkel et al. 2013a; Kenkel et al. 2013b), however, plasticity or specificity of coral-associated *Symbiodinium* and bacterial communities have also been shown to play a significant role in overall thermal tolerance (Rowan et al. 1997; Baker 2003; LaJeunesse 2010; Silverstein et al. 2015; Ziegler et al. 2017).

The clades, lineages, or species of *Symbiodinium* hosted by a coral are critical to its survival and resilience to stress. The genus *Symbiodinium* is genetically diverse and comprises at least nine divergent clades (clades A-I; Coffroth and Santos 2005). These clades can be further broken down into lineages, corresponding approximately to species level diversity (LaJeunesse 2001), with some species conferring variable benefits (Rowan et al. 1997; LaJeunesse and Trench 2000; Coffroth and Santos 2005). In particular, some *Symbiodinium* are more thermally tolerant than others (Warner et al. 1996; Rowan et al. 1997; Silverstein et al. 2017), specifically *Symbiodinium* clade D (Baker et al. 2004). In contrast, clade C is more thermally sensitive (Rowan 2004; Tchernov et al. 2004; Berkelmans and Van Oppen 2006), yet it includes *Symbiodinium thermophilum*, a thermally tolerant species within clade C endemic to the Red Sea (Hume et al. 2015). This example illustrates that making clade level generalizations is problematic due to the physiological diversity within a single *Symbiodinium* clade (Thornhill et al. 2017). Specific lineages within clades can also confer various advantages. For example, C1 enhances growth rate (Little et al. 2004), *S. thermophilum* confers heat tolerance (Hume et al. 2015), and B2 confers cold tolerance (Thornhill et al. 2008). Additionally, species D1a (*Symbiodinium trenchii)* has been shown to be both heat tolerant (Jones et al. 2008; LaJeunesse et al. 2009), and cold tolerant (Silverstein et al. 2017). However, the increased thermal tolerance of a coral which predominantly hosts clade D *Symbiodinium* appears to come at a cost of lower lipid stores, reproductive potential, growth, and carbon

fixation rates compared with corals that host other clades (Cantin et al. 2009; Jones and Berkelmans 2011; Cunning et al. 2015; Kennedy et al. 2015). Due to the high levels of variation in coral host-*Symbiodinium* interactions, it is essential to identify which lineages are present in order to help predict how a coral may respond to environmental stressors.

The majority of coral species host one dominant *Symbiodinium* lineage (Baker et al. 1997; Diekmann et al. 2002; Coffroth and Santos 2005) along with several non-dominant lineages (Silverstein et al. 2012), each proliferating primarily by asexual cloning (Thornhill et al. 2017). However, other corals can host multiple dominant lineages or clades (Rowan et al. 1997; Thornhill et al. 2017). Recent advances in genetic techniques, especially next-generation sequencing (NGS), have allowed researchers to identify cryptic and low-abundance symbionts comprising 0.1% or more of the total *Symbiodinium* community within a host (Kenkel et al. 2013b; Quigley et al. 2014). It is important to understand these low-abundance *Symbiodinium*, as they have the potential to play important roles in coral-algal holobiont physiology under ambient and stressful conditions (Correa et al. 2009; Jones and Berkelmans 2010; Davy et al. 2012; but see also Lee et al. 2016). Identifying trends in *Symbiodinium* community variation (including cryptic or low abundance lineages) within and between species across a coral reef may allow for a better understanding of the role of *Symbiodinium* communities in modulating coral response to environmental variation.

Symbiodinium communities have been shown to vary regionally (between reef systems; Garren et al. 2006; Kemp et al. 2015; Kennedy et al. 2015), locally (within a reef system; Garren et al. 2006), temporally (across time on the same reef; Warner et al. 2006), and within a colony (Kemp et al. 2015). Studies of this variation have revealed geographically endemic lineages of *Symbiodinium* which may play a significant role in local and regional scale coral

survival and stress tolerance (Rowan et al. 1997; Green et al. 2014; Kemp et al. 2015). While temperature stress may play a role in structuring *Symbiodinium* communities (Pettay et al. 2015), variations in other environmental factors have also been shown to drive *Symbiodinium* community composition. For example, physical processes and total suspended solids (a proxy for nutrients and flow) drive *Symbiodinium* associations within the *Orbicella annularis* species complex in Belize and Panama (Garren et al. 2006); however, on a regional scale (e.g., the entire Caribbean Sea), *O. annularis Symbiodinium* communities differed based on patterns of chronic thermal stress (Kennedy et al. 2016). Additionally, the presence of several subclades of *Symbiodinium* correlated with other environmental parameters, such as cooler summers, nutrient loading, and turbidity (Kennedy et al. 2016). Taken together, these studies demonstrate that variation in *Symbiodinium* communities can be driven by a variety of environmental parameters and may be specific to each coral species in each specific environment.

The majority of Caribbean *Symbiodinium* biogeography studies have focused on the *Orbicella* species complex (Garren et al. 2006; Kemp et al. 2015; Kennedy et al. 2016) as *Orbicella* spp. has experienced significant declines over the last two decades (Miller et al. 2009) and are now listed as 'threatened' under the Endangered Species Act. However, the variation in *Symbiodinium* communities of other more stress tolerant corals, such as *Sidereastrea siderea* and *S. radians* (Guzman and Tudhope 1998; Lirman et al. 2002; Lirman and Fong 2007; Lirman and Manzello 2009; Castillo et al. 2011b; Darling et al. 2012), remain relatively understudied. Here, we assess *Symbiodinium* community composition in three species of ubiquitous Caribbean corals (*Siderastrea siderea*, *S. radians*, and *Pseudodiploria strigosa*) across three distinct thermal regimes along the Belize Mesoamerican Barrier Reef System (MBRS) previously shown to influence coral community composition (Baumann et al.

2016). Coral-associated *Symbiodinium* communities were examined across an inshore-offshore thermal gradient and a latitudinal gradient to elucidate the role that coral species, local habitat, and thermal regime play in structuring *Symbiodinium* communities in the western Caribbean Sea.

Methods

Site selection and characteristics

Ten sites along the Belize MBRS were selected. These sites were previously characterized into three thermally distinct regimes (low_{TP}, mod_{TP}, $high_{TP}$) and exhibited variations in coral species diversity and richness (Baumann et al. 2016). $High_{TP}$ sites (inshore) were characterized by larger annual temperature variation, higher annual maximum temperatures, and are exposed to temperatures above the regional bleaching threshold of 29.7°C (Aronson et al., 2002) more often than mod_{TP} sites (mid-channel reefs) and low_{TP} sites (offshore) (Baumann et al. 2016). $High_{TP}$ sites were dominated by stress tolerant and weedy coral species while corals representing all four coral life histories (stress tolerant, weedy, competitive, and generalist; Darling et al. 2012) were present in low_{TP} and mod_{TP} sites (Baumann et al. 2016).

Sample Collection

In November 2014, five to ten (quantity depended on local availability) coral tissue microsamples (approx. 2 mm diameter) were collected at 3 to 5 m depth from three coral species (*Siderastrea siderea, S. radians, and Pseudodiploria strigosa*) at nine sites across four latitudes along the Belize MBRS (Fig 1; Table 1). Each latitudinal transect contained a low_{TP},

mod$_{TP}$, and high$_{TP}$ site. The transects from north to south were: Belize City, Dangriga, Placencia, and Punta Gorda (Fig 1). All three sites within the Punta Gorda and Placencia transects were sampled, but only the low$_{TP}$ and high$_{TP}$ sites were sampled along the Belize City and Dangriga transects due to time constraints. Samples collected at the Belize City high$_{TP}$ site were collected in October 2015, as no corals were located in the area in 2014, but patch reefs were located in 2015. Coral microsamples were collected at least 1m apart from one another to randomize micro-environmental and host genetic effects in order to attain more site-specific representative samples. Microsamples were collected from colony edges to avoid unnecessary damage to the larger colony and to limit effects of *Symbiodinium* zonation within an individual (Kemp et al. 2015). Tissue microsamples were placed on ice immediately following collection for transport to mainland Belize. Microsamples were then preserved in 96% ethanol and stored on ice at –20°C, and transported on ice to the coral ecophysiology lab at the University of North Carolina at Chapel Hill and stored at −20°C until DNA isolation.

Sea Surface Temperature

Daily 1-km horizontal resolution sea surface temperature (SST) estimates were acquired from the NASA Jet Propulsion Laboratory's Multi-Scale High Resolution SST (JPL MUR SST) product via NOAA Environmental Research Division's Data Access Program (ERDDAP- https://coastwatch.pfeg.noaa.gov/erddap/index.html) (Simons 2011b) and analyzed following Baumann et al (2016). Several additional temperature parameters were taken into account for this study, including: annual degree heating days (similar to degree heating weeks, as per Gleeson and Strong (1995)), annual minimum temperature, annual average temperature, annual winter average temperature, and annual summer average

temperature. Values for these parameters within the three thermal regimes are reported in Table S1.

DNA Extraction

Coral holobiont (coral, algae, and microbiome) DNA was isolated from each sample following a modified phenol-chloroform (Chomczynski and Sacchi 2006) method described in detail by Davies et al (2013). Briefly, DNA was isolated by immersing the tissue in digest buffer (100 mM NaCL, 10mM Tris-Cl pH 8.0, 25 mM EDTA pH 9.0, 0.5% SDS, 0.1 $mgml^{-1}$ Proteinase K, and 1 μgml^{-1} RNaseA) for 1 h at 42°C followed by a standard phenol-chloroform extraction. Extracted DNA was confirmed on an agarose gel and quantified using a Nanodrop 2000 Spectrophotometer (Thermo Scientific).

PCR amplification and metabarcoding

The ITS-2 region (350 bp) was targeted and amplified in each sample using custom primers that incorporated *Symbiodinium* specific ITS-2-dino-forward and its2rev2-reverse regions (Stat et al. 2009; Green et al. 2014; Quigley et al. 2014). Each primer was constructed with a universal linker, which allowed for the downstream incorporation of Illumina specific adapters and barcodes during the second PCR as well as four degenerative bases whose function was to increase the complexity of library composition. The forward primer was 5'-<u>GTCTCGTCGGCTCGG</u> + *AGATGTGTATAAGAGACAG* + NNNN + **CCTCCGCTTACTTATATGCTT**-3' where the underlined bases are the 5'- universal linker, italicized bases indicate spacer sequences, N's denote degenerative bases and the bold bases are the ITS-2-dino. The reverse primer was 5'-<u>TCGTCGGCAGCGTCA</u> + *AGATGTGTATAAGAGACAG* + NNNN + **GTGAATTGCAGAACTCGTG**-3'.

Each 20uL PCR reaction contained 5-100 ng DNA template, 12.4 µL MilliQ H_2O, 0.2 µM dNTPs, 1µM forward and 1µM reverse primers, 1X *Extaq* buffer, and 0.5 U (units) *Extaq* polymerase (Takara Biotechnology). PCR cycles were run for all samples using the following PCR profile: 95°C for 5 min, 95°C for 40 s, 59°C for 2 min, 72°C for 1 min per cycle and a final elongation step of 72°C for 7 min. The optimal number of PCR cycles for each sample was determined from visualization of a faint band on a 2% agarose gel (usually between 22 and 28 cycles) as per Quigley et al. (2014). PCR products were cleaned using GeneJET PCR purification kits (Fermentas Life Sciences) and then a second PCR reaction was performed to incorporate custom barcode-primer sequences (Quigley et al. 2014) modified for Illumina Miseq as in Klepac et al. (2015). Custom barcode primer sequences included 5'-*Illumina adaptor* + 6 bp **barcode sequence** + <u>one of two</u> <u>universal linkers</u>-3' (e.g.: 5'-*CAAGCAGAAGACGGCATACGAGAT* + **GTATAG** + <u>GTCTCGTGGGCTCGG</u>-3', or 5'-*AATGATACGGCGACCACCGAGATCTACAC* + **AGTCAA** + <u>TCGTCGGCAGCGTC-3'</u>). Following barcoding, PCR samples were visualized on a 2% agarose gel and pooled based on band intensity (to ensure equal contributions of each sample in the pool). The resulting pool was run on a 1% SYBR Green (Invitrogen) stained gel for 60 minutes at 90 volts and 120 mAmps. The target band was excised, soaked in 30 uL of milli-Q water overnight at 4°C, and the supernatant was submitted for sequencing to the University of North Carolina at Chapel Hill High Throughput Sequencing Facility across two lanes of Illumina MiSeq (one 2x250, one 2x300). The two lanes produced similar mapping efficiencies (73% and 73%, respectively; Table S3).

Bioinformatic Pipeline

The bioinformatic pipeline used here builds upon previous work by Quigley et al. (2014) and Green et al. (2014). Raw sequences were renamed to retain sample information and then all forward (R1) and reverse (R2) sequences were concatenated into two files, which were processed using CD-HIT-OTU(Li et al. 2012). CD-HIT-OTU clusters concatenated reads into identical groups at 100% similarity for identification of operational taxonomic units (OTUs). Each sample was then mapped back to the resulting reference OTUs and an abundance count for each sample across all OTUs was produced. A BLASTn search of each reference OTU was then run against the GenBank (NCBI) nucleotide reference collection using the representative sequence from each OTU to identify which *Symbiodinium* lineage was represented by each OTU (Table S2).

The phylogeny of representative sequences of each distinct *Symbiodinium* OTU was constructed using the PhyML tool (Guindon and Gascuel 2003; Guindon et al. 2010) within Geneious version 10.0.5 (http://geneious.com) (Kearse et al. 2012). PhyML was run using the GTR+I model (chosen based on delta AIC values produced from jModelTest (Guindon and Gascuel 2003; Darriba et al. 2012)) to determine the maximum likelihood tree. The TreeDyn tool in Phylogeny.fr was used to view the tree (Fig 2) (Chevenet et al. 2006; Dereeper et al. 2008; Dereeper et al. 2010). The reference sequences included in the phylogeny were accessed from GenBank (Table S6).

Statistical Analysis

OTU abundance analysis used the R (Team 2017) package *MCMC.OTU* and followed methods described in Green et al. (2014). First, outlier samples with low sequence coverage

(total log counts ≥2.5 standard deviations below the mean of all samples) were identified and removed, which removed 3 samples. Next, rare OTUs (<0.1% of the global sum of counts (as per Quigley et al. 2014)) were identified and discarded leaving 56 of the original 5,132 OTUs. Many remaining OTUs were identified as having the same *Symbiodinium* lineage (i.e., C1 or D1a) and these OTUs were regressed against one another. Positive correlations between OTUs within a lineage may indicate paralogous loci from the same genome (Kenkel et al. 2013b; Green et al. 2014). As a result, reads from OTUs within the same lineage that showed a positive R^2 and significant *p*-value following linear regression were pooled in order to control for possible overestimation of biodiversity (Thornhill et al. 2007). Pooling resulted in a final OTU table containing ten OTUs (Table S2). Raw reads, trimmed reads, mapped reads, and percentage of reads mapped per species were calculated and reported in Table 2. Final pooled OTUs were run through the MCMC.OTU package in R and fit to a model that included fixed effect for host species, collection site, and thermal regime (Table S4). Differences between fixed effects were calculated based on their sampled posterior distributions and statistical significance was calculated as per Matz et al. (2013). OTU count data were converted to relative abundances (%), which were used to generate Fig 3 (Table S5).

To visualize differences in symbiont communities between temperature regimes, latitude, and species, principal component analyses (PCA) were performed on all OTUs that passed filtering using the *vegan* package in R (Oksanen et al. 2013). Count data were transformed using Bray-Curtis similarity and were used as input for PCA. PERMANOVA was carried out on each PCA using the *adonis* function of the *vegan* package in R (Oksanen et al. 2013).

Results

Symbiodinium diversity and abundance across the Belize MBRS

Our analysis produced 118,834 unique sequences of which 89,211 mapped to 10 OTUs (Table 1). The dominant OTU (hereafter referred to as lineage) in *S. siderea* was C1.I (74.39%), while B1.I dominated *S. radians* (70.31%) and *P. strigosa* (51.74%) samples (Table S5, Fig 3). Nine out of ten *Symbiodinium* lineages were present in *S. siderea* and *P. strigosa* while all ten were present in *S. radians* (Table S5). The four most abundant lineages in *S. siderea* were C1.I, C1.III, D1a, and B1.I (74.39%, 12.94%, 9.29%, and 2.94%, respectively; Table S5, Fig 3A) and date of collection did not impact the dominate *Symbiodinium* lineages (all samples collected in 2014 except for Belize City high$_{TP}$ which were collected in 2015; Fig 3). *Symbiodinium* D1a (*S. trenchii*) was most abundant in *S. siderea* at low$_{TP}$ sites, particularly the low$_{TP}$ site along the most southern Punta Gorda transect (Table S5, Fig 3A) and lineage C1.III was more abundant in central and northern Belize (Belize City and Dangriga transects) compared to southern Belize (Figs 1, 3). Lineages C1.II, B1.II, G3, A4a, and B.BG were also present in *S. siderea* (Table S5, Fig 3A).

The four most abundant lineages in *S. radians* were B1.I, C1.I, B1.II, and C1.II (70.31%, 13.41%, 6.54%, and 2.19% respectively; Table S5, Fig 3B). B1.I was the dominant symbiont across all thermal regimes and all latitudes, but C1.I and C1.II were the most abundant *Symbiodinium* lineages in several samples from the central Placencia transect (Table S5, Fig 3B). Lineage C1.II was only present in proportions above 1% in 2 samples, both from the mod$_{TP}$ site along the Placencia transect (Table S5, Fig 3B). D1a (*S. trenchii*) was only present in low abundance in *S. radians* (Table S5, Fig 3B). Lineages C1.III, D1a, G3, A4a, B.BG, and C3 were also present in *S. radians* (Table S5, Fig 3B).

The four most abundant lineages in *P. strigosa* were B1.I, C1.I, C1.II, and C1.III (51.74%, 21.87%, 16.92%, and 6.24%, respectively). C1.II was the most abundant lineage at the low_{TP} site in the Placencia transect, but B1.I was most abundant at all other sites (Table S5, Fig 3). C1.I was the second most abundant lineage in mod_{TP} and $high_{TP}$ sites and C1.II was the second most abundant lineage in the low_{TP} site (Table S5, Fig 3C). D1a (*S. trenchii*) was only present in low abundance in *P. strigosa* (Table S5, Fig 3C). Lineages D1a, B1.II, G3, A4a, and B.BG were also present in *P. strigosa* (Table S5, Fig 3C).

Host species specificity in Symbiodinium community composition

Symbiodinium communities differed significantly between *S. siderea* and the other two coral host species (Table S4, Fig 4A, *p*-value=0.001). This difference appears to be driven by higher relative abundances of C1.I and D1a (*S. trenchii*) in *S. siderea* compared to *P. strigosa* and *S. radians* (Fig 3A). Within *S. siderea*, *Symbiodinium* communities varied by thermal regime site, and latitude (Table S4, Fig 4B). *Symbiodinium* communities in *S. radians* and *P. strigosa* did not differ significantly by thermal regime, site, or latitude (Table S4).

Discussion

Host-specificity drives Symbiodinium community composition

This study indicates that *Siderastrea siderea* hosts significantly different *Symbiodinium* communities from *S. radians* and *P. strigosa* on the Belize MBRS (Table S5, Fig 3), providing evidence to support previous findings of high rates of host-specific *Symbiodinium* associations within the Caribbean Sea where at least 62 genetically different *Symbiodinium* have been found and where >50% of *Symbiodinium* lineages have been found in only one coral genus (Finney 2010; Thornhill et al. 2017). This trend contrasts that of the Indo-Pacific where *Symbiodinium* diversity is lower and a few host-generalist *Symbiodinium* associate with many corals (Finney

2010). The three coral species studied here were found to be associated with the two most abundant *Symbiodinium* clades in the Caribbean (LaJeunesse et al. 2003): B1 in *S. radians* and *P. strigosa* colonies and C1 in *S. siderea* (Table S5, Fig 3). These associations are consistent with previous studies that identified the same dominant *Symbiodinium* in these species on the Belize MBRS (Finney 2010). However, our data contrast with findings of other studies on the same species elsewhere in the Caribbean which have identified other dominant *Symbiodinium* lineages in these host species (e.g., C3 and B5a in S. siderea and B5 and C46a in S. radians; Thornhill et al. 2006; Finney 2010). This supports previous evidence for regional endemism within the Caribbean Sea (Thornhill et al. 2009; Finney 2010). *Symbiodinium* clade G, a lineage found in Octocorals (Van Oppen et al. 2005), Foraminifera (Pochon et al. 2001) , and Pacific Porites spp. (Stat et al. 2015), was also observed to be a minor player in the symbiont communities of *S. radians* and *P. strigosa* (Table S5, Fig 3). This results indicates that this clade is present in the Caribbean Sea, however because this clade is not traditionally associated with Scleractinian corals, we cannot be confident that its presence is as a symbiont, a contaminant from the local environment, or that it was ingested as food. Differences in *Symbiodinium* communities between coral host species appear to be driven by the relative abundance of B1 and C1 as well as the presence or absence of D1a (Fig 4A). Presence of multiple lineages of C1 and B1 in this study (Table S2, Table S5) support previous evidence of phylogenetic partitioning, or highly specific lineages, in clades B and C (Santos et al. 2004; LaJeunesse et al. 2005; Finney 2010; Kemp et al. 2015). Interestingly, *Symbiodinium* communities were more similar between *S. radians* and *P. strigosa* than between *S. radians* and *S. siderea,* indicating that members of the same coral genus do not necessarily share a common dominant *Symbiodinium* partner, a phenomenon previously observed in *Siderastrea*

spp. and *Orbicella spp.* across the Caribbean Sea (Finney 2010). Finney et al (2010) show that *S. radians* and *S. siderea* exhibit different dominant *Symbiodinium* in both Belize (B5 vs. C1) and Barbados (B5 vs. C3). A similar trend is seen in *O. faveolata* and *O. annularis* (B17 vs. D1a in Belize and C7 vs. B1 in Barbados) (Finney 2010). These results suggest that *Symbiodinium* communities may not be influenced by coral host genus. Previously, it has been shown that symbiont acquisition strategy does not play a large role in determining *Symbiodinium* communities, however geographic distance and differences in environmental variables between habitats have been proposed as possible drivers of symbiont community composition (Finney 2010; Thornhill et al. 2017). Coral life history strategy (Darling et al. 2012) or energetic demands may also play a role. Future research is needed to better understand this process. Differences in *Symbiodinium* communities between *S. siderea* and *S.* radians/ P. *strigosa* is suggestive that corals species are differentially affected by the environmental gradients sampled here.

Thermal regime affects Symbiodinium community composition in S. siderea, but has no effect on other species

Symbiodinium communities varied significantly across thermal regimes in *S. siderea* (Table S4, Fig 4B), supporting previous evidence that habitat type (Bongaerts et al. 2010) and temperature (Tong et al. 2017) are correlated with differences in *Symbiodinium* associations. *Symbiodinium* communities did not differ significantly across thermal regimes in *S. radians* or *P. strigosa*, possibly due to low sample size at each sampling site for these two coral species (Table 1; Fig 3). *Symbiodinium* communities did not differ between thermal regimes in *S. radians* or *P. strigosa* (Table S4), In this study, only temperature parameters were quantified, yet it is likely that they did not account for all of the variance in *Symbiodinium* communities for any coral host species investigated as other local impacts, such as nutrients, light

availability, and/or sedimentation may play a role (Buddemeier and Fautin 1993; Glynn et al. 2001; Ulstrup and Van Oppen 2003; Baker et al. 2004; Ulstrup et al. 2006; Frade et al. 2008).

Role of local impacts on Symbiodinium communities

It has previously been shown that prevalence of specific *Symbiodinium* types within a coral host species can differ based on local scale environmental parameters such as nutrient loading and turbidity (Kennedy et al. 2016). While these variables were not quantified in this study, chlorophyll-a (*chl-a*), a proxy for nutrient input, has previously been shown to be positively correlated with thermal regime in Belize. Specifically, $high_{TP}$ sites had higher *chl-a* than low_{TP} sites across the Belize MBRS (Baumann et al. 2016). Therefore, a PERMANOVA that shows significant differences in *Symbiodinium* communities between thermal regimes includes a confounding effect of nutrient input (Table S4). Since significant differences in *Symbiodinium* communities occurred between thermal regimes in *S. siderea* only, it is possible that nutrient loading or turbidity played a role in *Symbiodinium* variation within *S. siderea*, but may not have significantly influenced *Symbiodinium* communities in *S. radians* or *P. strigosa*. However, the magnitude of this influence cannot be teased apart from the effect of thermal regime without extensive quantification of nutrient concentrations across the Belize MBRS.

Coral host may play a role in thermal tolerance

In this study, the relative abundance of thermally tolerant *Symbiodinium* D1a (*S. trenchii*) was not associated with inshore reefs as in Toller at al. (2001), marginal reefs as in Hennige et al. (2010) and LaJeunesse et al. (2003), sites exposed to the highest temperatures as in Baker et al. (2004), or sites exposed to the widest range of thermal fluctuations as in Abrego et al. (2009), Fabricius et al. (2004), and LaJeunesse et al. (2010; 2010). Instead, *S. trenchii* was most prevalent at the southern Punta Gorda low_{TP} and mod_{TP} sites (Table S1, S5,

Fig 3). Since *S. trenchii* is often associated with recently bleached and/or recovering corals (Baker 2001; Baker et al. 2004), but can be replaced or outcompeted following recovery (Thornhill et al. 2006), it is possible that a recent bleaching event may have occurred at these sites, however these data are not available. In summer 2014, temperatures at all sites in this study exceeded the published local bleaching threshold of 29.7°C (Aronson et al. 2002b) (Fig S1), yet *S. trenchii* was only the dominant symbiotic partner in eight *S. siderea* samples, all of which were from the same two sites (Punta Gorda low_{TP} and mod_{TP}; Fig 3). The presence of *S. trenchii* in several *P. strigosa* corals taken from the Punta Gorda mod_{TP} site provides additional evidence of temperature stress at these sites (Punta Gorda low_{TP} and mod_{TP}). This result suggests that corals at these sites had either bleached recently or retained *S. trenchii* as a dominant symbiont following past bleaching, possibly as a way to increase thermal tolerance (LaJeunesse et al. 2014). Lower thermal tolerance has been proposed previously for *S. siderea (Castillo et al. 2011b)* and *Orbicella faveolata (Carilli et al. 2009c)* at these sites (Punta Gorda low_{TP} and mod_{TP}) and may be due to nutrients, sediments, and low salinity terrestrial runoff exported from Guatemala and Honduras by currents that wash over this area of the Belize MBRS (Paris and Cherubin 2008; Carilli et al. 2009a; Carilli et al. 2009c). Low abundances of *S. trenchii* at other low_{TP} and mod_{TP} sites corroborates this hypothesis, as estimated thermal stress occurred at all latitudes at roughly the same magnitude (Fig S1). Overall, lack of *S. trenchii* in $high_{TP}$ sites indicates that regardless of warmer and more variable conditions, these three coral species do not associate with this thermally tolerant symbiont. Therefore, presumed increased thermal tolerance at $high_{TP}$ sites may be due to local adaptation of the coral host (Howells et al. 2013; Kenkel et al. 2013b) or strains of *Symbiodinium* (Howells et al. 2012;

Hume et al. 2016). Further research into coral host and symbiont local adaptation would be needed to confirm this hypothesis.

Conclusion

This study demonstrates that *Symbiodinium* communities associated with corals in Belize are dependent on both host species as well as environmental variables. *S. siderea Symbiodinium* communities were divergent from *S. radians* and *P. strigosa* (Fig 3; Fig 4A). Thermal regime played a role in driving *Symbiodinium* community composition in *S. siderea* but not *S. radians* or *P. strigosa*, suggesting that local impacts such as nutrients, sediment, or light availability may also influence *Symbiodinium* communities on the Belize MBRS. Additionally, low abundance of *S. trenchii* in inshore $high_{TP}$ sites indicates thermal tolerance at these sites must be conferred through alternative mechanisms, such as local adaptation.

Tables

Transect	Thermal regime	Collection Date	Lat (°N)	Long (°W)	SSID	SRAD	PSTR
Belize City	Low	Nov 2014	17.64363	88.0264	n=10	---	---
Belize City	High	Oct 2015	17.48685	88.1207	n=10	---	---
Dangriga	Low	Nov 2014	17.078	88.01285	n=9	---	---
Dangriga	High	Nov 2014	16.79491	88.27699	n=10	---	---
Placencia	Low	Nov 2014	16.45816	88.01295	n=7	n=7	n=5
Placencia	Mod	Nov 2014	16.49995	88.16527	n=6	n=7	n=6
Placencia	High	Nov 2014	16.4654	88.31315	n=9	n=9	n=5
Sapodilla	Low	Nov 2014	16.15729	88.25073	n=8	---	---
Sapodilla	Mod	Nov 2014	16.13013	88.33234	n=6	---	n=6
Sapodilla	High	Nov 2014	16.2245	88.62943	n=8	n=6	---

Table 1: Sampling locations and sample size for *S. siderea* (SSID), *S. radians* (SRAD), and *P. strigosa* (PSTR). Locations are listed in order of descending latitude (Northernmost to Southernmost). '-' represent an instance where sample size is equal to zero (n=0).

Species	Raw reads	Trimmed reads	Mapped reads	Mapping efficiency
S. siderea	46161	28453	22048	73%
S. radians	51081	46812	35290	75%
P. strigosa	88888	43928	31873	69%
Total	186130	118834	89211	75%

Table 2: Average number of raw reads, trimmed reads, and mapped reads including mapping efficiency (% of trimmed reads that mapped) for each species.

Figures

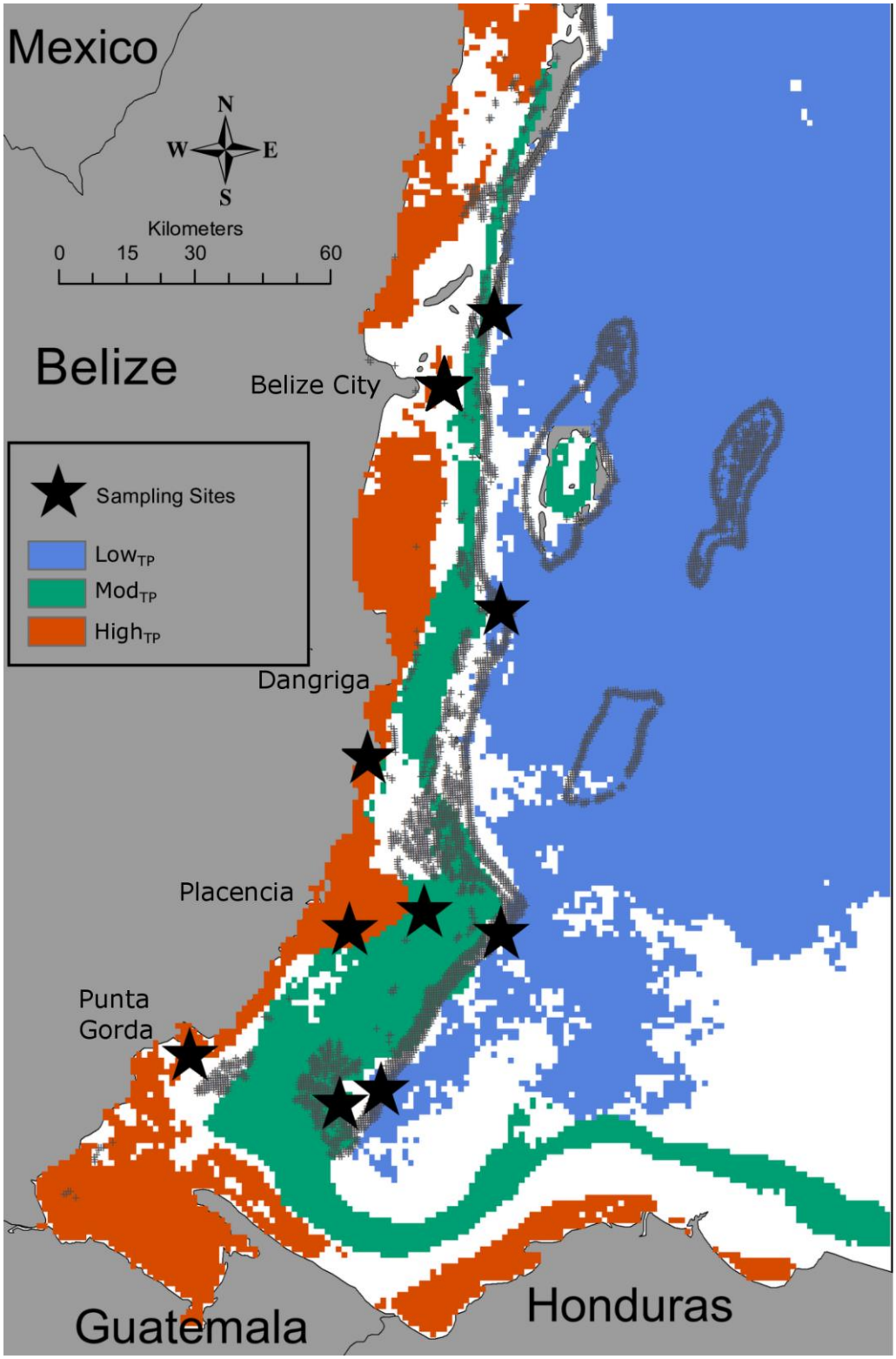

Fig 1: Thermal regime designations for sampling sites on the Belize MBRS (Baumann et al. 2016). Stars indicate sites where coral tissue samples were collected for *Symbiodinium* community analysis. Low$_{TP}$, mod$_{TP}$, and high$_{TP}$ are defined based on combined averages of annual maximum temperature, annual temperature range, annual days above the bleaching threshold, and annual longest streak of

consecutive days above the bleaching threshold. Low_{TP} sites exhibit the lowest values for all parameters measured and $high_{TP}$ sites exhibit the highest. A more detailed description of classification of these thermal regimes can be found in Baumann et al. (2016).

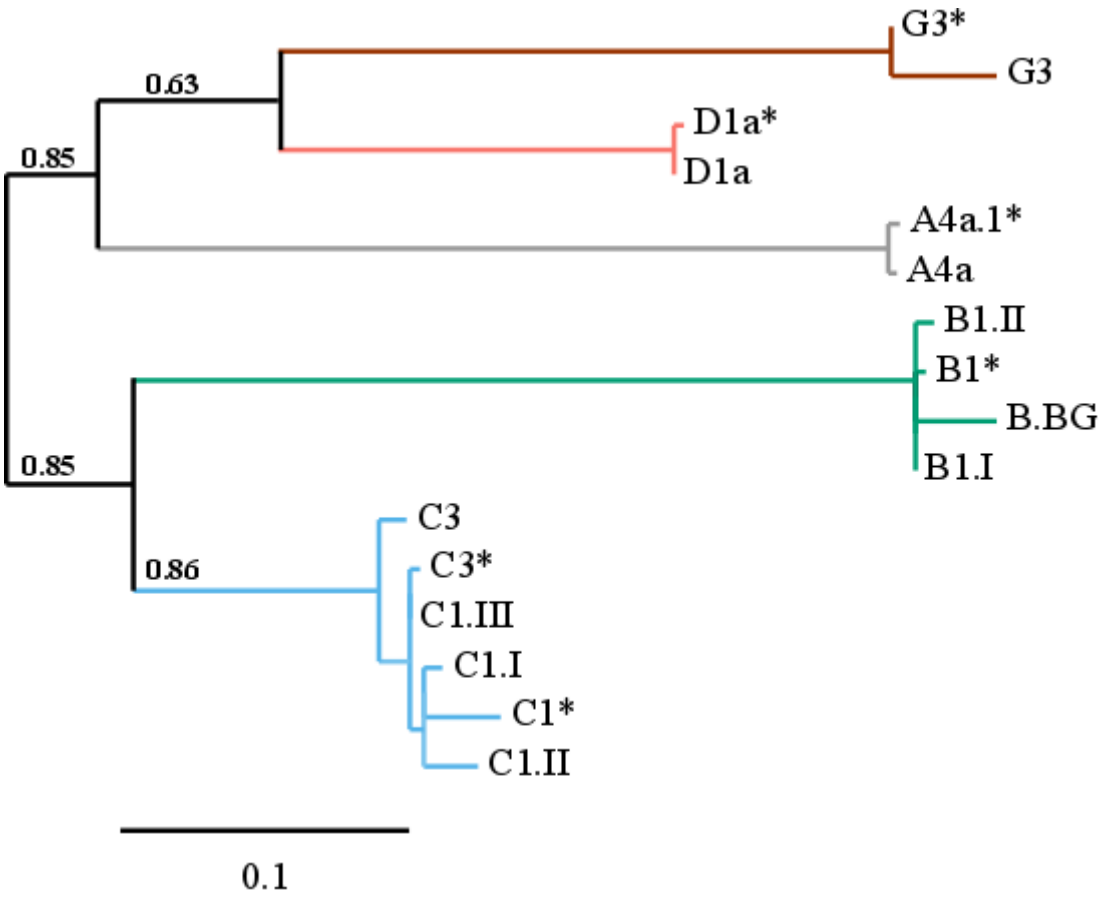

Fig 2: Phylogenetic analysis of ITS-2 sequences of representative OTUs from this study in addition to reference sequences for each clade (indicated by *). Branch support values are shown on the branches at divisions between distinct clades. The scale bar represents replacements per nucleotide site.

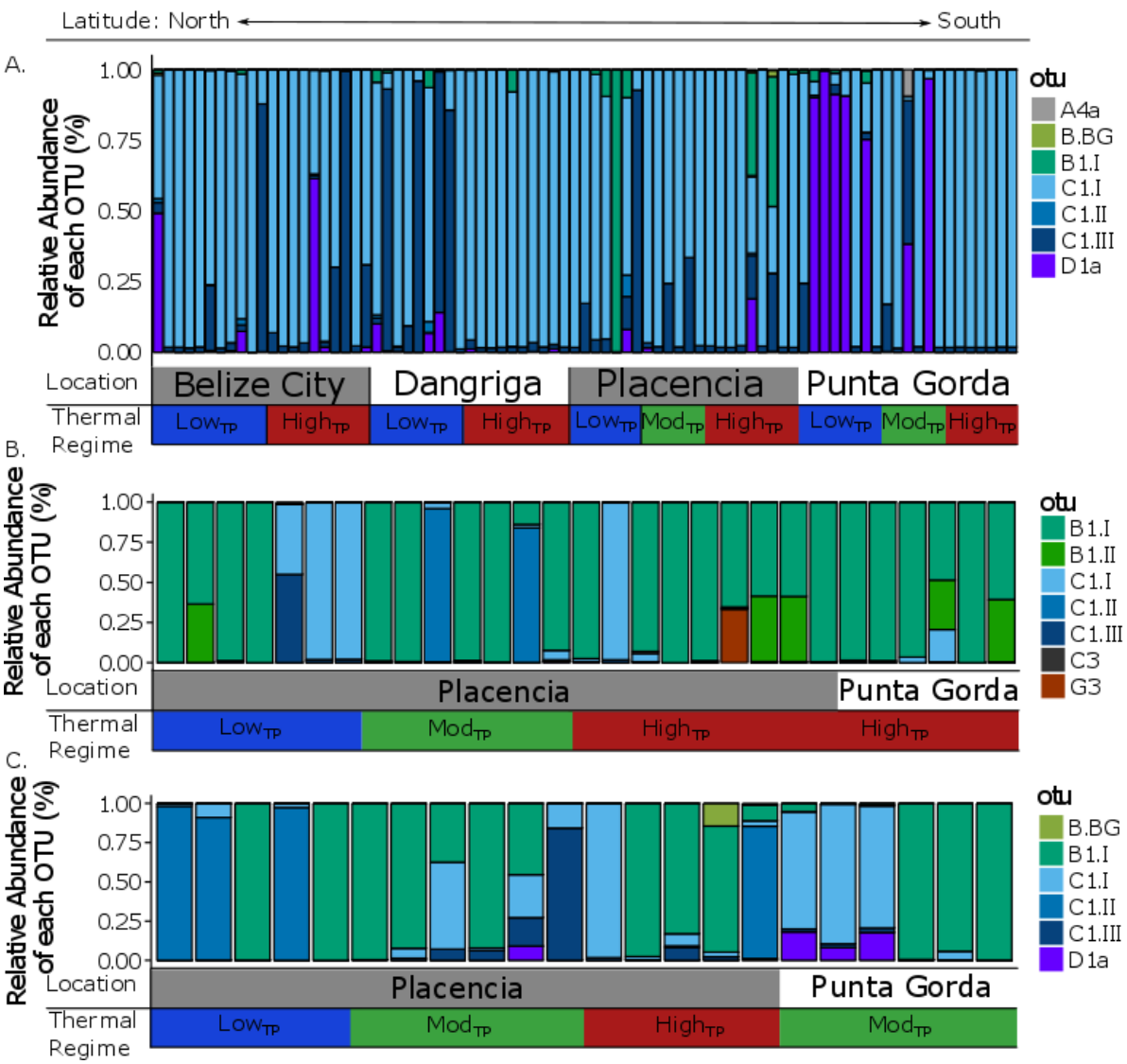

Fig 3. Relative abundance (%) of each OTU (lineage) in *S. siderea* (A), *S. radians* (B), and *P. strigosa* (C). Each column represents an individual sample. Columns are arranged by latitudinal transect (as indicated by site names in alternating gray and white boxes) and then by thermal regime (blue boxes indicate low$_{TP}$ sites, green boxes indicate mod$_{TP}$ sites, and red boxes indicates high$_{TP}$ sites.

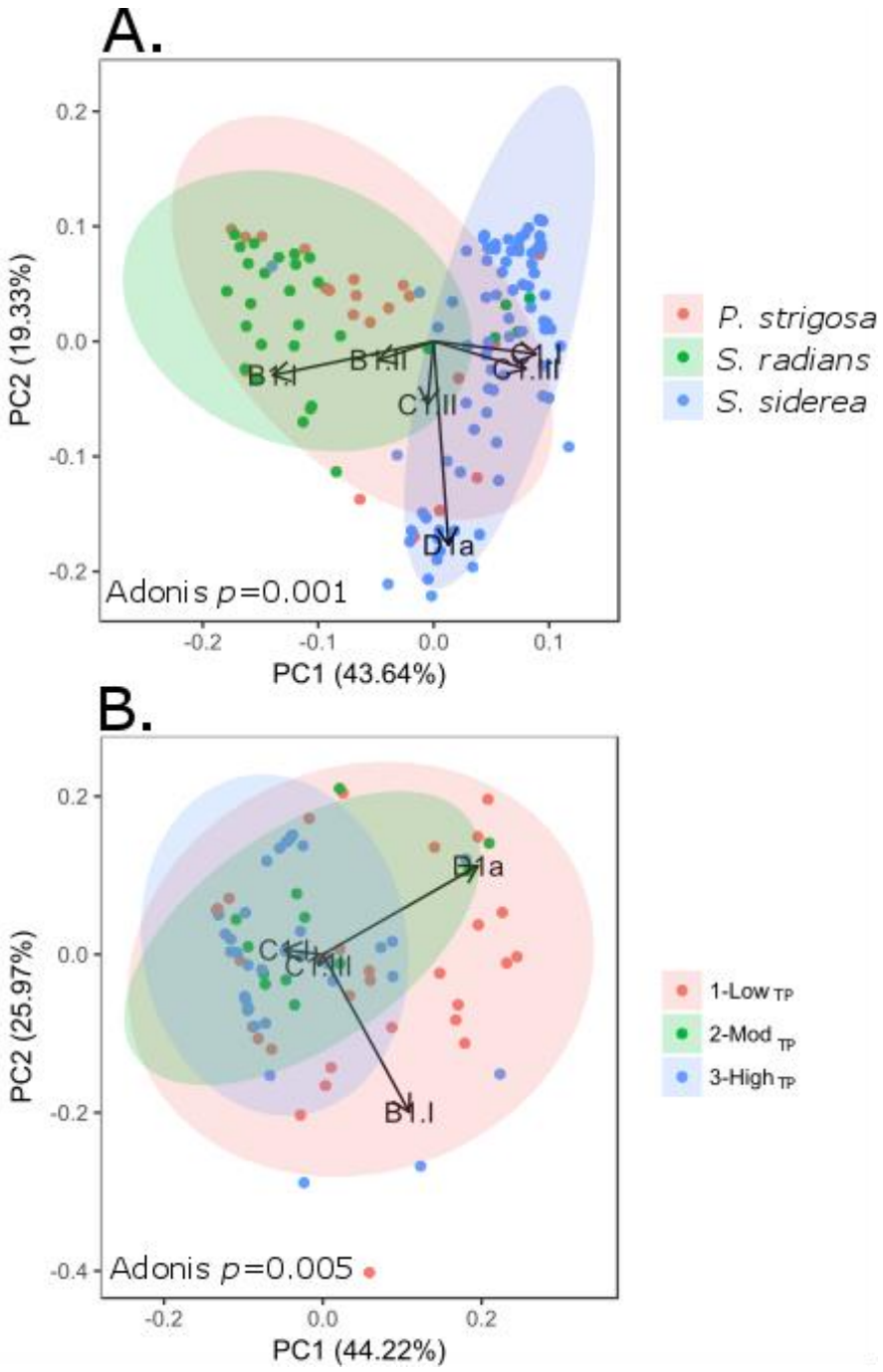

Fig 4. Principal component analysis (PCA) plots of *Symbiodinium* communities by species (A) and by thermal regime for *S. siderea* (B). Percentages on each axis indicate the amount of variation explained by each axis. Adonis *p-values* indicate significant results of PERMANOVA tests. See Table S4 for additional PERMANOVA results. Black arrows indicate loadings showing the magnitude and direction of the effect of each OTU on the total variance. Colored ellipses indicate 95% confidence intervals.

CHAPTER 4: NEARSHORE CORALS ON THE MESOAMERICAN BARRIER REEF SYSTEM ON PACE TO CEASE GROWING AS EARLY AS 2110

Introduction

Global oceanic change has impacted marine ecosystems worldwide (Walther et al. 2002), causing range expansions (Elmhagen et al. 2015), habitat contractions(Smale and Wernberg 2013), decreased productivity (O'Reilly et al. 2003), pest outbreaks(Kurz et al. 2008), phase shifts (Connell and Russell 2010), and alterations in ecosystem structure and function (Knowlton 2001; Hoegh-Guldberg and Bruno 2010). In tropical oceans, sea surface temperatures (SST) have increased by up to 1° C over the past century (Deser et al. 2010). As corals inhabiting tropical oceans already live near their thermal maximum (Glynn 1993), even small increases in ocean temperature can have dire consequences for their health and viability. Increased seawater temperature is the primary cause of widespread coral bleaching—a phenomenon in which the obligate coral-algal symbiosis essential for the survival of reef-building corals breaks down, resulting in a white or 'bleached' appearance (Jokiel and Coles 1990). Mass coral bleaching events have caused significant coral mortality across reef ecosystems globally (Hughes et al. 2017a). These mass bleaching events are of particular concern in the Caribbean Sea, where seawater temperature has increased at higher rates than in other tropical basins (Chollett et al. 2012a). This warming has caused coral cover to decrease by up to 80% in recent decades (Gardner et al. 2003), declines in the structural complexity of local reefs (Alvarez-Filip et al. 2009), and previously dominant, massive, long-lived coral species to be replaced by smaller short-lived species (Green et al. 2008). If present warming

trends continue, bleaching events on Caribbean coral reefs are predicted to increase in both frequency and severity, potentially occurring every two years as soon as 2030 (Donner et al. 2007a) and annually by 2040 (Van Hooidonk et al. 2015b). This increased rate of bleaching, triggered by exposure to more intense, frequent and/or prolonged thermal stress, is predicted to negatively impact rates of coral growth and survival even in more thermally tolerant species.

Coral growth response to temperature has been shown to be parabolic (Pratchett et al. 2015). Moderate increases in temperature below the thermal maximum promote coral growth (Lough and Barnes 2000; Pratchett et al. 2015), while temperature increases above the thermal maximum cause coral growth to decline (Pratchett et al. 2015). The duration of corals' responses to thermal stress can vary based on local factors, as coral growth rates on reefs with higher local stress have been shown to recover to pre-stress growth levels slower than conspecifics from reefs with lower local stress (Carilli et al. 2009c). Nevertheless, more sustained decreases in skeletal extension and calcification have been attributed primarily to ocean warming (Lough and Barnes 2000), independent of other local stressors.

Irrespective of cause, declining coral growth rates may increase the incidence of post-settlement mortality in young corals by increasing the duration of exposure to size-specific agents of mortality (Pratchett et al. 2015). As a result, the dominant species of Caribbean coral reefs should continue to shift from fast-growing and structurally complex corals (e.g., *Acropora* sp.) to smaller, fast-growing species (Green et al. 2008) (e.g., *Porites* sp.) and larger, slow-growing, domical, stress-tolerant species (e.g., *S. siderea*) (Alvarez-Filip et al. 2013). Such shifts in community structure, coupled with decreasing growth rates of surviving corals and increased juvenile mortality, may reduce structural complexity of reefs and decrease rates of gross community calcification. If gross community calcification fails to exceed gross $CaCO_3$

dissolution, this will lead to net community dissolution, degradation of the physical reef structure, and collapse of the reef ecosystem that relies upon this structure (Alvarez-Filip et al. 2013; Pratchett et al. 2015). Although thermal stress is known to be one of the most negative stressors impacting rates of coral calcification and skeletal extension, coral growth is also impacted by disease, changing ocean chemistry (e.g., ocean acidification), eutrophication, increased sedimentation, food availability, storm activity, and other anthropogenic and non-anthropogenic stressors (Pratchett et al. 2015).

Sedimentation and nutrient loading, shown to negatively impact coral skeletal growth parameters (Dodge et al. 1974; Tomascik 1990), are often higher on nearshore reefs than on offshore reefs due to proximity to land—the ultimate source of sediments and nutrients (Dodge et al. 1974; Heyman and Kjerfve 1999). For example, nearshore massive *Porites* sp. corals on the Great Barrier Reef (GBR) have exhibited decreasing growth rates since 1930, while growth rates in offshore and mid-channel reefs have remained relatively stable (D'Olivo et al. 2013). Conversely, *Orbicella annularis* corals exhibited elevated skeletal extension rates in less turbid waters in Jamaica (Dodge et al. 1974), as did *Porites* spp. in Indonesia (Tomascik 1990), suggesting that higher water quality supports higher rates of coral growth. However, growth rates of *O. annularis* in Mexico (Carricart-Ganivet and Merino 2001) and *Porites* spp. on the GBR (Lough et al. 1999) are reported to be higher in more turbid waters. Furthermore, in areas of the Florida Keys, nearshore corals exhibited higher growth rates than offshore corals despite their exposure to higher levels of local stress (Lirman and Fong 2007).

Elevated and/or increasing growth rates on nearshore reefs with generally lower water quality may be driven by historical exposure to greater temperature variability, which has been shown to confer resilience to corals exposed to anthropogenic thermal stress (Carilli et al.

2012). Notably, in southern Belize, forereef *S. siderea* corals exhibited declining skeletal extension over the past century, while skeletal extension of nearshore and backreef corals remained relatively stable (Castillo et al. 2011a). Declining skeletal extension in forereef *S. siderea* was correlated with increasing SST, while skeletal extension for backreef and nearshore corals was uncorrelated with SST, suggesting that forereef corals are more vulnerable to thermal stress. The authors attributed this to the fact that forereef corals were historically exposed to less diurnal and seasonal thermal variability, and therefore could be less adapted for anthropogenic warming than backreef and nearshore corals (Castillo et al. 2012).

These differences in historical extension rates in nearshore, backreef, and forereef corals highlight the geographic variability in corals' response to warming and raise questions about the ultimate driver (s) (e.g., nutrients, sedimentation, and history of thermal exposure) of this variability. Understanding the role that these factors play in corals' response to ocean warming will provide insight into corals' ability (or inability) to maintain localized ecosystem function as the oceans continue to warm. This should allow for improved, site-specific management of coral reef ecosystems during this interval of rapid global change.

Here, we investigate the geographic variability of two scleractinian coral species' response to warming throughout the Mesoamerican Barrier Reef System (MBRS). Century-scale skeletal extension rates were quantified for two abundant and widely distributed massive Caribbean reef-building corals—*Siderastrea siderea* and *Pseudodiploria strigosa*—across numerous nearshore-offshore (i.e., nearshore-backreef-forereef) transects of the Belize MBRS. These transects were selected to represent stress gradients, decreasing from nearshore-to-offshore, because corals in nearshore habitats are exposed to higher summer temperatures, increased thermal variability (diurnal and seasonal), more days per year above the bleaching

threshold (Baumann et al. 2016), elevated nutrients (vis-à-vis chlorophyll-a) (Baumann et al. 2016), and greater local anthropogenic stress (e.g., sedimentation, pollution) than offshore corals (backreef, forereef, atolls) due to their proximity to mainland Belize (Heyman and Kjerfve 1999; Carilli et al. 2010).

A total of 134 coral cores were extracted from 19 reef sites across numerous inshore-offshore transects along the entire *ca.* 300 km Belize portion of the MBRS. Colonies of *S. siderea* were sampled from five distinct reef environments (nearshore, backreef, forereef, atoll backreef, atoll forereef) while *P. strigosa* colonies were sampled from two reef environments (nearshore, forereef; Fig. 1). Skeletal extension rates were reconstructed from the thickness of annual high-low density bands identified via X-ray computed tomography (CT). Because skeletal extension rates in both species were strongly linearly correlated with CT-derived calcification rates, the investigation was confined to the skeletal extension data. These data were evaluated for reef-zone differences in annual coral extension rate, slope of coral extension vs. time, and correlation with mass-bleaching events.

Materials and Methods

Site Description

This research was conducted along the coast of the Belize portion of the Mesoamerican Barrier Reef System (MBRS)—a 1,200 km network of reefs in the western Caribbean sea extending south from the tip of the Yucatan Peninsula in Mexico, traversing the entire coast of Belize and the Atlantic coast of Guatemala, and culminating in the Islas de la Bahia (Bay Islands) off the coast of Honduras (Fig 1).

Extraction of coral cores

A total of 134 coral cores (93 *S. siderea* and 31 *P. strigosa*) were collected from 19 sites along the Belize MBRS in 2009, 2012, and 2015 (Table S3). All *P. strigosa* cores were collected in 2015. Thirty-seven *S. siderea* cores were collected in 2015, while the remaining 56 *S. siderea* cores were collected in 2009 and 2012. Cores were obtained from five different reef zones (nearshore, backreef, forereef, atoll backreef, atoll forereef) (Fig 1). Backreef, forereef, atoll backreef, and atoll forereef are referred to collectively as offshore reefs. Nearshore coral cores were obtained from within 10 km of the coast of Belize at 4 different latitudes. Backreef and forereef coral cores were obtained on the shoreward and seaward sides of the reef crest, respectively. Corals were transported back to UNC Chapel Hill and CT scanned whole in order to quantify skeletal density, extension, and calcification (see supplementary methods for CT procedures).

Skeletal density, extension, and calcification

Siderastrea siderea and *P. strigosa* are known to deposit one low-density and one high-density growth band per year (seasonally) (Guzman and Tudhope 1998; Helmle et al. 2000). Semi-annual density bands were visualized on 8-10 mm thick "slabs" of stacked images (0.6 mm slices) using "mean" projection mode. Mean projection mode utilizes the mean density of each pixel within the 8-10 mm slab, in contrast to min projection mode that uses the minimum density at that pixel within the slice, and maximum projection mode that uses the maximum density (Carilli et al. 2017). Each annual band pair was demarcated using the "length" tool (ROI drawing tool) in Osirix. Annual linear extension rates for cores were estimated from the thickness of high-density and low-density annual couplets for each core

either using the applet RUNNINGCORALGUI (for cores from 2009 and 2012) or manual delineation (see supplementary methods). Three sets of linear transects were drawn down the length of the cores using the ROI tool in Horos. The linear extension of each seasonal light and dark band was then quantified from the total length of the line tool data in pixels, which was then converted to cm.

Extension, density, and calcification rate were quantified for all corals collected in 2015 (38 *P. strigosa* and 37 *S. siderea*), while only extension was quantified for corals collected in 2009 and 2012 (56 *S. siderea*). Density and calcification rate (calculated from linear extension and density) were not available for cores collected prior to 2015 because the cores were slabbed and sampled for geochemical analysis before they could be CT-scanned with an appropriate density standard. Density of cores collected in 2015 was determined as described above. Corals were oriented with the growth axis parallel to the length of the scanning table to decrease impacts of beam-hardening on density.

Statistical Analyses

Statistical analyses were performed on individual *S. siderea* and *P. strigosa* core chronologies rather than on a single master chronology for corals from different sub-environments of the reef system (Castillo et al. 2011a). This statistical approach was employed to address the inherent hierarchical nature of coral skeletal growth data. Although all three skeletal growth parameters (skeletal density, extension rate, calcification rate) were quantified for the cores collected in 2015, we focus here on annual skeletal extension because extension is highly correlated with calcification rate (i.e., annual skeletal density does not vary with time; (Fig S1; Lough and Barnes 1997,2000; Pratchett et al. 2015).

Annual skeletal extension rates within a core are inevitably highly correlated across time and therefore are not independent observations, but are approximately independent amongst different cores within the same reef sub-environment. A linear regression of annual skeletal extension with time was achieved by fitting a set of mixed effects models that treated the individual core as a structural variable (Tables 1, S4, supplementary methods). A residual temporal correlation structure was employed to determine if random effects adequately accounted for the correlation over time. To assess the need for random effects, the method of generalized least squares was employed to fit a corresponding set of models with residual correlation structures but without random effects. The use of mixed effects and time series methods to model coral skeletal growth data correctly distinguishes observational units from sampling units, recognizes that sampling variation exists both within and between core time series records, and addresses the temporal autocorrelation structure that is inherently present in such data. The use of mixed effects and time series methods also properly accounts for data imbalance—the fact that some cores provide a longer time series of annual skeletal extension than others. Further information on model testing is available in the supplementary methods.

Declining skeletal extension rates for nearshore corals

The slopes of the annual skeletal extension rates vs. time for nearshore *S. siderea* from the late 19th century to present (Fig. 2A, B) and nearshore *P. strigosa* from the mid-20th century to present (Fig. 3A, B) were significantly negative (*p*-values <0.001; Table S1), indicating declining rates of skeletal extension for both coral species on nearshore reefs on the Belize MBRS. In contrast, *S. siderea* and *P. strigosa* colonies from the backreef, forereef, atoll backreef, and atoll forereef (collectively defined as "offshore" because of their >30 km

distance from mainland Belize) exhibited relatively stable rates of skeletal extension through time (Fig. 2A, B).

Declining skeletal extension rates for nearshore *S. siderea* and *P. strigosa* corals may be driven by increasing seawater temperatures on nearshore reefs (Carilli et al. 2012; Pratchett et al. 2015), although local stressors such as eutrophication and sedimentation may have also played important roles (Fabricius 2005; Wiedenmann et al. 2013). Nearshore reefs on the Belize MBRS are exposed to warmer summers and more variable water temperatures than their offshore counterparts, and are subject to greater intervals when temperatures are above the regional bleaching threshold (Castillo et al. 2012; Baumann et al. 2016). Additionally, the average SST across all reef zones of the Belize MBRS has increased since 1880 ($p<0.01$; Fig. S2A) and average summer SST across this reef ecosystem has increased by approximately 0.5°C since 1985 (Castillo et al. 2012). However, moderate increases in temperature (below a coral's thermal optimum) have been shown to increase coral growth rates (Castillo et al. 2014; Pratchett et al. 2015), which may partially explain why nearshore corals exhibit faster growth down-core (i.e., when seawater temperatures were still below the corals' thermal optimum) than their offshore counterparts in the present study (Fig. 2C; Fig. 3C).

Although temperature increases up to and slightly beyond a coral species' thermal optimum can increase coral skeletal growth rates (Pratchett et al. 2015), temperatures surpassing this thermal optimum by more than a degree have been shown to negatively impact coral growth (Lough and Cantin 2014; Pratchett et al. 2015). This negative impact of elevated temperature on coral skeletal growth rate is driven not only by the magnitude of the warming, but also by its duration (Pratchett et al. 2015). Century-scale declines in skeletal extension rates of nearshore colonies along the Belize MBRS and relatively stability in extension rate of

backreef and forereef colonies (Fig. 2; Fig. 3) suggest that a critical threshold of thermal stress (e.g., frequency and/or intensity) may have been exceeded for nearshore *S. siderea* and *P. strigosa* corals, but not for forereef and backreef colonies.

The authors are not aware that a thermal optimum has been established for *P. strigosa*; however, Castillo et al (2014) identified a thermal optimum for *S. siderea* in the range of 28 ºC. Furthermore, a regional bleaching threshold (always warmer than a species' thermal optimum) of 29.7 °C has been identified for various species of corals across the Belize MBRS (Aronson et al. 2002b). Although corals at all sites on the Belize MBRS are exposed to temperatures above this threshold each year, nearshore reefs on the Belize MBRS are exposed to between 54 and 78 days per year above the bleaching threshold of 29.7 °C, with sustained intervals above the bleaching threshold lasting up to 7.5 consecutive days. In contrast, offshore reef sites experience only 20 to 40 days above the bleaching threshold annually, with sustained intervals above the bleaching threshold lasting fewer than 4.8 consecutive days (Baumann et al. 2016).

These observations, combined with the observation that extension rates on nearshore reefs have been declining over the past century while extension rates for offshore reefs have been relatively stable over the past century, suggest that the thermal threshold for temperature-related declines in coral growth lies somewhere between temperatures at these two reef locations. Alternatively, other environmental factors, such as ocean acidification, eutrophication, and/or sedimentation, may be driving the negative growth trends observed for nearshore reefs, but not for offshore reefs, of the Belize MBRS (Pratchett et al. 2015).

Previous work has demonstrated that poor water quality impairs coral growth rates on nearshore reefs (D'Olivo et al. 2013). Specifically, coral calcification rates on nearshore reefs

of the GBR are declining on multi-decadal timescales, while calcification rates on offshore reefs are increasing. This declining growth on nearshore reefs is attributed to the impacts of wet season river discharge of sediment and nutrients, a trend that is exacerbated by warming (D'Olivo et al. 2013). In the present study, it is possible that increasing nutrient and sediment loading (Heyman and Kjerfve 1999; Thattai et al. 2003), coupled with increasing water temperatures and duration of time when water temperatures exceed the species' bleaching threshold, are responsible for the decline in skeletal extension rates observed on nearshore reefs of the Belize MBRS.

In Belize, human population densities have increased 39% in coastal cities and agricultural land area has quadrupled since the mid-21st century (Fig. S2B, C). It is therefore likely that runoff and eutrophication in nearshore environments of the MBRS have also increased over time (Heyman and Kjerfve 1999; Carilli et al. 2009a). This increase in runoff and eutrophication should impact water quality more negatively at nearshore reefs than at offshore reefs that are further from the pollution source(Heyman and Kjerfve 1999). If temperature and eutrophication continue to increase, nearshore coral growth rates should continue to decline—with offshore corals potentially following suit as these stressors impact more distal portions of the Belize MBRS. Although there is metagenomic evidence that nearshore *S. siderea* and possibly *P. strigosa* have begun acclimatizing to these elevated temperatures (Davies et al. 2017), the observation that skeletal extension rates have continued declining for both species up to present time in nearshore reefs of the MBRS indicate that such acclimatization within nearshore corals is insufficient for maintaining stable rates of skeletal growth amidst the deteriorating environmental conditions of nearshore environments.

Further evidence of the combined effects of warming and local stress on nearshore coral skeletal extension is observed at the southernmost nearshore site in the present study. At this location, *S. siderea* cores were extracted from two nearshore reefs, one nearer to the coast at Sheepshead Caye (6 km from mainland Belize; point A in Fig. 1) and one further from the coast at Snake Cayes (13 km from mainland Belize; point B in Fig. 1). The cores collected from Snake Cayes (farther from mainland; NS14, NS15, NS16) exhibited the lowest skeletal extension rates of any nearshore core analyzed in the present study (Table S7; Table S8; Fig. S3), but did not exhibit declining skeletal extension rates with time (Castillo et al. 2011a), while those from Sheepshead Caye (closer to mainland) did exhibit declining skeletal extension rates with time.

Corals from Sheepshead Caye were exposed to warmer and more variable temperatures, on average, than corals from Snake Cayes (Baumann et al. 2016), and since corals from Sheepshead Caye are nearer to the mainland, it is likely that they are subject to greater eutrophication and sedimentation than corals from Snake Cayes (Fig. S2). The impacts of higher temperature, greater thermal variability, increased sedimentation, and/or eutrophication appear to have combined to cause declining skeletal extension rates at Sheepshead Caye, while the relatively lower temperature, thermal variability, sedimentation, and/or eutrophication, owing to Snake Cayes' greater distance from the mainland, were insufficient to cause coral growth at that location to significantly decline with time. These shore-distance gradients in skeletal extension trends within nearshore reefs of the southern MBRS recapitulate the regional scale, nearshore-offshore MBRS trend in coral skeletal extension rates, in which extension rates of nearshore corals have declined with time, while

extension rates of offshore (backreef, forereef, atoll) corals have exhibited relative stability with time.

Extension rates of nearshore corals have decreased to the level of offshore conspecifics

Nearshore *S. siderea* and *P. strigosa* exhibited higher skeletal extension rates than offshore conspecifics from at least 1990 to 2009 (Table S2; Table 3; Fig. 2C, 3C; *p*-values <0.001). This trend is visually apparent as far back as 1965, but decreasing sample size further back in time diminishes the statistical significance of this relationship (Table S2; Table 3; Fig. 2C, 3C). After 2009, however, skeletal extension rates of nearshore *S. siderea* and *P. strigosa* converge with those of their offshore conspecifics (*p*-values: 0.986 and 0.186, respectively; Table S2; Table 3; Fig. 2C; Fig. 3C) owing to the decline in skeletal extension rates for the nearshore corals.

The results from the present study suggest that warmer and more nutrient-rich nearshore reef environments historically supported higher skeletal extension rates than offshore reef environments (Table S2; Table 3; Fig. 2C; Fig. 3C; Fig. S3). On the Belize MBRS, nearshore reefs have historically experienced higher temperatures than offshore reefs (Baumann et al. 2016) and since warming below a species' thermal optimum can increase coral growth rates (Pratchett et al. 2015), it is not surprising that nearshore corals historically (pre-2010) exhibited higher skeletal extension rates than offshore corals inhabiting historically cooler waters. Furthermore, proximity to shore (i.e., source of nutrients and sediments) dictates that nutrient levels and sediment load are likely higher on nearshore reefs than on offshore reefs (Fig. S2) (Heyman and Kjerfve 1999; Chérubin et al. 2008).

Although decreased light availability from increased turbidity (i.e., elevated suspended sediment, algal blooms) can inhibit coral growth (Fabricius 2005) and nutrient enrichment [and subsequent altering of nitrogen (N):phosphorus (P) ratio] (Wiedenmann et al. 2013; Rosset et al. 2017) can increase bleaching susceptibility and lead to decreased growth rates (Dodge et al. 1974; D'Olivo et al. 2013), some coral species, including *S. siderea* and *P. strigosa*, metabolize N from ingested sediments and particulates (Mills and Sebens 2004; Mills et al. 2004). This N may augment coral nutrition during intervals of increased sedimentation and eutrophication, potentially mitigating some of the negative impacts of these processes. Additionally, exposure to increased N and P, when coupled with heterotrophic feeding, has been shown to enhance coral calcification, even when the corals are exposed to thermal stress (Ezzat et al. 2015). A combination of enhanced nutrition and elevated temperatures (below the bleaching threshold) may have been responsible for nearshore corals growing faster than offshore corals before 2010 (Fig. 2C; Fig. 3C).

However, the recent convergence of extension rates for nearshore and offshore colonies of *S. siderea* and *P. strigosa* (Fig. 2) suggests that the advantage that nearshore corals appear to have historically had over offshore corals has now been lost, perhaps due to the intense warming, eutrophication, and sedimentation targeting nearshore environments over recent decades (Figs. 2, 3, S2; Table S2; Table 3). These declining trends in skeletal extension may also have significant impacts on the geomorphology of nearshore reef environments, as slowing growth can result in reef-scale flattening and a loss of structural complexity that may impact the ecological function of nearshore reefs (Alvarez-Filip et al. 2009) and may ultimately impair their ability to keep pace with rising sea level.

Recent bleaching events differentially impact corals across reef environments

Mass coral bleaching was documented in the Caribbean in 1997-1998, 2005, 2010, and 2014-2016 (see methods and Donner et al., 2017). The skeletal extension data from the present study was evaluated to determine whether recent mass bleaching events in the Caribbean Sea impacted coral skeletal extension within each reef zone of the Belize MBRS (Andréfouët et al. 2002). Overall, skeletal extension was significantly lower during bleaching years than during non-bleaching years for *S. siderea* ($p<0.001$; Table S6), but not for *P. strigosa*, although there were some bleaching years in which *P. strigosa* exhibited significantly lower extension than during non-bleaching years (Table S5; Fig. 4). These relationships between bleaching and extension did not vary significantly by reef zone for either species (Table S6). However, skeletal extension was anomalously low for *S. siderea* on the forereef and backreef of the atolls during the 1997-1998 bleaching event and on the backreef of the atolls following the 2005 bleaching event (Table S5; Fig. 4), for nearshore *S. siderea* and *P. strigosa* following the 2010 bleaching event (Table S5; Fig. 4), and for nearshore *S. siderea* and forereef corals of both species during the 2014 bleaching event (Table S5; Fig. 4). Notably, anomalously low skeletal extension rates were also observed for some non-bleaching years in both species (e.g., in 1985 for nearshore *S. siderea* and in 1992 for nearshore *P. strigosa*; Table S5; Fig. 4), potentially due to other stressors (e.g. storms, human activity, or sedimentation (Pratchett et al. 2015; Hughes et al. 2017a)) or unreported/small-scale bleaching.

Anomalously low skeletal extension rates for both nearshore and forereef conspecifics in the same year were observed only in *S. siderea* in 2014, indicating that the impact of this bleaching event on growth of this species was more widespread than past bleaching events, possibly resulting from the cumulative impacts of increased temperatures, bleaching, and/or

local stressors in the preceding years. The 2010 bleaching event correlated with low extension for both species in the nearshore reef zone, but not in the other reef zones, demonstrating that the impact of individual bleaching events on coral skeletal extension varied across reef zones, even though the general relationship between all bleaching events and coral extension did not vary significantly across reef zones.

Although single mass bleaching events were correlated with low rates of skeletal extension within some reef zones, no single bleaching event was correlated with low rates of skeletal extension across all reef zones, underscoring the variability in how individual bleaching events impact skeletal extension across coral species and reef environments. Therefore, the declining skeletal extension rates observed on nearshore reefs of the Belize MBRS cannot be confidently attributed to the increasing frequency of mass bleaching events in recent years. Instead, the steady nature of the decline in skeletal extension of the investigated species in nearshore reef environments suggests that it has been caused by the comparably steady increase in seawater temperatures over the same interval, which is also the root cause of the bleaching events themselves. Nevertheless, the increasing frequency of the bleaching events may indeed be exacerbating the deleterious impacts of steady anthropogenic warming on skeletal extension rates in these nearshore reef environments.

Results predict that nearshore colonies of *P. strigosa* will cease growing by year 2110

Extrapolating from historical growth trends, skeletal extension of nearshore *S. siderea* corals of the MBRS is expected to decline by 23% by year 2100 and to cease entirely by year 2374 ± 17, while skeletal extension of nearshore *P. strigosa* of the MBRS is expected to decline by 89% by year 2100 and to cease entirely by year 2110 ± 34. Although both species are considered stress-tolerant (Darling et al. 2012), substantial differences in their historical trends

in skeletal extension suggest that *S. siderea* is more stress-tolerant than *P. strigosa*. Less stress-tolerant corals would naturally be expected to suffer even more depressed extension and to cease growing earlier. Coral reefs are predicted to transition to a state of net dissolution by the end of the present century due to the impacts of ocean acidification on carbonate sediment dissolution, assuming little to no decline in coral calcification (Eyre et al. 2018). Our results suggest that coral calcification on nearshore reefs along the Belize MBRS will decline drastically over the next century, even in the most stress-tolerant species, suggesting that nearshore reef platforms (i.e., living corals and algae plus non-living reef frameworks and sediments) of the MBRS will experience net dissolution well before the end of the century. The resulting degradation of the three-dimensional reef structure and collapse of the associated reef ecosystem will lead to species extirpation and/or extinction, decreasing coral diversity and evenness, reef-flattening, and loss of reef complexity and habitat on nearshore reefs of the MBRS (Alvarez-Filip et al. 2009; Alvarez-Filip et al. 2013).

These predicted declines in coral growth assume that the temporal trends in coral extension observed over the cored interval can be linearly extrapolated into the future, which is predicated on the assumptions that the primary coral stressors (e.g., warming, acidification, eutrophication, sedimentation, pollution) will continue changing at the same rate and that corals' responses to these stressors will be linear. However, continued improvement of local water quality and reduction in global CO_2 emissions (if achieved) have the potential to mitigate some of these projected growth decreases. For example, emissions scenarios lower than or on par with the commitments of the Paris Agreement have been projected to potentially increase or at least maintain stable growth rates for Bermudan corals (Hall et al. 2015). Conversely, further deterioration of water quality and/or acceleration of warming and acidification beyond

rates observed over the cored interval and/or development of synergistic impacts amongst stressors would accelerate future declines in coral extension.

Declining skeletal extension in nearshore corals foretells deterioration of entire MBRS

The results of the present study reveal a clear difference in historical growth trends between nearshore and offshore corals of the Belize MBRS. Nearshore *S. siderea* and *P. strigosa* historically exhibited higher skeletal extension rates compared to their offshore conspecifics (Fig. 2; Fig. 3). This higher growth of nearshore corals was likely driven by historically warmer temperatures—favorable to the extent that they were below the corals' thermal optimum—and lower local environmental stress (Heyman and Kjerfve 1999; Thattai et al. 2003) (Fig. S2), although other factors may have played a role. However, extension rates of nearshore *S. siderea* and *P. strigosa* have now declined to levels similar to their historically slower growing offshore conspecifics owing to seawater temperatures more frequently exceeding the corals' thermal optima and from higher local environmental stress in nearshore environments.

Although skeletal extension trends of offshore corals have exhibited relative stability over the observed interval, the decline in extension rate of nearshore colonies that are presently experiencing sustained thermal stress beyond their thermal optimum may foretell future declines in the growth of offshore colonies once their thermal optima are more consistently exceeded.

Declines in extension of nearshore colonies of both species do not reliably correlate with mass bleaching events—suggesting that the long-term decline in nearshore coral extension cannot be unequivocally attributed to the increasing frequency of mass bleaching

events. Instead, long-term increases in seawater temperature and local stressors (e.g., eutrophication and sedimentation), which are typically more pronounced in nearshore environments owing to their mainland proximity, are the more likely drivers of the observed decline in nearshore coral growth. Any advantage historically conferred to corals by inhabiting the nearshore environment, vis-à-vis thermal acclimation and/or increased heterotrophic uptake of N and/or C in particle-rich nearshore waters, has now been lost.

Furthermore, continued declines in coral growth could lead to complete stoppage of growth by year 2110 for nearshore *P. strigosa* and by year 2370 for nearshore *S. siderea*. Such a scenario would cause baseline dissolution rates of coral skeletons, which have also been shown to increase with warming(Ries et al. 2016), to exceed rates of gross coral calcification. This, coupled with increasing carbonate sediment dissolution (Eyre et al. 2018), would result in the net reef dissolution (i.e., gross dissolution > gross calcification) and eventual collapse and disappearance of nearshore reef structures (Eyre et al. 2014).

Although nearshore corals historically exhibit higher rates of growth than offshore corals, rapid deterioration of environmental conditions in nearshore environments has caused growth rates of nearshore corals to approach those of their offshore conspecifics. Such declines in these and other reef species are reducing the biodiversity, structure, and ecosystem function of the Belize MBRS (Alvarez-Filip et al. 2009; Alvarez-Filip et al. 2013). Continued protection and management of these reefs should include monitoring land use to limit increases in sedimentation and eutrophication of reefs (particularly nearshore reefs), as well as local, regional, and global action to reduce CO_2 emissions and stabilize global temperatures and ocean pH. The rapid and persistent decline in skeletal extension of two species of nearshore corals underscores the urgency of this action, which might afford corals of the Belize MBRS

sufficient time to acclimatize to and, hopefully, survive this interval of rapid climate and oceanic change.

Tables

Species	Reef Zone	Slope	Slope *p-value*
S. siderea	AFR	0.00024	0.599
	ABR	-0.00056	0.141
	BR	0.00013	0.591
	FR	-0.00030	0.182
	NS	-0.00108	**<0.001**
P. strigosa	FR	-0.00183	0.329
	NS	-0.00755	**<0.001**

Table 1: Slope of extension rate by reef zone from linear mixed effects models by species and time scale. Significant *p-values* ($p<0.05$) are in bold and indicate a difference from zero. 95% confidence intervals (CI) that do not overlap indicate significant differences between reef zones (see Fig 2, 3, S2, S3).

Figures

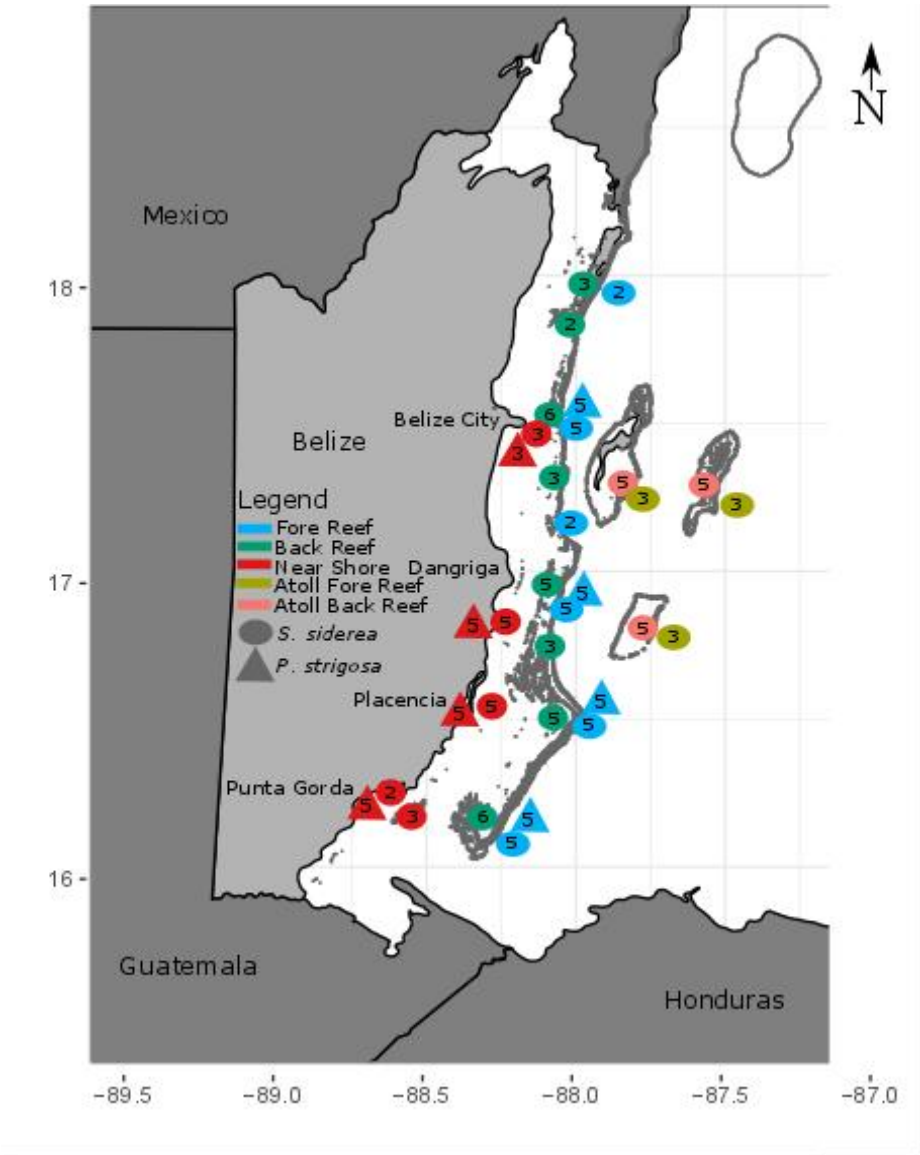

Fig 1: Map of reef sites on the Belize Mesoamerican Barrier Reef where *Sidereastrea siderea* and *Pseudodiploria strigosa* cores were extracted in 2009, 2012, and 2015. Circles and triangles represent core extraction sites for *S. siderea* and *P. strigosa*, respectively. Colors denote reef zone (nearshore = red, backreef = green, forereef = blue, atoll backreef = pink, and atoll forereef = yellow). Numbers denote total cores extracted for a particular species at a specific site.

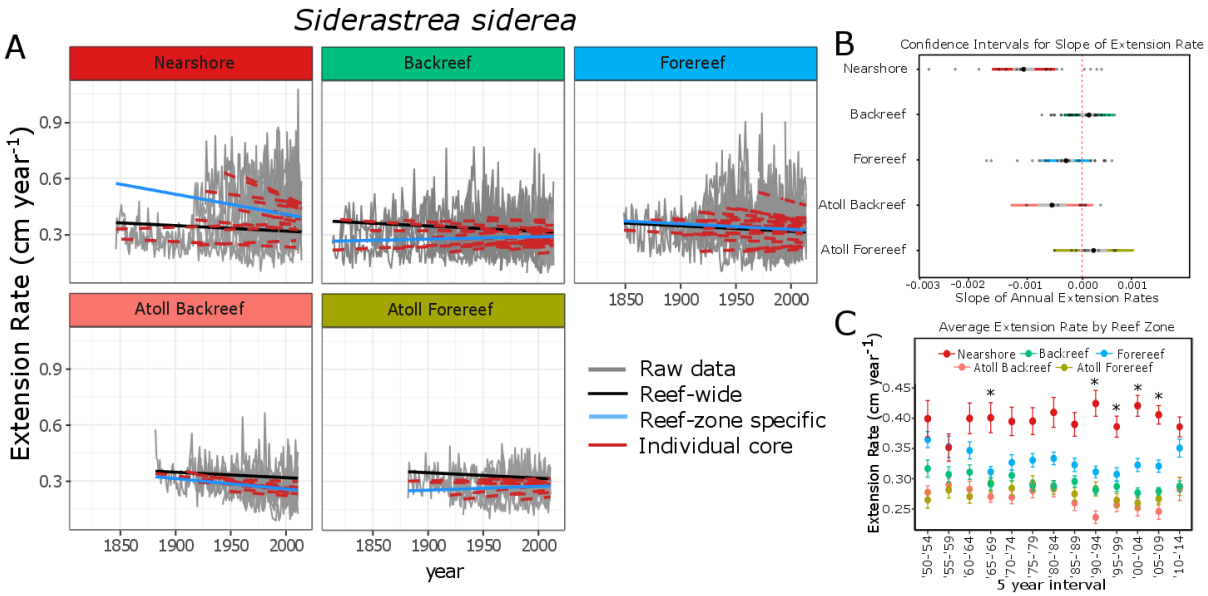

Fig 2: (A) Results of linear model of extension rate (cm year^{-1}) for *S. siderea* by reef zone for the 1814-to-present interval. Gray lines are raw extension data, black lines are average linear models of extension for all *S. siderea* cores across all reef zones, blue lines are average linear models of extension for all *S. siderea* cores within each reef zone, and red lines are linear models of extension for individual *S. siderea* cores within reef zones. (B) Slopes of linear models describing extension vs. time for each reef zone, with small points representing individual cores and large points representing average slopes of all cores within a reef zone (gray bars and colored bars are 50% and 95% confidence intervals (CI), respectively, of average slope for each reef zone). Slopes are significantly different from each other if their 95% CI do not overlap. Likewise, slopes are significantly different from zero if their 95% CI do not overlap with the red dashed 0 line. (C) Five-year averages of skeletal extension rate by reef zone ± 1 SE. Asterisks indicate statistically significant differences ($p < 0.05$) between nearshore and forereef values.

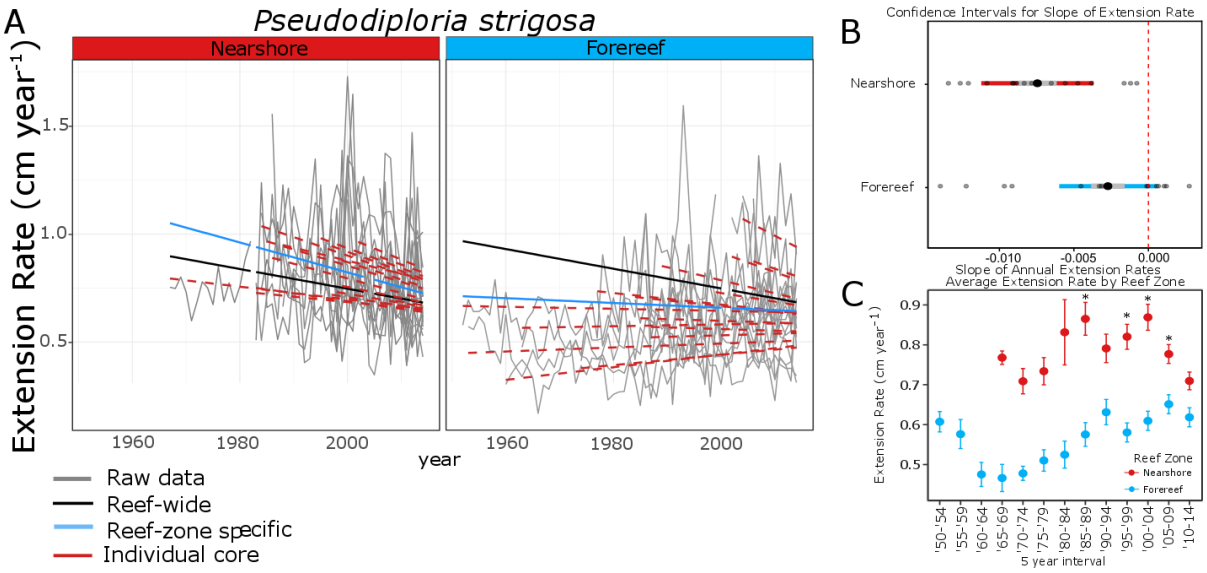

Fig 3: Results of linear model of extension rate (cm year^{-1}) for *P. strigosa* by reef zone for the 1950-to-present interval. Gray lines are raw extension data, black lines are average linear models of extension for all *P. strigosa* cores across all reef zones, blue lines are average linear models of extension for all *P. strigosa* cores within each reef zone, and red lines are linear models of extension for individual *S. siderea* cores within reef zones. (B) Slopes of linear models describing extension vs. time for each reef zone, with small points representing individual cores and large points representing average slopes of all cores within a reef zone (gray bars and colored bars are 50% and 95% confidence intervals (CI), respectively, of average slope for each reef zone). Slopes are significantly different from each other if their 95% CI do not overlap. Likewise, slopes are significantly different from zero if their 95% CI do not overlap with the red dashed 0 line. (C) Five-year averages of skeletal extension rate by reef zone ± 1 SE. Asterisks indicate statistically significant differences ($p < 0.05$) between nearshore and forereef values.

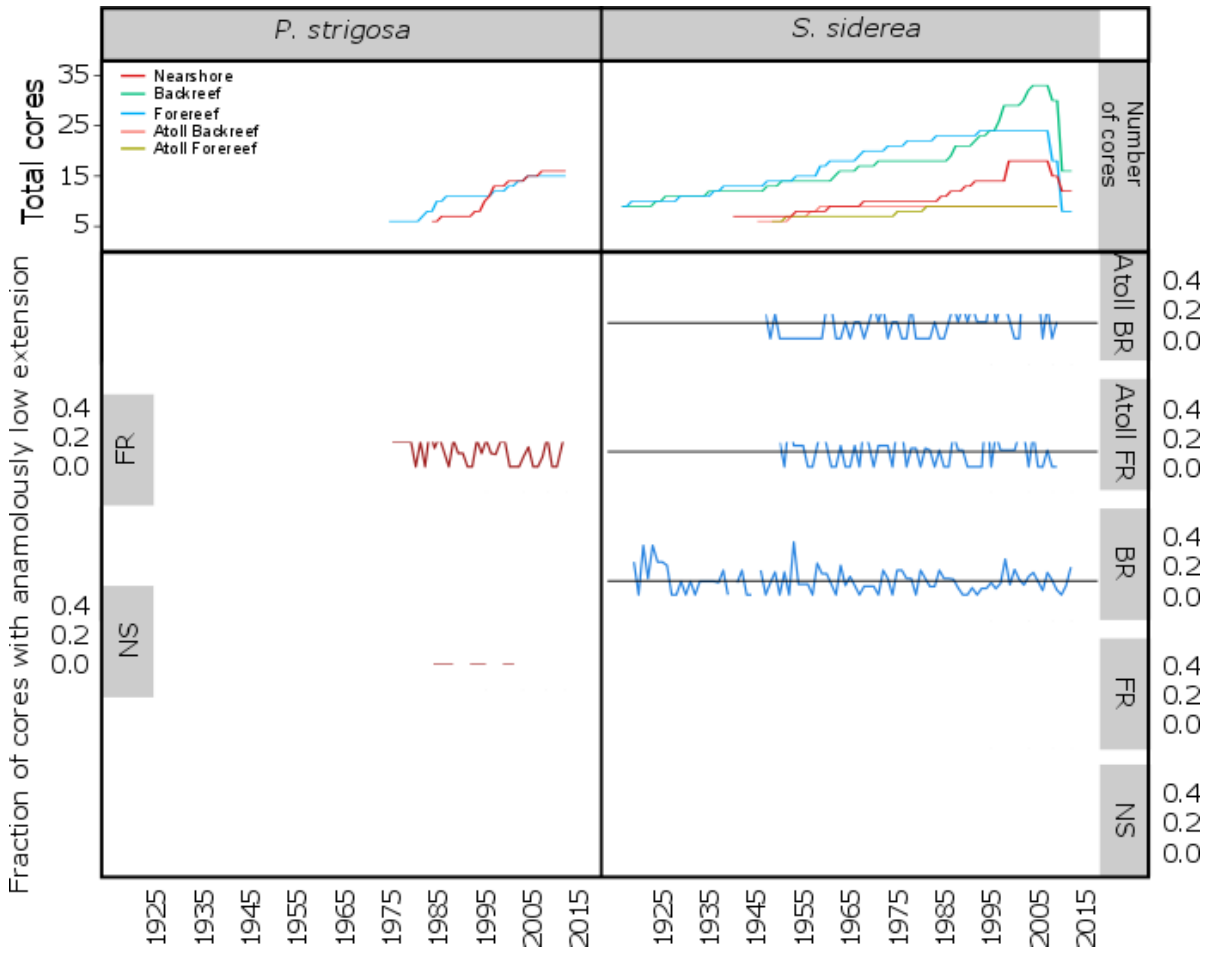

Fig 4: Graphs of total number of cores extracted from each reef zone per species per year (top panel) and fraction of cores within each reef zone exhibiting anomalously low extension rates (i.e., annual extension rate in lowest 10% of core) per year (bottom panel). Higher values in bottom panel indicate higher proportion of cores within a reef zone exhibiting anomalously low extension within a given year. Black horizontal lines indicate time-averaged ratios for each reef zone (separated by species). Vertical dashed lines at 1997, 2005, 2010, and 2014 indicate known bleaching events in the Caribbean (note: first mass bleaching event in Belize was recorded in 1997-1998).

CHAPTER 5: ACCLIMATIZATION TO ENVIRONMENTAL HETEROGENEITY LIMITED BY LOCAL ADAPTATION IN *SIDEREASTREA SIDEREA* BUT NOT *PSEUDODIPLORIA STRIGOSA* CORALS

Introduction

Tropical coral reef ecosystems cover less than 1% of the surface area of the planet, yet they support up to 35% of all species living in the global oceans (Nybakken and Bertness 2005). Coral reefs are also an important source of protein (Azam and Worden 2004) and economic gain for human populations worldwide, as coral reef tourism and fisheries generate $9.6 billion and $5.7 billion USD annually, respectively (Cesar et al. 2003). However, coral reefs are facing significant threat due to a combination of rising ocean temperatures, acidification, and local stressors (Caldwell et al. 1965; Pandolfi et al. 2003; Hoegh-Guldberg et al. 2007). These stressors, coupled with disease outbreaks and loss of urchin grazers have led to a precipitous decline in coral cover in the Caribbean since the 1970s (Gardner et al. 2003). As a result, most of the coral species responsible for the structural complexity of Caribbean coral reefs have been significantly impacted, while more opportunistic or stress-tolerant species have increased in abundance (Gardner et al. 2003; Baumann et al. 2016). This change in reef complexity has led to the flattening of Caribbean reefs (Alvarez-Filip et al. 2009) and has resulted in phase-shifts in dominant coral genera causing decreased reef functionality (Alvarez-Filip et al. 2013). These phase-shifts may due to different coral life history strategies and/or resilience to modern stressors such as ocean warming (Darling et al. 2012; Darling et al. 2013). As the combined impacts of global and local stressors continue to

mount, corals that are best able to acclimatize and/or adapt to changing environmental conditions are most likely to persist under climate change.

Thermal tolerance and the capacity of corals to acclimatize and/or adapt has received renewed interests due to increasing threats from global and local anthropogenic stressors. Acclimatization is a plastic change in the phenotype of an organism over its lifetime using its existing genomic repertoire, while adaptation is a change in the genotype of an organism over generations in response to a stress (Coles and Brown 2003; Frias et al. 2010). These two responses are vital to ensure the continued survival and success of corals as climate change persists, especially to acute stressors such as coral bleaching (i.e., the breakdown of the vital coral-*Symbiodinium* partnership that sustains reef-building corals), which are increasing in frequency and severity (Hughes et al. 2017b). Often, acclimatization in response to thermal stress impacting the coral holobiont (coral host, *Symbiodinium*, and any associated microbial community) is driven by changes to the dominant *Symbiodinium* community from more thermally sensitive *Symbiodinium* species to more thermally tolerant varieties (Jones et al. 2008; Howells et al. 2012; Howells et al. 2013). However, acclimatization and/or local adaptation also occurs in the coral host, as corals living in warmer reef environments have shown fewer signs of physiological stress following exposure to acute temperature stress events (Castillo and Helmuth 2005; Carilli et al. 2012; Rochman et al. 2013).

Exposure of corals to high frequency (daily) thermal variability has also been shown to reduce the incidence of coral bleaching on a variety of reefs worldwide (Jambeck et al. 2015). Reefs that experienced greater thermal variability exhibited lower declines in coral cover during the 1997-'98 El Nino mass bleaching event in the Western Indian Ocean

(Ateweberhan and McClanahan 2010). Also, mounding *Porites* spp. corals exposed to a higher degree of historical temperature variability were less impacted by the 2004 and 2009 bleaching events in Kiribati (Carilli et al. 2012). Indeed, previous exposure of corals to high frequency thermal variation provides thermal tolerance via acclimatization that exceeds the impact of shifts to thermally tolerant symbionts alone (Oliver and Palumbi 2011a). A follow-up study revealed that when *Acropora hyacinthus* corals were transplanted to an environment with a higher magnitude of daily thermal variation, they experienced both acclimatization and long-term adaptation that confers a heat tolerance improvement that would be expected from generations of strong natural selection in just 2 years (Palumbi et al. 2014). As a result, thermally variable reefs are presently being considered as conservation priorities (Jambeck et al. 2015) and acclimatization to heat stress, suggested to occur at rates near of 0.1°C increases per decade (Gregory 2009; Hall et al. 2015), provides hope that some species of corals will continue to persist under changing climate. As thermal stress and other impacts of climate change are projected to worsen, it is vital to understand the main drivers of change in coral reef communities and identify how reefs of the future may be structured in order to ensure their persistence and to protect the vital ecosystem and economic services they provide (Graham et al. 2014).

Limits to coral thermal tolerance and plasticity may slow or impede the process of acclimatization and/or adaptation. For example, corals that already live at their upper thermal tolerance limit (i.e., the Southern Red Sea) show decreased capacity for physiological acclimatization to warming, while those from cooler latitudes show greater potential for acclimatization, indicating that the upper thermal tolerances limits of modern corals can act as a barrier to acclimatization (Howells et al. 2013; Kirstein et al. 2016; Nadal et al. 2016).

Also, adaptation to native thermal regimes can be limiting to acclimatization potential, as *Acropora millepora* corals transplanted to reefs that experience warmer or cooler temperatures than their native environments grew slower than corals that remained in their native environments on the Great Barrier Reef (Howells et al. 2013). It should also be noted that not all coral species exhibit increasing thermal tolerance through acclimatization. *Oculina patagonica* corals from the Mediterranean Sea acclimated to warmer or more variable environments did not receive a boost in thermal tolerance of the coral host or *Symbiodinium* when exposed to varying degrees of experimental warming (Lönnstedt and Eklöv 2016). Similarly, exposing Caribbean *Porites astreoides* and *Acropora palmata* corals from low variability sites to conditions with greater temperature and pH variability did not confer greater tolerance to either stressor, suggesting that adaptation to native environmental conditions may have limited physiological plasticity (Camp et al. 2016). Lastly, *P. astreoides* corals transplanted from cooler and less thermally variable offshore reefs to warmer and more thermally variable nearshore reefs experienced significant growth reductions, indicating that such corals specialize to their home environment and incur a fitness tradeoff when moved or exposed to new conditions, thereby they are selected against in situation where environmental conditions change (Kenkel et al. 2015). Nonetheless, thermal tolerance conferred via acclimatization in parent corals is heritable (McCormick et al. 2014), indicating that corals that survive stressful conditions and then reproduce may be able to pass on advantages gained through acclimatization to larvae, which may increase coral cover or improve the capacity for thermal tolerance of those reefs.

Many tropical coral reef environments that exhibit high degrees of thermal variation are located more proximal to the coast in nearshore environments (Castillo et al. 2011b;

Oliver and Palumbi 2011a; Barshis et al. 2013; Palumbi et al. 2014; Baumann et al. 2016; Camp et al. 2016). Thermal tolerance, acclimatization, and/or local adaptation of corals from these environments are often compared to those from nearby offshore reefs. In the Caribbean, nearshore reefs are often degraded as a result of thermal stress combined with local land-based stressors. As a result of these stressors, nearshore environments exhibit lower coral diversity and cover than offshore reefs (Baumann et al. 2016; Camp et al. 2016), with the exception of nearshore environments on the Florida Reef Tract, which have higher coral cover than offshore reefs (Lirman and Fong 2007; Moore 2008; Kenkel et al. 2015). In spite of their degraded state, nearshore Caribbean reefs may harbor corals with a genetic or physiological pre-disposition to persist in future ocean conditions.

Here, we employ a reciprocal transplant experiment to assess the relative acclimatization and/or local adaptation capacity of two stress-tolerant Caribbean coral species, *Pseudodiploria strigosa and Siderastrea siderea* from nearshore and offshore environments on the Belize Mesoamerican Barrier Reef System (MBRS) over three winter months (December- March). Six colonies of each species were collected from a nearshore and offshore reef and sectioned so that 6 replicates of each genotype were present in each transplant treatment, allowing for analysis of individual and community level responses. We assessed whether degraded, less diverse, and more thermally variable nearshore habitats harbor more thermally tolerant corals that are armed with a genetic of phenotypically plastic physiological advantage to survive in this era of rapid climate change. Not only will this study further our understanding of the impacts of environmental control on thermal tolerance, it also has wide reaching implications for coral restoration, as current restoration methods involve harvesting resilient corals and transplanting them between reefs (Setälä et al. 2014;

Setälä et al. 2016). Identification of hotspots for thermal tolerance and/or resilience has the potential to improve restoration success. Also, nearshore coral reef environments are often not designated for protection due to their more degraded status. In Belize, only 1 nearshore reef is within a marine protected area (Taylor et al. 2016). Improved understanding of the valuable role these nearshore coral reef ecosystems may play in conferring coral thermal tolerance at local and regional scales can be utilized by policy-makers and coastal zone managers to improve protection for these environments.

Methods

Study sites description

Field work was conducted at a nearshore reef site (False Caye, 16.0391° N, 88.33694° W, and an offshore reef site (Silk Caye 16.45026° N, 88.04360° W) on the Belize Mesoamerican Barrier Reef System (MBRS). Nearshore reefs on the Belize MBRS have previously been characterized as having greater annual seawater temperature variations and higher incidence of temperatures exceeding the published regional coral bleaching threshold of 29.7°C (Aronson et al. 2002b). False Caye, the nearshore site, has experienced greater thermal variability over the past 15 years than has Silk Caye, the offshore site (Table 1; Fig 1A). Notably, over the course of this experiment, which occurred during the winter months (Dec 2017- March 2018), the nearshore site was actually slightly cooler than the offshore site (Table 1; Fig 1D). Additionally, remotely sensed chlorophyll-*a* has historically been slightly elevated and more variable (due to land-based influences) compared to the offshore site over the past 15 years (Table 1; Fig 1B) and over the course of this experiment (Table 1; Fig 1E). The availability of photosynthetically active radiation (PAR) at depth at each of the two reef

site has varied more at the nearshore site, although an overall difference in PAR between the sites is not clearly visible (Table 1; Fig 1C, 1F). Environmental data were extracted from satellite products on the NOAA Coastwatch ERDDAP database. Light availability at depth (Iz) was calculated using remote sensed PAR (at the ocean surface) and remote sensed diffusion attenuation coefficient (k490) complemented with the depth of each site using Beer's Law (Formula 1; Gordon 1989).

Formula 1: Beer's Law formula for light attenuation $Iz = PAR * 10^{-(k490 * depth)}$

Reciprocal transplant experimental design

In December 2017, 6 colonies of *S. siderea* and 6 colonies of *P. strigosa* were collected from False Caye (nearshore) and Silk Caye (offshore). The average size of parent colonies was 4792 cm^3 ±625 (±SD). Each colony was sectioned into 13 equitably sized fragments using a 25 cm diameter wet tile saw (*RIDGID* model R4092, Elyria , Ohio) lubricated with seawater. The saw was rinsed with freshwater after sectioning each individual colony. After sectioning, one fragment from each parent colony was labelled and immediately flash frozen on dry ice as a time 0 (T0) control. The remaining twelve fragments were affixed to plastic petri-dishes with super glue (Gluemasters cyanoacrylate, Henderson, Nevada) and each coral fragment was buoyantly weighed to quantify calcification. Half (6) of the fragments from each parent colony were returned to their native reef and half (6) were transplanted to the foreign reef (Fig 2), yielding 4 transplant treatments: Nearshore native (native to nearshore), Offshore native (native to offshore), Nearshore transplant (transplanted to nearshore from offshore), and Offshore transplant (transplanted to offshore from nearshore). Photos were taken of each fragment post-transplantation to qualitatively assess bleaching and mortality. Coral fragments remained on the reef for three months. In March,

2018 Time 1 (T1) photos were taken, all coral fragments were again buoyantly weighed, and 36 total fragments were flash frozen and shipped to the University of North Carolina at Chapel Hill for further analysis including quantification of energy reserves (total soluble protein), *Symbiodnium* density, and *Symbiodinium* chlorophyll-*a*.

Calcification, and Survivorship

In December 2017 (T0), each fragment was buoyantly weighed for quantification of calcification rates (Jokiel et al. 1978). In March (T1), each fragment was collected and buoyantly weighed to track changes in calcification between T0 and T1 (~90 days) using an Ohaus Scout® portable balance (Ohaus, Parsippany, NJ). A hook was affixed to the bottom of the balance to allow for hanging weights to be measured and the balance was placed over a bucket of seawater. Salinity and temperature of the seawater were quantified with a YSI 30 probe (Yellow Springs Incorporated, Yellow Springs, Ohio). Percent change in weight between T0 and T1 was calculated to represent net calcification (gross calcification + dissolution). Photographs were of each fragment were taken at T0 and T1 with a GoPro Hero 3+ camera (GoPro, San Mateo, Ca). These images were qualitatively analyzed to determine the number of coral fragments that experience whole or partial mortality. Partial mortality is defined as evidence of tissue recession or exposed skeleton relative to T0.

Symbiodinium density and chlorophyll-a

Fragments preserved during T0 and T1 collection periods were sectioned into 4 rectangular or triangular sub-fragments (dependent on colony geometry). The length, width, and height (when applicable) of each fragment were calculated using calipers or a NIST certified ruler (Fisher Scientific, Hampton, NH). Surface area of each fragment was calculated based on these measurements and the geometry of each individual fragment (Veal

et al. 2010). Tissue was airbrushed from one sub-fragment from each parent colony using deionized water. The resulting slurry was homogenized using a Tissue-Tearor® handheld homogenizer (BioSpec, Bartkesville, Oklahoma). 1 mL of the resulting homogenized slurry was aliquoted for symbiont density analysis as per Kenkel et al (2015). Briefly, a 1:1 mixture of formalin and Lugol's iodine was added to the aliquot to stain *Symbiodinium* cells for counting. *Symbiodinium* densities were determined by conducting 3-8 replicate cell counts of 10 µL samples using a haemocytometer and compound microscope (100x magnification) and counts were standardized to the surface area of their respective sub-fragment.

The remaining tissue slurry was centrifuged at 4400 rpm for 3 min to pellet out the endosymbiotic algae portion. Coral animal fraction (supernatant) was poured off, leaving the endosymbiotic algae pellet behind. Chlorophyll-*a* was extracted from the endosymbiotic algae pellet for 24 hr using a 90% acetone dark incubation at -20°C (Kenkel et al. 2015). Samples were diluted by adding 0.1 mL of extracted chlorophyll-*a* sample to 1.9 mL of 90% acetone. If samples were too high or too low to read on the fluorometer, samples were reanalysed by either diluting or concentrating the sample, respectively. Extracted chlorophyll-*a* content was measured using a Turner Design 10-AU fluorometer with the acidification method (Parsons et al. 1984) and expressed as µg of pigment per cm^2 of coral tissue surface area.

Protein content

Total soluble proteins (Rodrigues and Grottoli 2007) were measured for all frozen fragments from T0 and T1. Briefly, a sub-fragment (skeleton + animal tissue + endosymbionts) of each frozen coral fragment was ground with a mortar and pestle. The resulting slurry was centrifuged at 3500 rpm for 10 minutes to pellet the skeleton fraction.

The resulting supernatant (animal tissue + endosymbionts) was decanted to a clean 50-ml centrifuge tube. 5 mL of MilliQ water was added to the skeleton pellet to wash off any remaining tissue residue. The skeleton was vortexed and centrifuged at 3500 rpm for an additional 5 minutes. The resulting supernatant was added to the previous supernatant. The resulting tissue and endosymbiont slurry was homogenized using a Tissue-tearor handheld homogenizer (BioSpec, Bartkesville, Oklahoma). A 1 mL aliquot of the resulting tissue and endosymbiont slurry from each coral fragment was placed into a clean microcentrifuge tube. Glass microbeads were added to each tube and then each tube was vortexed for 20 minutes in order to break up cells and homogenize the slurry. Each tube was then centrifuged for 3 minutes at 4000 rpm to pellet the glass beads. 15 µL aliquots were taken from each tube and added to new tubes. MilliQ water was added to each to tube to bring the total volume in each tube to 250 µL. Total protein was quantified colorimetrically from each sample using a Bradford Assay (Pierce^{TM} Coomassie Protein Assay Kit). Spectrophotometric protein analyses were conducted on an Eppendorf BioSpectrometer® Basic measuring absorbance values at 562nm. Bovine Serum Albumin (BSA) standards of known protein concentration were run as standards and each sample was run in duplicate. If absorption values for a sample did not fall within the standard curve, that sample was diluted and re-run.

Statistical analyses

A two-way analysis of variance (ANOVA) was used to conduct pairwise comparisons of the influence of species (*S. siderea*, *P. strigosa*), transplantation treatment (Nearshore native, Nearshore transplant, Offshore native, Offshore transplant), and their interaction on percent change in coral weight (proxy for calcification) between T0 and T1, as in Howells et al. (2013). If the interaction was significant (p<0.050), a post-hoc Tukey's HSD test was used

to evaluate the significance of each pair-wise comparison. Survivorship was assessed qualitatively based on identification of partial mortality, mortality, or survival in photographs. Percentages were calculated for each of the four transplantation treatments within a species. Three-way ANOVAs were conducted to compare the influence of species, transplant site, time point (T0, T1), and their interactions on endosymbiont density, chlorophyll-*a* and total soluble proteins. As these data are pairwise and there are only two time points, ANOVA is a valid statistical framework for analyzing these data (Roark et al. 2009). If interactions were significant (p<0.050), a post-hoc Tukey's HSD test was used to evaluate the significance of each pair-wise comparison. Samples were confirmed to be independent in order to satisfy the main assumption of ANOVA tests (Roberts et al. 2006; Rochman et al. 2014; Rochman 2015). Assumptions of normality and homoscedascticity were not evaluated, as ANOVA modeling has been deemed robust enough to be meaningful even when these assumptions are violated (Roberts et al. 2006). Bonferonni corrections were not applied to decrease the likelihood of false negatives (Roark et al. 2009). All statistical analysis were conducted in R (R Core Team 2017).

Results

Survivorship and Fragment Status

Pseudodiploria strigosa fragments exhibited 100% survival at T1 in all 4 transplant treatments (i.e., nearshore and offshore native and transplant). *Siderastrea siderea* fragments exhibited 100% survival in 3 out of 4 transplant treatments, with 87.5% of offshore transplant (transplanted from nearshore to offshore) *S. siderea* fragments surviving (Fig 3). Whole

fragment mortality (i.e., death) and missing fragments were only observed for offshore transplant *S. siderea*.

Nearshore native *P. strigosa* fragments exhibited <10% partial mortality while no partial mortality occurred in nearshore transplants. Conversely, offshore native *P. strigosa* fragments exhibited no partial mortality while offshore transplant fragments exhibited <10% partial mortality (Fig 3).

Calcification

Across all transplant treatments, *P. strigosa* showed greater calcification rates (i.e., percent change in buoyant weight between T0 and T1) than did *S. siderea* (Fig 4, Table 2). All *P. strigosa* fragments experienced positive net calcification rates, while offshore native and transplant *S. siderea* fragments exhibited net dissolution (Fig 4, table 2). There was no significant difference in calcification rate between nearshore native and nearshore transplant fragments in either species (Fig 4, Table 2). There was no significant difference between offshore native and offshore transplant fragments for *P. strigosa*, but offshore transplant *S. siderea* fragments exhibited significantly greater net dissolution than did offshore native *S. siderea* (Fig 4, Table 2). Offshore transplants exhibited higher calcification rates than did their offshore natives (Fig 4, Table 2).

Symbiodinium density

Across all treatments *P. strigosa* showed higher symbiont densities than did *S. siderea* (Fig 5A, Table S1). *Symbiodinium* densities increased in nearshore native *P. strigosa* from T0 to T1 but did not change between T0 and T1 in any other transplant treatments.

Symbiodinium densities decreased in offshore transplant *S. siderea*, but did not change in any other transplant treatments (Fig 5A, Table S1).

Chlorophyll-a

Pseudodiploria strigosa corals exhibited higher chlorophyll-*a* levels than did *S. siderea* corals (Fig 5B, Table S2). There were no statistically significant difference in chlorophyll-*a* between T0 and T1 within any treatments of either species. Likewise, there were no significant difference in chlorophyll-*a* between treatments within either species (Fig 5B, Table S2).

Total soluble protein

Protein content was significantly lower in T1 *S. siderea* than in T0 (Fig 5C, Table S3), however, there were no statistically significant differences between T0 and T1 protein content within any individual treatment of either species. Likewise, there were no significant differences between treatments within either species (Fig 5C, Table S3).

Discussion

Current environment dictates calcification rate

Corals of both species transplanted from the offshore to the nearshore (nearshore transplant) and from the nearshore to the offshore (offshore transplant) showed calcification responses akin to native corals (Fig 4), providing evidence for plasticity (i.e., different growth responses in different environments) of calcification in response to environmental changes. This observation suggests that the current environment determines rates of calcification for *P. strigosa* and *S. siderea*. While there were no statistically significant

differences between native and immigrant *P. strigosa* in either environment (Fig 4), visible trends suggest that calcification responses in transplanted *P. strigosa* mimic those of native coral counterparts. In *S. siderea*, calcification responses in transplanted corals mimic those of their native counterparts, as nearshore native and transplant corals exhibit positive net calcification rates and offshore native and transplant corals exhibit net dissolution (Fig 4) between T0 and T1 (December – March). These trends, which show transplanted corals responding to their new environment similarly to corals native of that environment, indicate that *P. strigosa* and *S. siderea* corals both have the capacity to acclimatize to their environment, and that *S. siderea* corals may experience better growth (i.e. calcification and linear extension) in the nearshore site which is warmer, more thermally variable, and more nutrient rich than the offshore site (Fig 1; Table 1). These calcification rate trends are not seen in *Symbiodinium* density, chl-*a* concentration, or total soluble proteins (energy reserves), where there were no differences in response between any of the four experimental treatments in either species (Fig 5). These results contrast those of previous work on the weedy Caribbean coral, *Porites astreoides*, in which growth rates did not differ between transplant and native corals and where protein concentrations were higher in corals left in their native habitat than in transplant corals (Kenkel et al. 2015).

The acclimatization potential of *P. strigosa* and *S. siderea* to changing environmental conditions may be limited by local adaptation, as in other coral species (Howells et al. 2013; Kenkel et al. 2015). Transplants performing worse than natives within a treatment is an indicator of local adaptation within the native population (Wright et al. 2013). While no significant differences in calcification rate are seen between nearshore native and transplant *P. strigosa*, offshore transplant *P. strigosa* appear to have marginally lower calcification rates

than offshore natives, although this trend is not statistically significant (Table 2; Fig 4). Additionally, nearshore *P. strigosa* show increases in *Symbiodinium* densities over the course of the experiment, but nearshore transplants do not (Fig 5). Interestingly, chlorophyll-*a* did not increase with increasing *Symbiodinium* density, suggesting that increased *Symbiodinium* densities did not confer any energetic advantage (Fitt et al. 1993). Overall, there are indications of local adaptation in nearshore *P. strigosa* and that such adaptation may impede the acclimatization ability of nearshore corals upon transplant or exposure to novel environmental conditions.

In *S. siderea*, the impacts of local adaptation on acclimatization capacity are more palpable. Offshore transplant *S. siderea* have significantly lower calcification rates than do offshore natives (Table 2; Fig 4), exhibit declines in *Symbiodinium* density over the course of the experiment, and 75% of offshore transplant *S. siderea* show partial mortality (Fig 3, Fig 5A). The same trend is not seen in nearshore transplants, which exhibit a calcification rate that is not significantly different from nearshore natives (Fig 4). Interestingly, a similar study on the Pacific coral, *Acropora millepora*, showed that transplanted *A. millepora* corals exhibited lower growth rates than native corals (Howells et al. 2013). The authors attributed these lower growth rates to local adaptation. In the current experiment, declines in growth and/or physiology are only seen in offshore transplant *S. siderea*, indicating that local adaptation may most severely limit the plasticity of nearshore *S. siderea* when they are transplanted or exposed to novel environmental conditions.

S. siderea exhibit net dissolution offshore

Offshore native and transplant *S. siderea* exhibited greater partial mortality than did their nearshore counterparts (Fig 3). Indeed, offshore transplant *S. siderea* was the only treatment in which total fragment mortality was recorded. In addition, offshore native corals showed a negative calcification response (net dissolution) over the winter months and offshore transplants had an even lower calcification rate, compared to nearshore natives and transplants, which showed positive net calcification during the experiment (Fig 4). Taken together, this evidence suggests that *S. siderea* corals are better suited for nearshore conditions. In contrast, previous work has shown that nearshore corals (and corals transplanted to nearshore from offshore) grow slower than their offshore counterparts on the Florida Keys Reef Tract, likely due to heat and/or cold stress (specific to nearshore sites only) (Carpenter et al. 1972). However, while nearshore reefs in Belize have previously been characterized to experience warmer summers, greater annual thermal variability, and to experience a greater number of days above the bleaching threshold each year than offshore reefs (Castillo et al. 2012; Baumann et al. 2016), there was no evidence of a cold stress within the duration of this experiment (Fig 1D). Nearshore reefs also experience higher average chl *a* levels (a proxy for eutrophication risk or primary productivity; Chiappone et al. 2005) than offshore reefs (Baumann et al. 2016; Table 1). While all of these characteristics can negatively impact corals (Fabricius 2005; Hoegh-Guldberg et al. 2007), historical growth data along the Belize MBRS reveals that nearshore *P. strigosa* and *S. siderea* have historically grown faster than their offshore counterparts (Farrell and Nelson 2013). Nearshore growth rates of these two species are declining and appear similar to offshore counterparts on a reef system scale (Farrell and Nelson 2013). Our results reveal that local

scale trends mimic reef system trends for *P. strigosa*, but in *S. siderea*, nearshore corals and nearshore transplants are growing faster than their offshore counterparts, at least during the winter months.

One explanation for elevated growth rates in *S. siderea* nearshore compared to offshore is slightly warmer annual average temperatures in nearshore habitats (Fig 1; Baumann et al. 2016), which can speed up metabolic rates. Indeed, corals in warmer water grow faster than corals in cooler water on a global scale, at least up to a certain temperature threshold (Pratchett et al. 2015). However, over the time of this experiment (winter), the nearshore environment was actually slightly cooler than the offshore environment, likely negating the metabolic influence of temperature on growth (Fig 1D). It is also possible that nearshore corals are able to glean additional nutrients from particulate matter, which is in higher abundance in the nearshore (Table 1). Both species in this study have the capacity to ingest and take up Nitrogen from particulate matter (Mills et al. 2004) and increased concentrations of suspended particulate matter have been shown to correlate with elevated coral growth rates elsewhere in the Caribbean (Cole et al. 2014). As chl-*a* is elevated in the nearshore comparted to offshore on an annual scale and during the experimental interval (Fig 1B, E; Baumann et al. 2016), this additional source of nutrition may well provide a reasonable explanation for increased *S. siderea* growth nearshore.

Less clear are the reasons for offshore *S. siderea* corals to exhibit negative calcification rates (net dissolution). As experimental corals were sectioned and skeleton was exposed during the experiment, dissolution of skeleton is possible (Arthur et al. 2009). Additionally, aragonite saturation state (Ω) may have also been lower offshore than it was on nearshore reefs, as it is on the Florida Keys Reef Tract (Baillon et al. 2012), causing

increased rates of dissolution. It is important to note that several studies have revealed that *S. siderea* growth and calcification rates do not decrease due to low magnitude differences in pH or Ω similar to what corals in this experiment were likely to experience (Caldwell et al. 1965; Castillo et al. 2014). Indeed, *S. siderea* appears to be more resistant to both temperature and acidification stress than most other common Caribbean reef-building corals (Caldwell et al. 1965). As such, it seems likely that ocean acidification does not play a significant role here.

It is also likely that partial mortality and tissue recession influenced the low calcification rates of offshore *S. siderea*, as the incidence of partial mortality was highest in offshore native and transplant *S. siderea* (Fig 3). The cause of this partial mortality is as yet unknown. There were no visible signs of disease on any corals during the experiment and *Symbiodinium* chlorophyll-*a* (an indicator of symbiotic efficiency) and total soluble protein (an indicator of energy reserve usage) did not decrease during the experiment (Fig 5B, C). As such, these corals did not appear to lack vital nutrients translocated from the symbiont, nor did they show signs of energy reserve utilization, indicating that that although they showed partial mortality, there were no indications of nutrient deficiency due to breakdown on the coral-algal symbiosis. *S. siderea* are often thought of as early indicators of reef stress due to their tendency to bleach sooner than other species as a result of stress, with smaller colonies more likely to bleach than larger ones (Banks and Foster 2016). However, as previously mentioned, *S. siderea* corals seem markedly more resilient to temperature and acidification stress in laboratory studies (Caldwell et al. 1965; Castillo et al. 2014) and even when they do bleach in the wild, they exhibit resilience to mortality, with most colonies able to recover in under 9 months (Banks and Foster 2016). As such, it is possible that these offshore *S. siderea*

corals suffered mild bleaching and subsequent recovery between T0 and T1. However, low rates of complete mortality and lack of decline in *Symbiodinium* chl-*a*, and total soluble protein provide evidence that the stress that caused the partial mortality appears to be sub-lethal. Given the slow rate of growth exhibited by *S. siderea* (Castillo et al. 2011b; Castillo et al. 2012; Dustan et al. 2013; Farrell and Nelson 2013; Castillo et al. 2014) it is not surprising to see low (or even negative) growth rates of this species during the winter months. However, given this species' relative resilience (Caldwell et al. 1965), it would be very telling in terms of the acclimatization ability and habitat and growth preferences of *S. siderea,* should this trend of net dissolution continue through the summer season.

Conclusion

Transplanted corals of both *P. strigosa* and *S. siderea* showed calcification responses akin to native corals at their transplant locations providing evidence for plasticity of calcification (acclimatization) in response to environmental changes. *Pseudodiploria strigosa* corals did not exhibit net dissolution, declining *Symbiodnium* densities, chlorophyll-*a*, or proteins in any treatment, indicating that this species is resistant to the impacts of environmental heterogeneity.

Siderastrea siderea corals exhibited greater calcification rates over the winter months in nearshore habitats than in offshore habitats, even when transplanted from offshore to nearshore, possibly due to elevated availability of nutrients in the water column (Mills and Sebens 2004; Mills et al. 2004; Cole et al. 2014). Conversely, offshore native and transplant *S. siderea* exhibited net dissolution and high incidence of partial mortality. Transplant *S. siderea* growth rates mimicked those of corals native to the transplant habitat, indicating that they possess a degree of acclimatization capacity. Such plasticity is potentially limited by

local adaptation, especially in nearshore populations of *S. siderea*. Previous research on *S. siderea* suggests that the species is resilient to temperature and acidification stress, providing hope that although offshore native and transplant *S. siderea* appear to have struggled during winter months, they will likely recover and resume growth in the summer months.

Tables

Reef Location	Reef Zone	Annual Avg. SST (°C)	Annual SST Range (°C)	Annual Avg. Max SST (°C)	Annual Avg. Chl-*a* (mg/m^3)	Annual Avg. light at depth (W/m^2)
False Caye	Nearshore	28.21	6.10	30.92	1.34	63.61
Silk Caye	Offshore	28.14	5.33	30.62	0.50	56.73

Table 1: Annual average SST, SST range, max SST, chl-*a*, and light availability at depth of the transplant tables at the two transplant sites (2003-2017).

	Df	**Sum sq**	**Mean sq**	**F value**	***p*-value**
Species	1	23953	23953	357.03	**<0.001**
Transplant	3	18611	6204	92.47	**<0.001**
Species: Transplant	3	8269	2756	41.08	**<0.001**
Residuals	281	18852	67		

Tukey HSD Results	**Comparison**	***p*-value**
Species	SSID-PSTR	**<0.001**
Transplant	OS Transplant: NS Native	**<0.001**
	OS Native: NS Native	**<0.001**
	NS Transplant: OS Transplant	**<0.001**
	OS Native: OS Transplant	**<0.001**
	OS Native: NS Transplant	**<0.001**
Species: Transplant	SSID NS Native: PSTR NS Native	**<0.001**
	SSID OS Transplant: PSTR NS Native	**<0.001**
	SSID OS Native: PSTR NS Native	**<0.001**
	SSID OS Transplant: SSID NS Native	**<0.001**
	PSTR NS Transplant: SSID NS Native	**<0.001**
	PSTR OS Native: SSID NS Native	**<0.001**
	SSID OS Native: SSID NS Native	**<0.001**
	SSID OS Transplant: PSTR OS Transplant	**<0.001**
	PSTR NS Transplant: PSTR OS Transplant	**0.002**
	SSID OS Native: PSTR OS Transplant	**<0.001**
	PSTR NS Transplant: SSID OS Transplant	**<0.001**
	SSID NS Transplant: SSID OS Transplant	**<0.001**
	PSTR OS Native: SSID OS Transplant	**<0.001**
	SSID OS Native: SSID OS Transplant	**<0.001**
	SSID NS Transplant: PSTR NS Transplant	**0.001**
	SSID OS Native: PSTR NS Transplant	**<0.001**

	SSID OS Native: SSID NS Transplant	**<0.001**
	SSID OS Native: PSTR OS Native	**<0.001**

Table 2: Results of ANOVA and Tukey HSD tests comparing % change in weight between T0 and T1 within and between species and between transplant treatments.

Figures

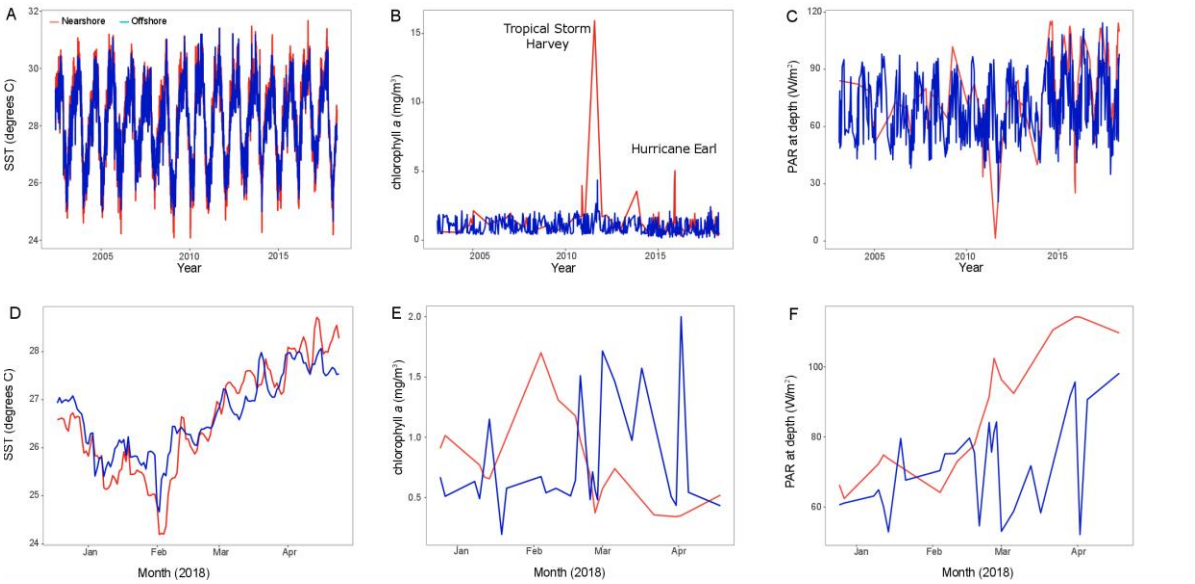

Figure 1: Daily satellite-derived SST (A), oceanic chlorophyll-*a* (B), and photosynthetically available radiation (PAR) at depth of transplanted corals (C) for nearshore (red) and offshore (blue) site from 2003-2018. Daily satellite-derived SST (D), oceanic chlorophyll-*a* (E), and PAR (F) for the nearshore (red) and offshore (blue) site from Dec 2017-May 2018 (duration of experiment).

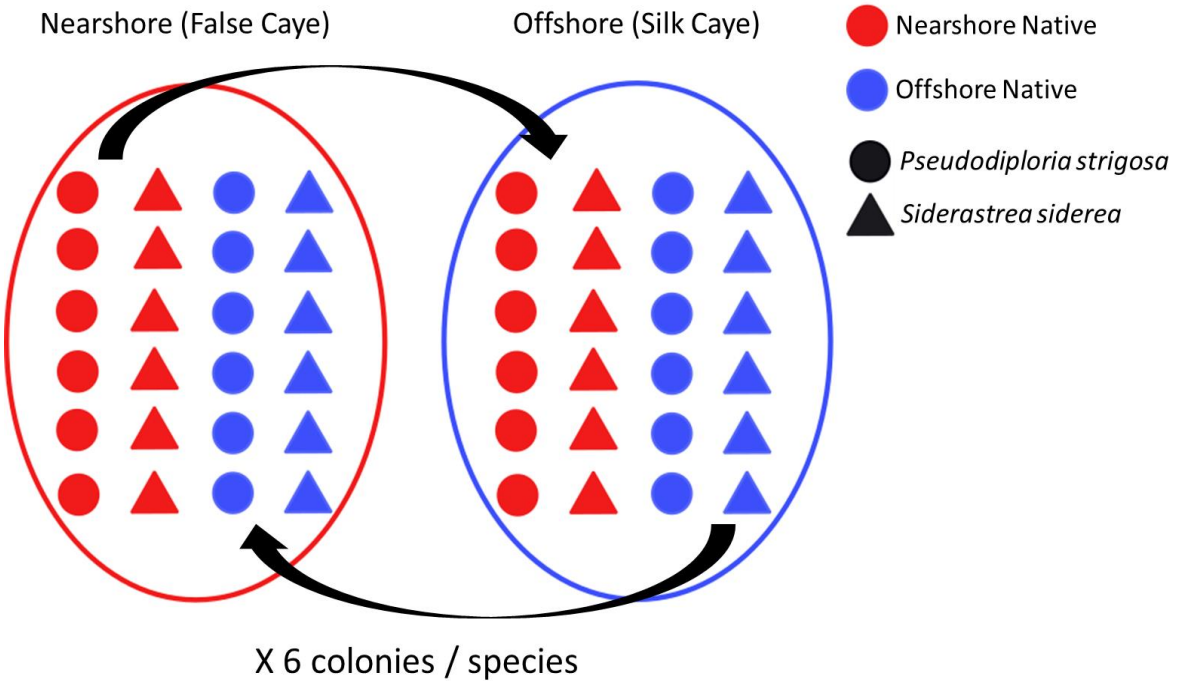

Figure 2: Reciprocal Transplant Experiment Schematic. Corals collected at False Caye (nearshore) are in red and corals collected at Silk Caye (offshore) are in blue. Triangles represent *P.* strigosa and circles represent *S. siderea*. Six colonies of each species of coral were collected at the nearshore and offshore site. Each colony was sectioned into 13 fragments. One fragment of each colony was immediately flash frozen. Six of the remaining fragments transplanted to their native reef six were transplanted to the foreign reef environment.

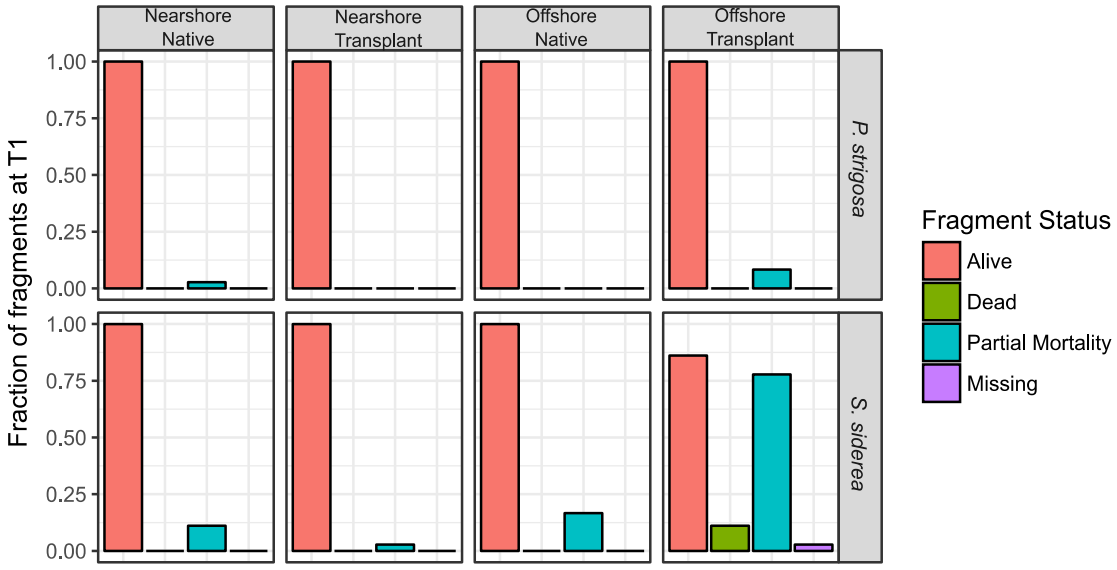

Figure 3: Fragment status and survivorship. Fraction of *P. strigosa* and *S. siderea* fragments alive, dead, exhibiting partial mortality, or missing at T1 (March, 2018) for each of the 4 transplant treatments.

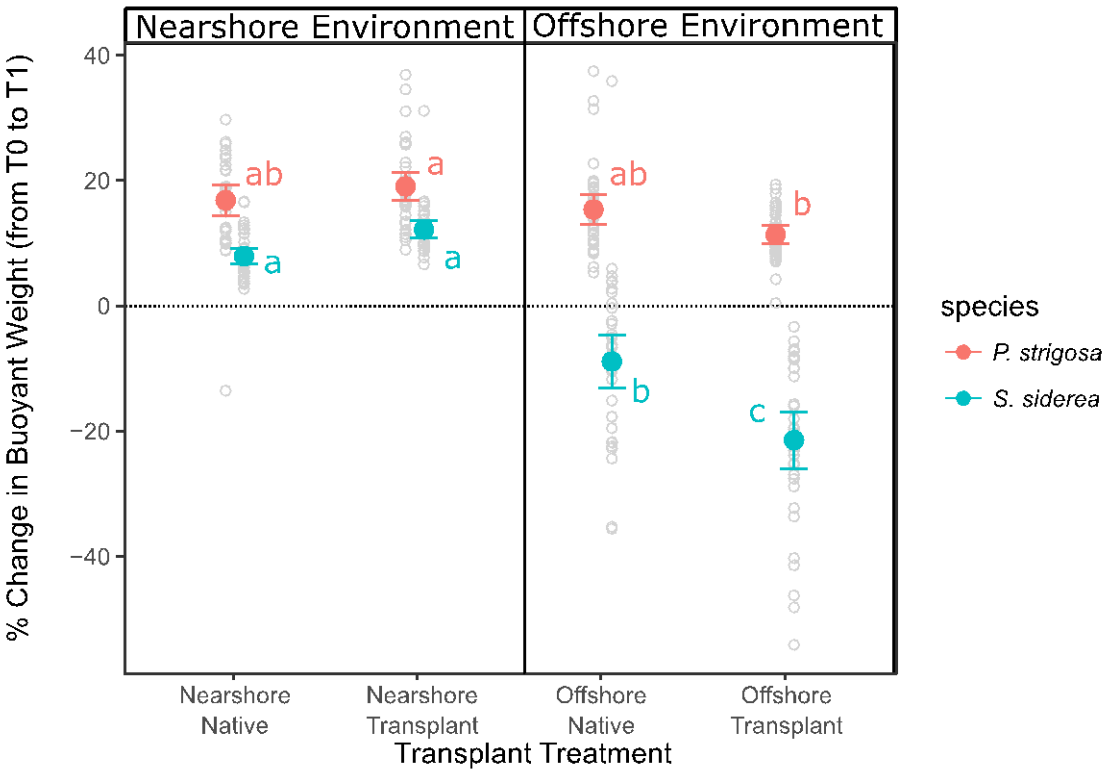

Figure 4: Percent change in coral buoyant weight between T0 and T1 for *P. strigosa* (red) and *S. siderea* (blue) within each transplant of the transplant treatments. Lowercase letters represent statistically significant differences between treatments within a species (color-coded).

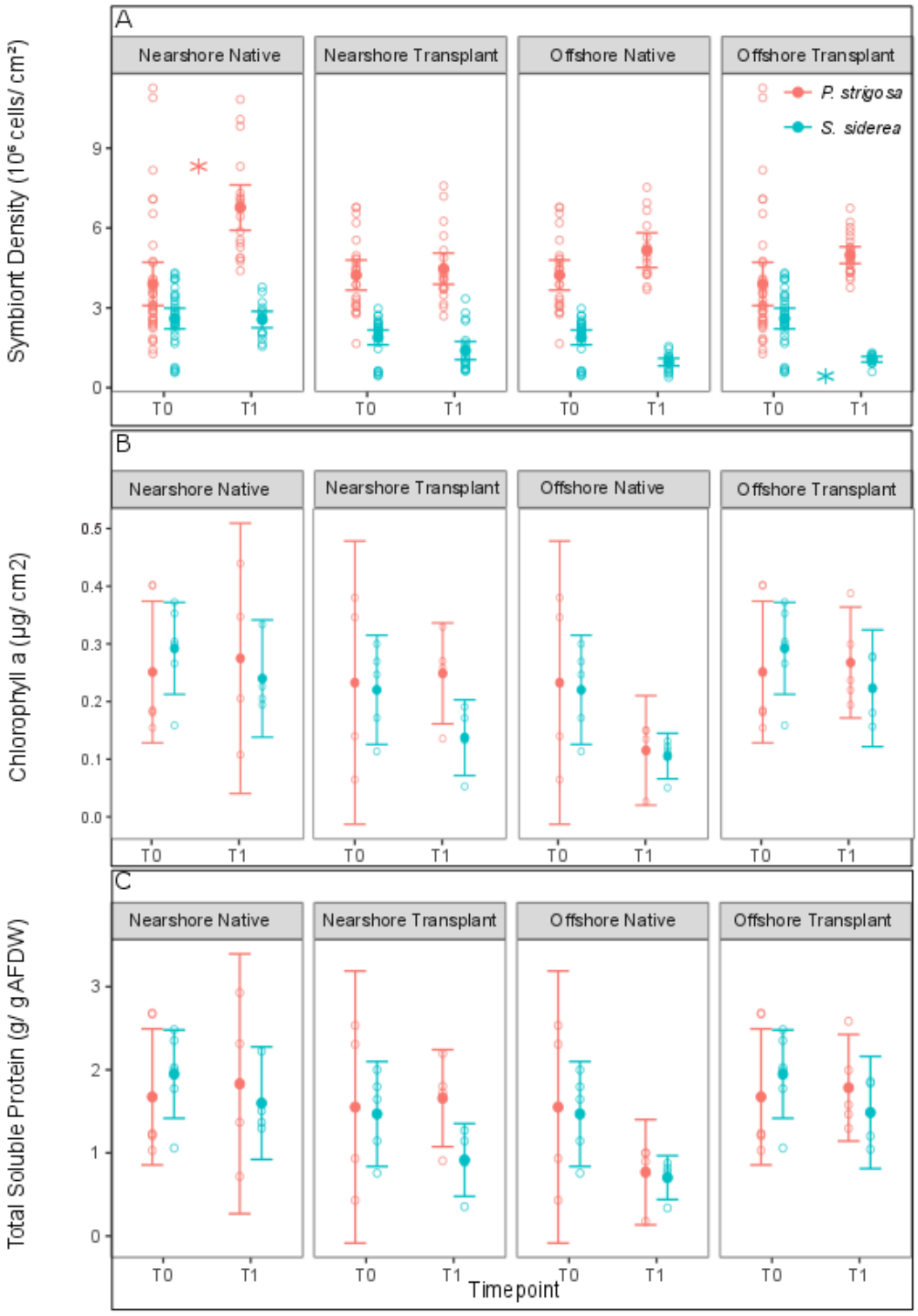

Figure 5: *Symbiodinium* density (A), *Symbiodnium* chlorophyll-*a* (B), and total soluble protein (C) by transplant treatment in *P. strigosa* (red) and *S. siderea* (blue). The asterisk represents statistically significant differences (p <0.05) between time points.

CHAPTER 6: CONCLUSIONS

This research has revealed that nearshore reefs on the Belize MBRS exhibit lower coral diversity, abundance, species richness, and cover than do offshore reefs. These nearshore reefs are exposed to higher annual temperatures, greater temperature variability, more time above the regional bleaching threshold, elevated *chl-a* concentrations, and likely increased sedimentation rates and lower flow than offshore reefs. Temperature parameters, most notably time spent above the bleaching threshold, correlated better with differences in coral community structure than did local nutrient concentrations. In addition, stress-tolerant and weedy coral life history strategies dominated at nearshore reefs while all 4 coral life histories were represented on offshore reefs. Due to exposure to generally more stressful environmental conditions, nearshore reefs may offer a snapshot into the projected future of coral reefs as they become increasingly exposed to local (pollution, runoff, land-use change, and overpopulation) and global (warming and acidification) stressors. Previously, such reefs have been suggested as possible refugia against climate change (Woesik et al. 2012). Globally, this would mean a shift towards dominance of stress-tolerant and weedy corals (McClanahan et al. 2014). Such a shift would dramatically impact the structure and function of reefs, essentially creating novel ecosystems (Graham et al. 2014). Nearshore reefs may host coral holobionts that are best suited to survive in future ocean conditions. Such resilience may be conferred through changes in *Symbiodinium* partners, local adaptation, acclimatization, or some combination of the three.

Symbiodinium communities associated with corals in Belize are dependent on both host species as well as environmental variables. *S. siderea Symbiodinium* communities were divergent from *S. radians* and *P. strigosa* indicating species specificity. Thermal regime played a role in driving *Symbiodinium* community composition in *S. siderea* but not *S. radians* or *P. strigosa*, suggesting that local impacts such as nutrients, sediment, or light availability may also influence *Symbiodinium* communities on the Belize MBRS. Additionally, low abundance of *S. trenchii* in inshore high$_{TP}$ sites indicates thermal tolerance at these sites must be conferred through alternative mechanisms, such as local adaptation or acclimatization.

Further exploration of the physiological differences between nearshore and offshore coral populations led to a study focused on the impacts of thermal history on coral growth rates. Through the analyses of 134 *S. siderea* and *P. strigosa* cores taken throughout the Belize MBRS a clear difference between nearshore and offshore growth rates was revealed. Nearshore *S. siderea* and *P. strigosa* historically exhibited higher skeletal extension rates compared to their offshore conspecifics, likely driven by historically warmer temperatures—favorable to the extent that they were below the corals' thermal optimum—and lower local environmental stress (Heyman and Kjerfve 1999; Thattai et al. 2003). However, extension rates of nearshore *S. siderea* and *P. strigosa* have now declined to levels similar to their historically slower growing offshore conspecifics owing to seawater temperatures more frequently exceeding the corals' thermal optima and from higher local environmental stress in nearshore environments. Although skeletal extension trends of offshore corals have exhibited relative stability over the observed interval, the decline in extension rate of nearshore colonies that are presently experiencing sustained thermal stress beyond their thermal optimum may foretell future

declines in the growth of offshore colonies once their thermal optima are more consistently exceeded. Instead, long-term increases in seawater temperature and local stressors (e.g., eutrophication and sedimentation), which are typically more pronounced in nearshore environments owing to their mainland proximity, are the more likely drivers of the observed decline in nearshore coral growth. Any advantage historically conferred to corals by inhabiting the nearshore environment, vis-à-vis thermal acclimation and/or increased heterotrophic uptake of N and/or C in particle-rich nearshore waters, appears to have been lost. However, the impact of local adaptation and/or acclimatization to local stressors on these growth declines remains unknown.

A nearshore-offshore reciprocal transplant experiment was started in December 2017 in order to attempt to elucidate differences in local adaptation and/or acclimatization capacity of nearshore and offshore *S. siderea* and *P. strigosa* on the Belize MBRS. *S. siderea* corals grew faster over the winter in nearshore habitats than in offshore habitats, even when transplanted from offshore to nearshore, possibly due to elevated availability of nutrients in the water column (Mills and Sebens 2004; Mills et al. 2004; Cole et al. 2014). Conversely, nearshore native and transplant *S. siderea* exhibited net dissolution and high incidence of partial mortality and visible bleaching. Transplant *S. siderea* growth rates mimicked those of corals native to the transplant habitat, indicating that they possess a degree of acclimatization capacity. Such plasticity is potentially limited by local adaptation, especially in nearshore populations of *S. siderea*. Although not statistically significant, trends seen in *S. siderea* appear to be mirrored in *P. strigosa*, but with a smaller amplitude, suggesting that this species is less prone to the impacts of environmental heterogeneity and/or stress in winter months. Previous research on *S. siderea* suggests that the species is resilient to temperature

and acidification stress, providing hope that although offshore native and transplant *S. siderea* appear to have struggled during winter months, they will likely recover and resume growth in the summer months.

Overall, while nearshore reefs are more degraded and less diverse than their offshore counterparts, there is clear evidence that some stress-tolerant corals such as *S. siderea* and *P. strigosa* have locally adapted and/or acclimatized to survive and in some cases, appear healthier on these degraded reefs relative to more pristine offshore reefs. Historically elevated growth rates on nearshore reefs were consistent across the entire Belize MBRS system, likely due to warmer summers boosting the growth metabolism of corals and increased dissolved and particulate nutrient availability on nearshore reefs compared to offshore reefs. However, recent declines in coral growth on nearshore reefs, likely due to mounting compounding stressors such as increased temperatures and nutrient concentrations, may limit the continued success of the few coral taxa that can survive on these reefs. As these nearshore reefs are modern analogs of future reefs under business as usual climate scenarios and continued population growth, further protection of these reefs and investigation of the physiological adaptations or strategies of plasticity present in corals living on these reefs is vital.

APPENDIX 1: SUPPORTING INFORMATION FOR CHAPTER 2

Additional detail of AGGRA and video survey methods

Six video transects (1 m x 20 m) were performed at each site using a GoPro® camera attached to a PVC stabilizing apparatus that allowed each diver to hold the camera steady with two hands while performing a transect. Six 20 m video transects per site has been shown to be sufficient to describe the coral community at a site (Cruz et al. 2008). Lead line of known length was attached to the camera rig to allow the diver to maintain a constant height above the substrate. Two lasers were placed on the camera rig 25 cm apart and were used to calibrate distances during video transect analysis. The entire apparatus, including the GoPro® camera, cost approximately $250, which is a more cost-effective option than commonly used stereo-video rigs that utilize much more expensive cameras and underwater housings. Video transects were analyzed in the same manner as the AGRRA transects. Length and width of each coral was recorded from measurements made while watching the video on a computer screen. The distance between the two lasers at each given stopped frame was used to calibrate the length and width measurements. Height of coral colonies was not recorded due to the two dimensional nature of the video recordings. Coral cover and coral density were also calculated using video transects. Video transects were calibrated in the field to be 1 m wide and 20 m long. However, due to shallow water and conditions at some sites the transects were less than 1 m wide, creating a slightly variable transect area, which was corrected for via the 25 cm laser scale.

All corals greater than 4 cm^2 in area (as measured by a metric ruler) at least partially inside of the video screen were surveyed following AGRRA guidelines (AGRRA 2003). The genus and species of each coral was identified and number and size of individual colonies of each species were recorded on underwater data sheets. The outward facing surfaces of each colony were analyzed for health and mortality using parameters defined by AGRAA (live, pale, bleached, new mortality, old mortality). After the data were collected, species diversity, abundance, species richness, and coral life history (Darling et al. 2012) were calculated for each site.

The results of the two survey methods were analyzed separately and then compared. It was determined that the data from the two transect methods could be combined for species richness, abundance, and Shannon diversity, as survey method was not a significant factor in the ANOVA (Table 3A). Percent coral cover was calculated using video transect data only, as the AGRRA method over-estimates coral cover. This is due to the fact that the AGRRA methodology requires any coral that is even partially within the transect to be quantified in full, leading to over-estimates of coral cover. Coral density (# of corals/ m^2) was also calculated from video transect data only.

Each method has downsides. AGRRA surveys are time consuming (1 hour per transect) and have the potential to overestimate coral cover. In addition, the diver must identify every coral individually while also maintaining buoyancy and safe diving practices, which can be difficult especially in rough weather. With video analysis, transects can be recorded much faster (less than 1 hour for 3 surveys) with approximately 150% of the AGRRA survey area covered using video in significantly less dive time. Videos were analyzed after the fact, allowing several researchers to analyze the video together and make a more thorough

identification of coral species than underwater AGRRA surveys allow for. While limitations in video framing and the two dimensional nature of the video prevent accurate measurements of individual size, coral cover can also be estimated more accurately than with AGRRA methodology. Overall, video analysis requires more time than field transects, but has the potential to be more accurate as the time crunch or other external stressors that may be experienced underwater are no longer present. The two methods are comparable in terms of results, however video surveys are more efficient in the field and are have previously been shown to have the potential to be more accurate (Lirman et al. 2007; Turner et al. 2015).

Figures

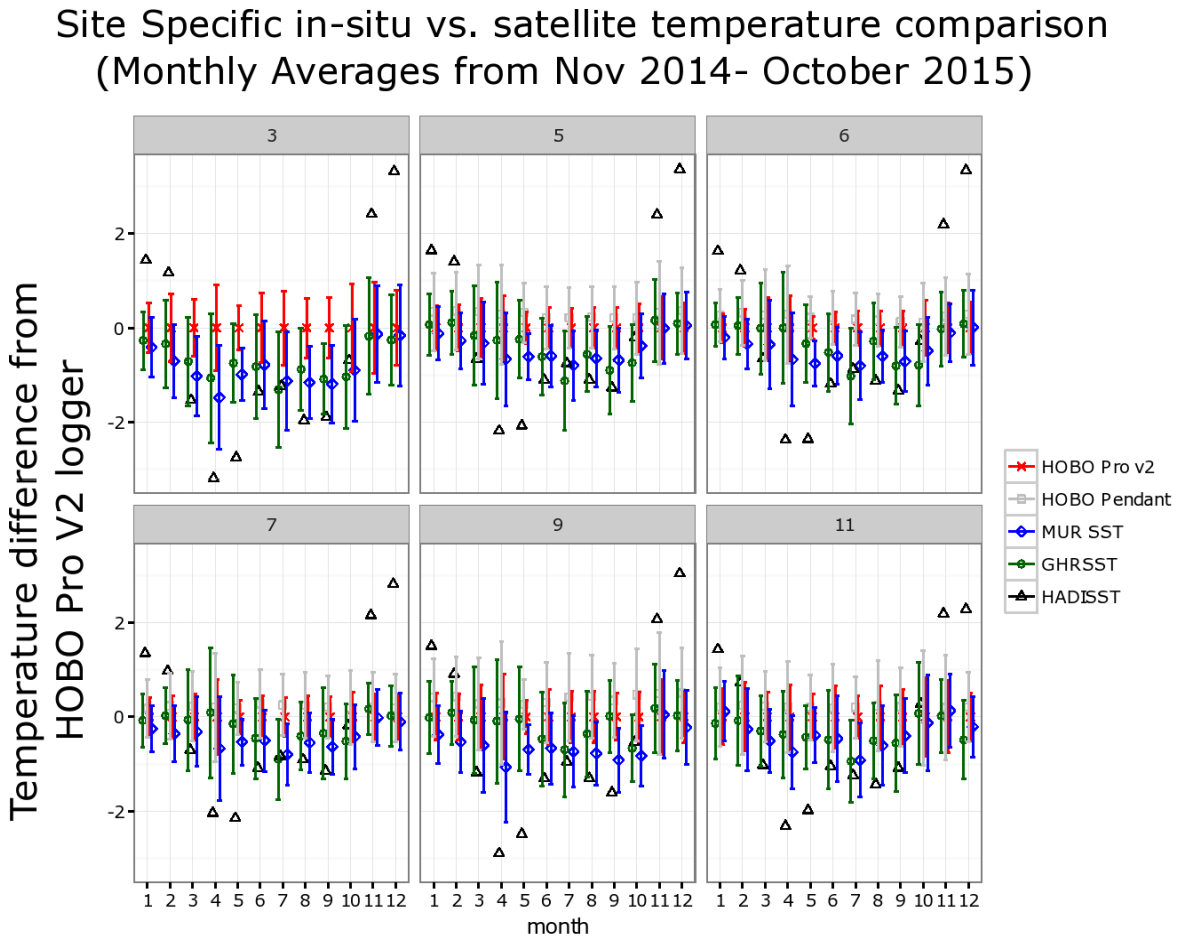

Fig S1. *In situ* temperature versus satellite SST products: A comparison of *in situ* temperature and MUR SST. *In situ* loggers were collected from 6 sites along the BBRS (site numbers are listed in the gray headers above each panel). Each panel shows a month by month comparison of *in situ* logger measurements and SST products. Zero on the y-axis represents the average value for the Hobo Pro V2 loggers at each site. Red errors bars the standard deviation over a month for each logger. Gray squares show average values for an additional *in situ* logger that was placed at the site (± 1 standard deviation). Blue, green, and black symbols show monthly average values for various SST products (± 1 standard deviation).

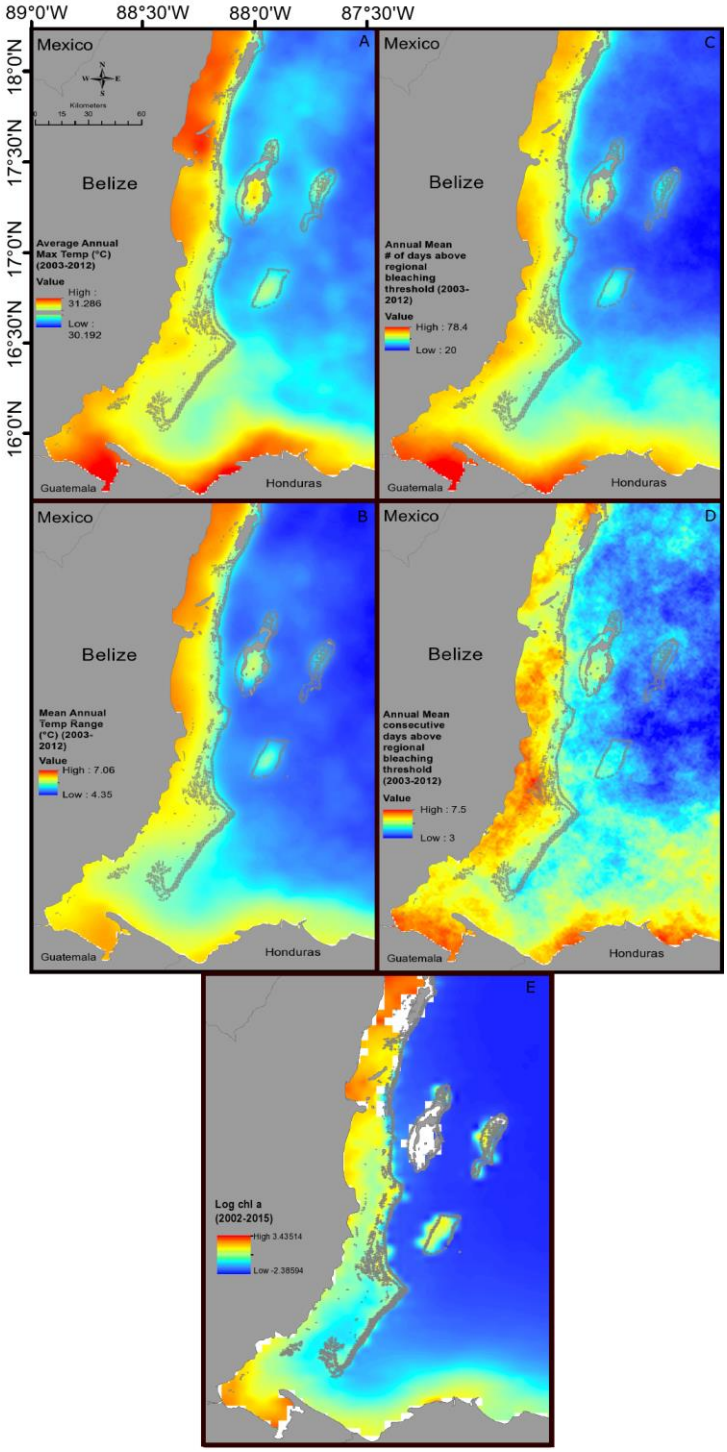

Fig S2. Temperature parameter and *chl-a* maps: Maps showing the 4 parameters used to calculate site type: yearly maximum temperature (A), Mean annual temperature range (B), Annual mean number of days above the bleaching threshold (C),Annual mean consecutive days above the bleaching threshold (D), and 13 year mean *chl-a* concentration from 2002-2015 (E). Maps generated from means calculated from daily satellite measurements taken from Jan 2003-Dec 2012.

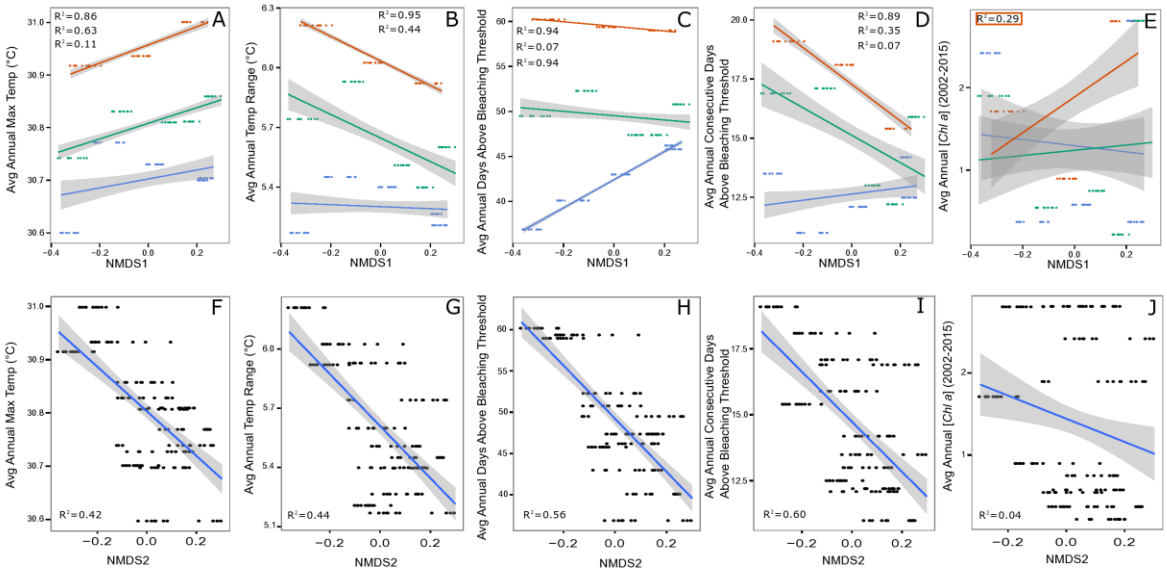

Fig S3. Linear regression of Physical Parameters vs. NMDS1 and NMDS2 by site type Linear regression of average annual max temp (A, F), average annual temp range (B, G), average annual days above the bleaching threshold (C, H), average annual consecutive days above the bleaching threshold (D, I), and *Chl-a* (E, J) vs. NMDS1 and NMDS2 by site type. R^2 values are included for each regression that yielded a significant slope (p <0.05).

Tables

Site Name	Site Type	Latitude (Degrees N)	Longitude (Degrees W)	Depth	Habitat
1- Dangriga Low	Low_{TP}	17.078	88.01285	3-5 m	Back-reef
2- Dangriga Mod	Mod_{TP}	16.99597	88.08416	3-5 m	Patch reef
3- Dangriga Ext	$High_{TP}$	16.79491	88.27699	3-5 m	Nearshore patch reef
4- Placencia Low	Low_{TP}	16.45816	88.01295	3-5 m	Back-reef
5- Placencia Mod	Mod_{TP}	16.49995	88.16527	3-5 m	Patch reef
6- Placencia Ext	$High_{TP}$	16.4654	88.31315	3-5 m	Nearshore patch reef
7- Sapodilla Low	Low_{TP}	16.15729	88.25073	3-5 m	Back-reef
8- Sapodilla Mod	Mod_{TP}	16.13013	88.33234	3-5 m	Patch reef
9- Sapodilla Ext	$High_{TP}$	16.2245	88.62943	3-5 m	Nearshore patch reef
10-Belize City Low	Low_{TP}	17.54239	88.06509	3-5 m	Back-reef
11- Belize City Mod	Mod_{TP}	17.64363	88.0264	3-5 m	Patch reef
12- Caulker Low	Low_{TP}	17.79846	88.00196	3-5 m	Back-reef
13- Caulker Mod	Mod_{TP}	17.82413	88.02581	3-5 m	Patch reef

Table S1. Site locations: Summary of survey sites, how they were classified, and where they were located (latitude/ longitude).

	NMDS1		NMDS2	
	p-value of slope	R^2	*p*-value of slope	R^2
Avg Annual Max Temp	**0.02**	0.0327	**<0.0001**	0.4154
Avg Annual Range	**0.0001**	0.0926	**<0.0001**	0.4361
Avg Annual Days Above Bleaching Threshold	**0.3**	0.0063	**<0.0001**	0.5644
Avg Annual Consecutive Days Above Bleaching Threshold	**<0.0001**	0.1026	**<0.0001**	0.6039
DOC	**<0.0001**	0.2673	0.5	0.0028
DIN	0.2	0.0093	0.8	0.0172
DON	**<0.0001**	0.3414	**0.02**	0.0338
Chl a	0.5	0.0035	**0.009**	0.0434

Table S2: Summary of *p*- and R^2 values for temperature and nutrient parameters vs. NMDS1 and NMDS 2. Significant *p*-values are in bold.

	low_{TP}		mod_{TP}		$high_{TP}$	
	p-value of slope	R^2	*p*-value of slope	R^2	*p*-value of slope	R^2
Avg Annual Max Temp	**0.01**	0.1119	<**0.0001**	0.6268	<**0.0001**	0.8627
Avg Annual Range	0.442	0.0104	<**0.0001**	0.4389	<**0.0001**	0.9514
Avg Annual Days Above Bleaching Threshold	<**0.0001**	0.9514	**0.04**	0.9514	<**0.0001**	0.9435
Avg Annual Consecutive Days Above Bleaching Threshold	**0.05**	.06612	<**0.0001**	0.6664	<**0.0001**	0.8946
DOC	<**0.0001**	0.3184	<**0.0001**	0.1892	**0.0119**	0.1676
DIN	<**0.0001**	0.2866	**0.0005**	0.5100	<**0.0001**	0.7958
DON	**0.0040**	0.1892	<**0.0001**	0.3611	<**0.0001**	0.7710
Chl a	0.6	0.0058	0.6	0.0046	**0.0006**	0.2878

Table S3. *p*-values and R^2 for Linear Regression of Physical Parameters vs. NMDS1 by Site Type: Summary of *p* and R^2 values for physical parameters vs. NMDS1 by site type. Significant *p*-values are in bold.

City/Town	Census Population 2010	Estimated Mid-year Pop 2010	Estimated Mid-year Pop 2015
Orange Walk	13708	13707	13687
San Pedro	11767	11884	16444
Belize City	57169	57264	60963
Belmopan	13939	14077	19458
Dangriga	9593	9606	10108
Punta Gorda	5351	5365	5910
Country Total	322453	323598	368310

Table S4. Population of major towns in Belize: Populations of major towns in Belize in 2010 and 2015. Data source: Statistical Institute of Belize.

APPENDIX 2: SUPPORTING INFORMATION FOR CHAPTER 3

Tables

Thermal regime	Annual min temp (°C)	Annual max temp (°C)	Annual temp range (°C)	Annual average temp (°C)	Annual winter avg temp (°C)	Annual summer avg temp (°C)	Annual days above bleaching threshold (days/year)	Longest streak of days above bleaching threshold (days/year)	Annual degree heating days (days)
Low_{TP}	25.41	30.74	5.33	28.17	26.38	29.48	41.29	12.40	2.12
Mod_{TP}	25.09	30.85	5.76	28.05	26.34	29.38	51.31	16.23	3.46
$High_{TP}$	24.989	30.99	6.00	28.13	26.49	29.56	55.68	17.16	5.14

Table S1: Temperature parameters for each of the three thermal regimes. Parameters reported are annual averages calculated from NASA JPL MUR SST for the interval 2003-2014 (time of sample collection).

OTU (name)	Blast hit	E-value	OTU accession #
C1.1	C1	$6e^{-177}$	JN558041.1
B1.1	B1	$1e^{-178}$	JN558059.1
C1.II	C1	$3e^{-174}$	JN558041.1
C1.III	C1	$2e^{-175}$	JN558041.1
D1a	D1a	$1e^{-172}$	KU842718.1
B1.II	B1	$2e^{-171}$	JN558059.1
G3	G3	$2e^{-161}$	LK392377.1
A4a	A4a	$4e^{-158}$	FN429762.1
B.BG	B19	$8e^{-145}$	DQ865212.1
C3	C3	$8e^{-150}$	HG515026.1

Table S2: NCBI Blast hits, E-values, and accession numbers for each OTU.

Illumina Lane	Raw reads	Trimmed reads	Mapped reads	Mapping efficiency
1	69187	48461	36793	73%
2	17834	2098	1521	72%

Table S3: Average number of raw reads, trimmed reads, and mapped reads including mapping efficiency (% of trimmed reads that mapped) for each lane of Illumina.

Model		Degrees of freedom	Sum Squares	Mean Squares	F Model	R^2	*P*-value
All species x species	Species	2	4.0163	2.008	25.506	0.285	**0.001**
	Residuals	128	10.0775	0.079		0.715	
	Total	130	14.0938			1.000	
SSID x thermal regime	Thermal Regime	2	0.279	0.140	3.869	0.090	**0.001**
	Residuals	78	2.812	0.036		0.910	
	Total	80	3.091			1.000	
SSID x latitude	Latitude	3	0.246	0.082	2.224	0.078	**0.025**
	Residuals	77	2.845	0.037		0.920	
	Total	80	3.091			1.000	
SSID x site	Site	9	0.859	0.078	2.414	0.278	**0.013**
	Residuals	71	2.232	0.032		0.722	
	Total	80	3.091			1.000	
SRAD x thermal regime	Thermal Regime	2	0.270	0.135	2.030	0.135	0.098
	Residuals	26	1.729	0.066		0.865	
	Total	28	1.999			1.000	
SRAD x latitude	Latitude	1	0.066	0.066	0.958	0.034	0.367
	Residuals	27	1.930	0.071		0.966	
	Total	28	1.999			1.000	
SRAD x site	Site	3	0.277	0.092	1.343	0.139	0.235
	Residuals	25	1.722	0.069		0.861	
	Total	28	1.999			1.000	
PSTR x thermal regime	Thermal Regime	2	0.323	0.162	1.715	0.160	0.139
	Residuals	18	1.697	0.094		0.840	
	Total	20	2.020			1.000	
PSTR x latitude	Latitude	1	0.067	0.067	0.656	0.033	0.294
	Residuals	19	1.953	0.103		0.967	
	Total	20	2.020			1.000	
PSTR x site	Site	3	0.344	0.115	1.163	0.170	0.572
	Residuals	17	1.676	0.099		0.830	
	Total	20	2.020			1.000	

Table S4: Results of PERMANOVA on principal component analysis of *Symbiodinium* communities between coral species' and within coral species by thermal regime, individual site, and latitudinal transect. Significant *p-values* ($p<0.05$) are in bold.

Species	Thermal Regime	C1.1	B1.1	C1.II	C1.III	D1a	B1.II	G3	A4a	B.BG	C3
SSID	Low_{TP}	63.68 %	4.42%	0.53%	15.23 %	16.10 %	0.03%	N/A	0.02%	0.01%	N/A
	Mod_{TP}	68.59 %	0.07%	<0.01 %	19.11 %	11.43 %	<0.01 %	N/A	0.79%	<0.01 %	N/A
	$High_{TP}$	86.11 %	2.51%	0.08%	8.84%	2.34%	0.02%	<0.01 %	0.02%	0.08%	N/A
	All	74.39 %	2.94%	0.25%	12.94 %	9.29%	0.02%	<0.01 %	0.13%	0.04%	N/A
SRAD	Low_{TP}	34.24 %	51.73 %	0.03%	8.44%	0.02%	5.20%	N/A	0.16%	N/A	0.17 %
	Mod_{TP}	2.06%	71.82 %	25.73 %	0.20%	0.15%	0.04%	N/A	<0.01 %	N/A	N/A
	$High_{TP}$	8.99%	78.27 %	<0.01 %	0.20%	0.13%	10.20 %	2.22%	N/A	<0.01 %	N/A
	All	13.41 %	70.31 %	6.22%	2.19%	0.11%	6.54%	1.15%	0.04%	<0.01 %	0.41 %
PSTR	Low_{TP}	2.64%	40.00 %	57.28 %	0.03%	<0.01 %	0.01%	0.01%	0.01%	<0.01 %	N/A
	Mod_{TP}	29.48 %	55.59 %	0.02%	10.39 %	4.47%	0.05%	N/A	N/A	N/A	N/A
	$High_{TP}$	22.85 %	54.32 %	17.14 %	2.51%	0.19%	<0.01 %	N/A	0.17%	2.90%	N/A
	All	21.87 %	51.74 %	16.92 %	6.24%	2.48%	0.03%	<0.01 %	0.04%	0.66%	N/A

Table S5: Relative abundance of each *Symbiodinium* lineage within each species of coral host at each thermal regime. N/A indicates that the haplotype in question was not present.

Reference Sequence	GenBank Accession Number	Associated Publication
G3*	AM748600	Pochon et al., 2007
D1a*	EU074894	Thornhill et al., 2009
A4a.1*	FN429762	Green et al., 2009
B1*	KP730723	Kemp et al., 2015
C3*	AJ621536	Pochon et al., 2004
C1*	KR002400	Grajales et al., 2015

Table S6: GenBank accession numbers and associated publications for reference sequences used in constructing phylogeny (Fig 2).

Figures

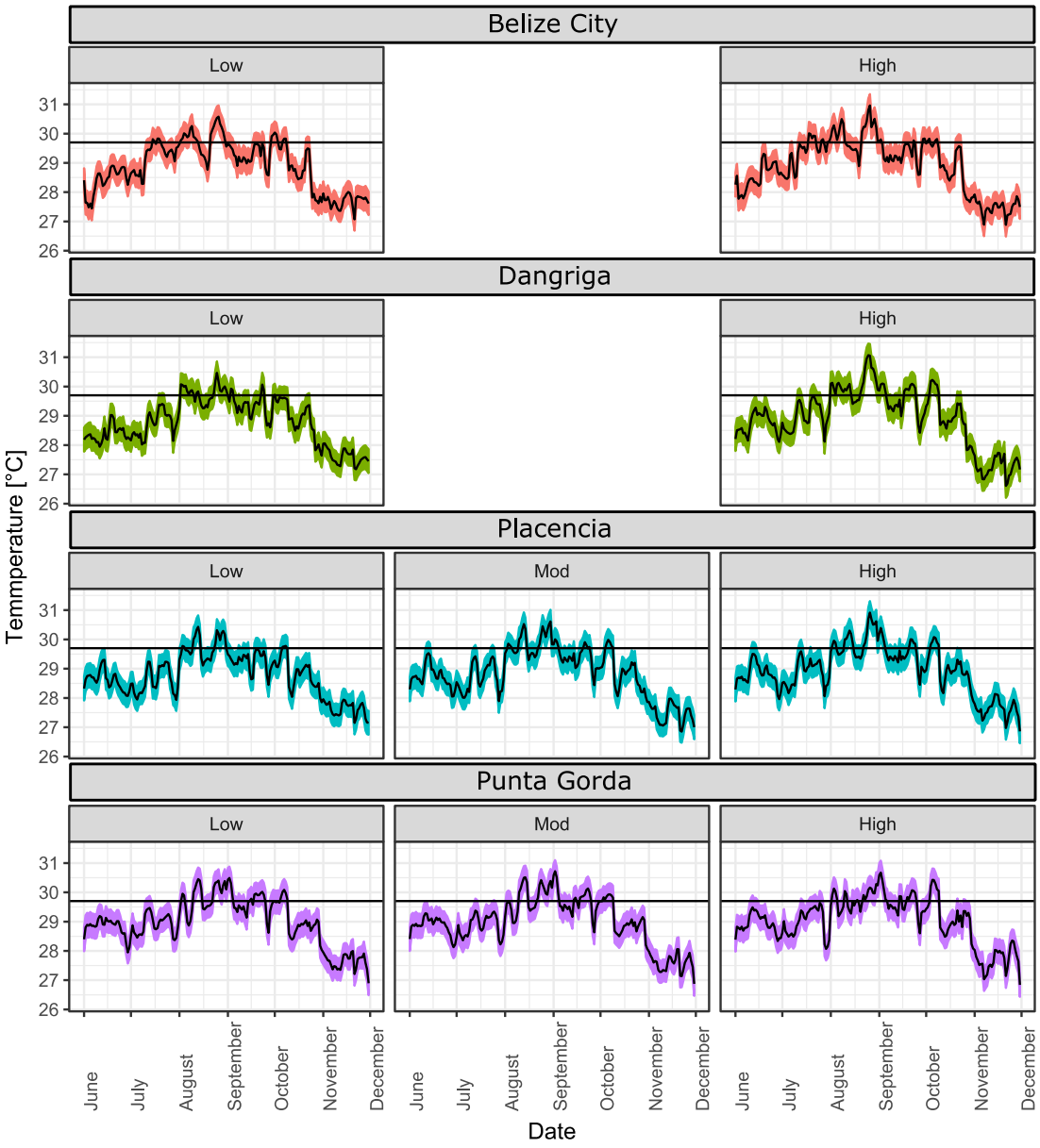

Fig S1: MUR SST values for each sampling site from June 2014- December 2014. The black horizontal line indicates the published bleaching threshold of 29.7°C for Belize.

APPENDIX 3: SUPPORTING INFORMATION FOR CHAPTER 4

Tables

Species	ANOVA parameter	Df	Sum sq	Mean Sq	F value	*p*-value
S. siderea	Reef Zone	4	8.170	2.042	171.76	**<0.001**
	Bins	12	0.280	0.023	1.960	**0.024**
	Reef Zone: Bins	48	0.620	0.013	1.080	0.325
	Residuals	4241	50.420	0.012		
	Tukey HSD results	**Reef Zone**	**diff**	**lwr**	**upr**	***p*-value**
		FR-ABR	0.069	0.044	0.093	**<0.001**
		NS-ABR	0.154	0.128	0.180	**<0.001**
		FR-AFR	0.049	0.025	0.074	**<0.001**
		NS-AFR	0.135	0.109	0.161	**<0.001**
		FR-BR	0.038	0.020	0.055	**<0.001**
		NS-BR	0.123	0.104	0.143	**<0.001**
		NS-FR	0.086	0.066	0.106	**<0.001**
	Bins	**Reef Zone: Bins**	**diff**	**lwr**	**upr**	***p*-value**
	1950-1954	NS:FR	0.034	-0.059	0.128	1.000
	1955-1959	NS:FR	-0.001	-0.091	0.088	1.000
	1960-1964	NS:FR	0.053	-0.033	0.139	0.976
	1965-1969	NS:FR	0.090	0.008	0.172	**0.011**
	1970-1974	NS:FR	0.068	-0.001	0.146	0.271
	1975-1989	NS:FR	0.065	-0.013	0.142	0.363
	1980-1984	NS:FR	0.076	0.000	0.153	0.053
	1985-1989	NS:FR	0.067	-0.008	0.142	0.196
	1990-1994	NS:FR	0.113	0.043	0.184	**<0.001**
	1995-1999	NS:FR	0.079	0.011	0.147	**<0.001**
	2000-2004	NS:FR	0.098	0.035	0.161	**<0.001**
	2005-2009	NS:FR	0.085	0.022	0.148	**<0.001**
	2010-2014	NS:FR	0.035	-0.046	0.116	1.000

Table S1: Results of ANOVA and Tukey HSD tests of binned five-year averaged extension rates by reef zone (Fig 2C, Fig 3C) for *S. siderea*. The significance cutoff was $p<0.05$. For *S. siderea*, the interaction between reef zone and five-year bins was not significant, but pairwise

comparisons of nearshore and forereef at each bin are still ecologically relevant. Only significant (p<0.05) p-values are shown for Tukey results except for the interactive effects of Reef Zone:Bins, where all p-values are shown.

Species	**ANOVA parameter**	**Df**	**Sum sq**	**Mean Sq**	**F value**	***p*-value**
P. strigosa	Reef Zone	1	9.070	9.069	220.199	**<0.001**
	Bins	12	1.700	0.142	3.441	**<0.001**
	Reef Zone: Bins	9	1.100	0.122	2.958	**0.002**
	Residuals	837	34.470	0.041		
	Tukey HSD results	**Reef Zone**	**diff**	**lwr**	**upr**	***p*-value**
		NS-FR	0.208	0.181	0.236	**<0.001**
		Bins	**diff**	**lwr**	**Upr**	***p*-value**
		2010s-2000s	-0.078	-0.148	-0.009	**0.018**
	Bins	**Reef Zone: Bins**	**diff**	**lwr**	**upr**	***p*-value**
	1950-1954	NS:FR	N/A	N/A	N/A	N/A
	1955-1959	NS:FR	N/A	N/A	N/A	N/A
	1960-1964	NS:FR	N/A	N/A	N/A	N/A
	1965-1969	NS:FR	0.301	-0.162	0.765	0.786
	1970-1974	NS:FR	0.231	-0.142	0.604	0.853
	1975-1989	NS:FR	0.224	-0.140	0.587	0.861
	1980-1984	NS:FR	0.307	0.023	0.590	0.017
	1985-1989	NS:FR	0.290	0.0117	0.463	**<0.001**
	1990-1994	NS:FR	0.160	-0.002	0.322	0.059
	1995-1999	NS:FR	0.240	0.094	0.386	**<0.001**
	2000-2004	NS:FR	0.259	0.128	0.391	**<0.001**
	2005-2009	NS:FR	0.126	0.003	0.249	**0.039**
	2010-2014	NS:FR	0.091	-0.029	0.212	0.477

Table S2: Results of ANOVA and Tukey HSD tests of binned five-year averaged extension rates by reef zone (Fig 2C, Fig 3C) for *P. strigosa*. The significance cutoff was p<0.05. For *P. strigosa*, both parameters of the ANOVA and their interaction were significant. However, only significant differences between reef zones within the same five-year bin are shown, as they are most pertinent to the study question. Only significant (p<0.05) p-values are shown for Tukey results, except for the interactive effects of Reef Zone:Bins, where all p-values are shown.

Core ID	species	Year collected	Latitude	Longitude
BCL-P-1	*P. strigosa*	2015	17.64363	-88.0264
BCL-P-2	*P. strigosa*	2015	17.64363	-88.0264
BCL-P-3	*P. strigosa*	2015	17.64363	-88.0264
BCL-S-1	*S. siderea*	2015	17.64363	-88.0264
BCL-S-2	*S. siderea*	2015	17.64363	-88.0264
BCL-S-3	*S. siderea*	2015	17.64363	-88.0264
BR-06	*S. siderea*	2009	16.14045	-88.26015
BR-07	*S. siderea*	2009	16.14067	-88.260067
BR-08	*S. siderea*	2009	16.14167	-88.26
BRA	*S. siderea*	2012	18.00000	-87.904167
BRB	*S. siderea*	2012	18.00006	-87.904556
BRC	*S. siderea*	2012	18.00006	-87.904556
BRD	*S. siderea*	2012	17.83358	-87.992694
BRE	*S. siderea*	2012	17.83358	-87.992694
BRF	*S. siderea*	2012	17.50444	-88.049722
BRG	*S. siderea*	2012	17.50444	-88.049722
BRH	*S. siderea*	2012	17.50444	-88.049722
BRI	*S. siderea*	2012	17.29936	-87.803972
BRJ	*S. siderea*	2012	17.29936	-87.803972
BRK	*S. siderea*	2012	17.30267	-87.802333
BRL	*S. siderea*	2012	17.21122	-87.557139
BRM	*S. siderea*	2012	17.21122	-87.557139
BRN	*S. siderea*	2012	17.21122	-87.557139

BRO	*S. siderea*	2012	16.72683	-87.846028
BRP	*S. siderea*	2012	16.72683	-87.846028
BRQ	*S. siderea*	2012	16.72683	-87.846028
BRR	*S. siderea*	2012	16.88745	-88.066
BRS	*S. siderea*	2012	16.88745	-88.066
BRT	*S. siderea*	2012	16.88745	-88.066
BRU	*S. siderea*	2012	17.40353	-88.03825
BRV	*S. siderea*	2012	17.40353	-88.03825
BRW	*S. siderea*	2012	17.40353	-88.03825
DL-S-1	*S. siderea*	2015	17.078	-88.01285
DL-S-2	*S. siderea*	2015	17.078	-88.01285
DL-S-3	*S. siderea*	2015	17.078	-88.01285
DL-S-4	*S. siderea*	2015	17.078	-88.01285
DL-S-5	*S. siderea*	2015	17.078	-88.01285
FR-02	*S. siderea*	2009	16.13715	-88.252883
FR-04	*S. siderea*	2009	16.13722	-88.253167
FR-05	*S. siderea*	2009	16.13722	-88.253783
FR-09	*S. siderea*	2009	16.0917	-88.287933
FR-11	*S. siderea*	2009	16.09812	-88.27235
FR-12	*S. siderea*	2009	16.10227	-88.27235
FR-13	*S. siderea*	2009	16.1033	-88.2686
FRA	*S. siderea*	2012	17.97228	-87.916417
FRB	*S. siderea*	2012	17.97228	-87.916417
FRC	*S. siderea*	2012	17.49561	-88.045278
FRD	*S. siderea*	2012	17.49561	-88.045278
FRE	*S. siderea*	2012	17.49561	-88.045278
FRF	*S. siderea*	2012	17.27889	-87.810278
FRG	*S. siderea*	2012	17.27889	-87.810278
FRH	*S. siderea*	2012	17.27867	-87.8105
FRI	*S. siderea*	2012	17.20811	-87.55725

FRJ	*S. siderea*	2012	17.20811	-87.55725
FRK	*S. siderea*	2012	17.20811	-87.5575
FRL	*S. siderea*	2012	16.71056	-87.854167
FRM	*S. siderea*	2012	16.71056	-87.854167
FRN	*S. siderea*	2012	16.71056	-87.854167
FRO	*S. siderea*	2012	16.50817	-87.984694
FRP	*S. siderea*	2012	16.50817	-87.984694
FRQ	*S. siderea*	2012	16.50817	-87.984694
FRR	*S. siderea*	2012	17.19467	-88.052333
FRS	*S. siderea*	2012	17.19467	-88.052333
G-IR-BZ-40-S	*S. siderea*	2015	17.48683	88.12069
G-IR-BZ-41-S	*S. siderea*	2015	17.48684	88.12069
G-IR-BZ-43-S	*S. siderea*	2015	17.48683	88.12067
G-IR-BZ-44-P	*P. strigosa*	2015	17.48683	88.12064
G-IR-BZ-45-P	*P. strigosa*	2015	17.48694	88.12061
G-IR-BZ-46-P	*P. strigosa*	2015	17.48699	88.12048
G-IR-DG-23-S	*S. siderea*	2015	16.79468	88.27585
G-IR-DG-24-S	*S. siderea*	2015	16.79451	88.27585
G-IR-DG-25-S	*S. siderea*	2015	16.79463	88.27573
G-IR-DG-26-P	*P. strigosa*	2015	16.79474	88.27563
G-IR-DG-27-P	*P. strigosa*	2015	16.79474	88.27568
G-IR-DG-28-S	*S. siderea*	2015	16.79478	88.27568
G-IR-DG-29-S	*S. siderea*	2015	16.79484	88.27561

G-IR-DG-30-P	*P. strigosa*	2015	16.79466	88.27583
G-IR-DG-31-P	*P. strigosa*	2015	16.79484	88.27502
G-IR-DG-32-P	*P. strigosa*	2015	16.79471	88.27676
G-IR-PC-51-P	*P. strigosa*	2015	16.46482	88.31298
G-IR-PC-52-P	*P. strigosa*	2015	16.46472	88.31308
G-IR-PC-53-P	*P. strigosa*	2015	16.46472	88.31321
G-IR-PC-54-S	*S. siderea*	2015	16.46453	88.31326
G-IR-PC-55-S	*S. siderea*	2015	16.46451	88.31331
G-IR-PC-56-P	*P. strigosa*	2015	16.46441	88.31346
G-IR-PC-57-P	*P. strigosa*	2015	16.46417	88.31373
G-IR-PH-01-S	*S. siderea*	2015	16.22445	-88.62798
G-IR-PH-02-S	*S. siderea*	2015	16.19226	-88.62881
G-IR-PH-03-P	*P. strigosa*	2015	16.19225	-88.62853
G-IR-PH-04-P	*P. strigosa*	2015	16.19324	-88.62814
G-IR-PH-05-P	*P. strigosa*	2015	16.19334	-88.62817
G-IR-PH-06-P	*P. strigosa*	2015	16.19334	-88.62817
G-IR-PH-07-P	*P. strigosa*	2015	16.19309	-88.62824
G-OR-GP-58-P	*P. strigosa*	2015	17.38327	-88.01745
G-OR-GP-59-S	*S. siderea*	2015	17.38347	-88.01757
G-OR-GP-60-P	*P. strigosa*	2015	17.38347	-88.01757
G-OR-GP-61-P	*P. strigosa*	2015	17.38342	-88.01758
G-OR-GP-62-S	*S. siderea*	2015	17.38348	-88.01761
G-OR-GP-63-P	*P. strigosa*	2015	17.38349	-88.01755

G-OR-GP-64-P	*P. strigosa*	2015	17.38352	-88.01754
G-OR-GS-33-S	*S. siderea*	2015	16.48028	87.99103
G-OR-GS-34-S	*S. siderea*	2015	16.4803	87.99087
G-OR-GS-35-P	*P. strigosa*	2015	16.48015	87.9907
G-OR-GS-36-P	*P. strigosa*	2015	16.48018	87.99065
G-OR-GS-37-P	*P. strigosa*	2015	16.48013	87.99047
G-OR-GS-38-P	*P. strigosa*	2015	16.48004	87.99036
G-OR-GS-39-P	*P. strigosa*	2015	16.47999	87.99022
G-OR-SC-08-P	*P. strigosa*	2015	16.15124	-88.23985
G-OR-SC-09-P	*P. strigosa*	2015	16.15124	-88.23985
G-OR-SC-10-P	*P. strigosa*	2015	16.15124	-88.23985
G-OR-SC-11-P	*P. strigosa*	2015	16.15124	-88.23985
G-OR-SC-12-P	*P. strigosa*	2015	16.15124	-88.23925
G-OR-TC-13-S	*S. siderea*	2015	17.05705	-88.00252
G-OR-TC-14-P	*P. strigosa*	2015	17.05705	-88.00254
G-OR-TC-15-P	*P. strigosa*	2015	17.05698	-88.00236
G-OR-TC-16-P	*P. strigosa*	2015	17.05698	-88.00236
G-OR-TC-17-P	*P. strigosa*	2015	17.05711	-88.0022
G-OR-TC-18-S	*S. siderea*	2015	17.05496	-87.95861
G-OR-TC-19-S	*S. siderea*	2015	17.05496	-87.95861
G-OR-TC-20-S	*S. siderea*	2015	17.05496	-87.95861
G-OR-TC-21-P	*P. strigosa*	2015	17.05501	-87.95867
G-OR-TC-22-S	*S. siderea*	2015	17.05501	-87.95878

GS-P-1	*P. strigosa*	2015	16.45816	-88.01285
GS-P-2	*P. strigosa*	2015	16.45816	-88.01285
GS-S-1	*S. siderea*	2015	16.45816	-88.01285
GS-S-2	*S. siderea*	2015	16.45816	-88.01285
GS-S-3	*S. siderea*	2015	16.45816	-88.01285
GS-S-4	*S. siderea*	2015	16.45816	-88.01285
GS-S-5	*S. siderea*	2015	16.45816	-88.01285
NS-14	*S. siderea*	2009	16.19238	-88.567633
NS-15	*S. siderea*	2009	16.19195	-88.568067
NS-16	*S. siderea*	2009	16.19163	-88.5684
NSA	*S. siderea*	2012	16.51019	-88.272944
NSB	*S. siderea*	2012	16.51019	-88.272944
NSC	*S. siderea*	2012	16.51019	-88.272944
SL-S-1	*S. siderea*	2015	16.15701	-88.25074
SL-S-2	*S. siderea*	2015	16.15704	-88.25074
SL-S-3	*S. siderea*	2015	16.15715	-88.25074

Table S3: Core ID numbers and GPS locations for all cores collected in 2009, 2012, and 2015.

Species	Time Scale	Linear mixed effects model	ARMA parameters	AIC
S. siderea	1814-present	$\text{Extension}_{ij} = \beta_0 + u_{0i} + \beta_1(\text{Year}_{ij} - 2013) + \varepsilon_{ij}$	N/A	-12796.45
		$\text{Extension}_{ij} = \beta_0 + u_{0i} + \beta_1(\text{Year}_{ij} - 2013) + \varepsilon_{ij}$	(1, 0)	-13140.24
		$\text{Extension}_{ij} = \beta_0 + u_{0i} + \beta_1(\text{Year}_{ij} - 2013) + \varepsilon_{ij}$	(0, 1)	-13086.33
		$\text{Extension}_{ij} = \beta_0 + u_{0i} + \beta_1(\text{Year}_{ij} - 2013) + \varepsilon_{ij}$	(0, 2)	-13139.42
		$\text{Extension}_{ij} = \beta_0 + u_{0i} + \beta_1(\text{Year}_{ij} - 2013) + \varepsilon_{ij}$	(1, 1)	-13240.46
		$\text{Extension}_{ij} = \beta_0 + u_{0i} + \beta_1(\text{Year}_{ij} - 2013) + \varepsilon_{ij}$	(2, 0)	-13177.59
		$\text{Extension}_{ij} = \beta_0 + u_{0i} + \beta_1(\text{Year}_{ij} - 2013)*\text{reef\_zone} + \varepsilon_{ij}$	(1, 1)	**-13270.12**
		$\text{Extension}_{ij} = \beta_0 + u_{0i} + \beta_1(\text{Year}_{ij} - 2013)*\text{transect} + \varepsilon_{ij}$	(1, 1)	-13243.53
		$\text{Extension}_{ij} = \beta_0 + u_{0i} + \beta_1(\text{Year}_{ij} - 2013)*\text{site} + \varepsilon_{ij}$	(1, 1)	-13269.41
	1980-present	$\text{Extension}_{ij} = \beta_0 + u_{0i} + \beta_1(\text{Year}_{ij} - 2013) + \varepsilon_{ij}$	N/A	-5248.548
		$\text{Extension}_{ij} = \beta_0 + u_{0i} + \beta_1(\text{Year}_{ij} - 2013) + \varepsilon_{ij}$	(1, 0)	-5305.349
		$\text{Extension}_{ij} = \beta_0 + u_{0i} + \beta_1(\text{Year}_{ij} - 2013) + \varepsilon_{ij}$	(0, 1)	-5295.490
		$\text{Extension}_{ij} = \beta_0 + u_{0i} + \beta_1(\text{Year}_{ij} - 2013) + \varepsilon_{ij}$	(0, 2)	-5315.134
		$\text{Extension}_{ij} = \beta_0 + u_{0i} + \beta_1(\text{Year}_{ij} - 2013) + \varepsilon_{ij}$	(1, 1)	-5335.969
		$\text{Extension}_{ij} = \beta_0 + u_{0i} + \beta_1(\text{Year}_{ij} - 2013) + \varepsilon_{ij}$	(2, 0)	-5325.521

		$Extension_{ij} = \beta_0 + u_{0i} + \beta_1(Year_{ij} - 2013)*reef\_zone + \varepsilon_{ij}$	(1, 1)	**-5366.971**
		$Extension_{ij} = \beta_0 + u_{0i} + \beta_1(Year_{ij} - 2013)*transect + \varepsilon_{ij}$	(1, 1)	Failed to converge
		$Extension_{ij} = \beta_0 + u_{0i} + \beta_1(Year_{ij} - 2013)*site + \varepsilon_{ij}$	(1, 1)	Failed to converge
P. strigosa	1950-present	$Extension_{ij} = \beta_0 + u_{0i} + \beta_1(Year_{ij} - 2012) + \varepsilon_{ij}$	N/A	-563.8245
		$Extension_{ij} = \beta_0 + u_{0i} + \beta_1(Year_{ij} - 2012) + \varepsilon_{ij}$	(1, 0)	-591.6096
		$Extension_{ij} = \beta_0 + u_{0i} + \beta_1(Year_{ij} - 2012) + \varepsilon_{ij}$	(0, 1)	-587.3708
		$Extension_{ij} = \beta_0 + u_{0i} + \beta_1(Year_{ij} - 2012) + \varepsilon_{ij}$	(0, 2)	-592.3536
		$Extension_{ij} = \beta_0 + u_{0i} + \beta_1(Year_{ij} - 2012) + \varepsilon_{ij}$	(1, 1)	-592.3774
		$Extension_{ij} = \beta_0 + u_{0i} + \beta_1(Year_{ij} - 2012) + \varepsilon_{ij}$	(2, 0)	-592.6698
		$Extension_{ij} = \beta_0 + u_{0i} + \beta_1(Year_{ij} - 2012)*reef\_zone + \varepsilon_{ij}$	(2, 0)	**-596.5716**
		$Extension_{ij} = \beta_0 + u_{0i} + \beta_1(Year_{ij} - 2012)*transect + \varepsilon_{ij}$	(2, 0)	Failed to converge
		$Extension_{ij} = \beta_0 + u_{0i} + \beta_1(Year_{ij} - 2012)*site + \varepsilon_{ij}$	(2, 0)	-594.9496
	1980-present	$Extension_{ij} = \beta_0 + u_{0i} + \beta_1(Year_{ij} - 2012) + \varepsilon_{ij}$	N/A	-408.4174
		$Extension_{ij} = \beta_0 + u_{0i} + \beta_1(Year_{ij} - 2012)*reef\_zone + \varepsilon_{ij}$	N/A	**-410.9907**
		$Extension_{ij} = \beta_0 + u_{0i} + \beta_1(Year_{ij} - 2012)*transect + \varepsilon_{ij}$	N/A	-403.3668
		$Extension_{ij} = \beta_0 + u_{0i} + \beta_1(Year_{ij} - 2012)*site + \varepsilon_{ij}$	N/A	-406.5723

Table S4: Linear mixed effects model testing for extension of *S. siderea* (1814-present). Underlined AIC value indicates best ARMA correlation structure for general model. Bold AIC value indicates the model with best (lowest) AIC, which was then used in the subsequent analysis. For all species and timescales, a model with reef zone as a fixed factor had the lowest AIC. ARMA parameters varied by species and timescale. For *P. strigosa* (1980-present), no ARMA parameters were used as all models including ARMA failed to converge. ARMA (1, 1) correlation structure combines an autoregressive model of order 1 with a moving average model of order 1. Here "*i*" references the core and "*j*" denotes an individual annual observation within that core. The term "u_{0i}" denotes the random intercept, which is constant for observations coming from the same core but different for observations coming from different cores.

Species	**Reef Zone**	**Year**	**Estimated value**	**SE**	**t- value**	***p*-value**
S. siderea	Nearshore	1985	0.314	0.080	3.937	<0.001
		2011	0.314	0.080	3.937	<0.001
		2014	0.164	0.080	2.056	0.044
	Backreef	1921	0.141	0.067	2.109	0.038
		1923	0.252	0.067	3.771	<0.001
		1925	0.252	0.067	3.771	<0.001
		1926	0.141	0.067	2.109	0.038
		1955	0.276	0.067	4.127	<0.001
	Forereef	1930	0.125	0.056	2.240	0.028
		1958	0.125	0.056	2.240	0.028
		1972	0.175	0.056	3.135	0.002
		2014	0.175	0.056	3.135	0.002
	Atoll Backreef	1997	0.251	0.095	2.648	0.011
		2004	0.473	0.095	4.993	<0.001
		2005	0.362	0.095	3.821	<0.001
		2006	0.251	0.095	2.648	0.011
	Atoll Forereef	1954	0.253	0.077	3.279	0.002
		1961	0.205	0.077	2.662	0.011
		1970	0.205	0.077	2.662	0.011
		1977	0.205	0.077	2.662	0.011
		1996	0.364	0.077	4.719	<0.001
P. strigosa	Nearshore	1992	0.218	0.087	2.516	0.022
		2011	0.245	0.087	2.825	0.012
	Forereef	2014	0.173	0.080	2.170	0.039

Table S5: Results of least squares regression models of extension anomaly. Only significant *p*-values (<0.05) are reported here. Significance indicates that extension within the specified species and reef zone was significantly lower in the tested year than the mean modeled extension anomaly ratio for the reef zone.

S. siderea		DF	Sum Sq	Mean Sq	F value	*p*-value
	Bleaching years vs. non-bleaching years	1	0.149	0.149	19.079	**<0.001**
	Reef zone	4	0.016	0.004	0.524	0.7183
	BL years: reef zone	4	0.124	0.031	3.973	**0.004**
	Residuals	367	2.861	0.008		
P. strigosa		**DF**	**Sum Sq**	**Mean Sq**	**F value**	***p*-value**
	Bleaching years vs. non-bleaching years	1	0.008	0.008	0.980	0.326
	Reef zone	1	0.002	0.002	0.228	0.635
	BL years: reef zone	1	0.003	0.003	0.361	0.550
	Residuals	63	0.518	0.008		

Table S6: ANOVA results for fraction of corals with low extension by bleaching vs. non-bleaching year and reef zone.

	DF	**Sum Sq**	**Mean Sq**	**F value**	***p*-value**
Core ID	17	11.43	0.6725	57.61	**<0.001**
Residuals	1017	11.87	0.0117		

Table S7: ANOVA results for average core extension rate (cm/yr) in nearshore *S. siderea* corals.

Core ID	diff	lwr	upr	p-value
GIRBZ43S-GIRBZ40S	-0.16508	-0.29548	-0.03469	0.0014393
GIRDG23S-GIRBZ43S	0.131198	0.000798	0.261597	0.0466792
GIRDG24S-GIRBZ43S	0.150038	0.019638	0.280437	0.0076711
GIRDG28S-GIRBZ43S	0.159479	0.044179	0.274779	<0.001
GIRPC54S-GIRBZ41S	0.166003	0.07811	0.253895	<0.001
GIRPC54S-GIRBZ43S	0.218337	0.124458	0.312217	<0.001
GIRPC54S-GIRDG25S	0.161652	0.077314	0.24599	<0.001
GIRPC55S-GIRBZ41S	0.137215	0.044944	0.229486	<0.001
GIRPC55S-GIRBZ43S	0.18955	0.091559	0.287541	<0.001
GIRPC55S-GIRDG25S	0.132864	0.043972	0.221757	<0.001
GIRPH01S-GIRBZ41S	0.113717	0.027955	0.199479	<0.001
GIRPH01S-GIRBZ43S	0.166052	0.074164	0.25794	<0.001
GIRPH01S-GIRDG25S	0.109366	0.027251	0.191482	<0.001
GIRPH02S-GIRBZ43S	0.134289	0.03405	0.234527	<0.001
GIRPH02S-GIRPC54S	-0.08405	-0.15656	-0.01154	0.0068265
NS14-GIRBZ40S	-0.17836	-0.28957	-0.06716	<0.001
NS14-GIRDG23S	-0.14447	-0.25568	-0.03327	<0.001
NS14-GIRDG24S	-0.16331	-0.27452	-0.05211	<0.001
NS14-GIRDG28S	-0.17275	-0.2658	-0.07971	<0.001
NS14-GIRDG29S	-0.14317	-0.25437	-0.03196	0.0010335
NS14-GIRPC54S	-0.23161	-0.29623	-0.16699	<0.001
NS14-GIRPC55S	-0.20283	-0.27329	-0.13236	<0.001
NS14-GIRPH01S	-0.17933	-0.24102	-0.11764	<0.001
NS14-GIRPH02S	-0.14756	-0.22112	-0.07401	<0.001
NS15-GIRBZ40S	-0.26154	-0.37012	-0.15296	<0.001
NS15-GIRBZ41S	-0.14879	-0.23423	-0.06335	<0.001
NS15-GIRBZ43S	-0.09645	-0.18804	-0.00486	0.0269485
NS15-GIRDG23S	-0.22765	-0.33623	-0.11907	<0.001

NS15-GIRDG24S	-0.24649	-0.35507	-0.13791	<0.001
NS15-GIRDG25S	-0.15314	-0.23492	-0.07136	<0.001
NS15-GIRDG28S	-0.25593	-0.34582	-0.16605	<0.001
NS15-GIRDG29S	-0.22634	-0.33492	-0.11777	<0.001
NS15-GIRPC54S	-0.31479	-0.37478	-0.2548	<0.001
NS15-GIRPC55S	-0.286	-0.35224	-0.21976	<0.001
NS15-GIRPH01S	-0.26251	-0.31933	-0.20568	<0.001
NS15-GIRPH02S	-0.23074	-0.30026	-0.16122	<0.001
NS15-NS14	-0.08318	-0.14443	-0.02193	<0.001
NS16-GIRBZ40S	-0.26426	-0.36962	-0.1589	<0.001
NS16-GIRBZ41S	-0.15151	-0.23282	-0.0702	<0.001
NS16-GIRBZ43S	-0.09917	-0.18692	-0.01142	0.010105
NS16-GIRDG23S	-0.23037	-0.33573	-0.12501	<0.001
NS16-GIRDG24S	-0.24921	-0.35457	-0.14385	<0.001
NS16-GIRDG25S	-0.15586	-0.23331	-0.0784	<0.001
NS16-GIRDG28S	-0.25865	-0.34462	-0.17268	<0.001
NS16-GIRDG29S	-0.22906	-0.33442	-0.1237	<0.001
NS16-GIRPC54S	-0.31751	-0.37146	-0.26357	<0.001
NS16-GIRPC55S	-0.28872	-0.34954	-0.2279	<0.001
NS16-GIRPH01S	-0.26522	-0.31562	-0.21483	<0.001
NS16-GIRPH02S	-0.23346	-0.29784	-0.16908	<0.001
NS16-NS14	-0.0859	-0.14124	-0.03056	<0.001
NSA-GIRDG28S	-0.09882	-0.19415	-0.00348	0.032877
NSA-GIRPC54S	-0.15767	-0.22556	-0.08979	<0.001
NSA-GIRPC55S	-0.12889	-0.20236	-0.05542	<0.001
NSA-GIRPH01S	-0.10539	-0.17049	-0.04028	<0.001
NSA-NS14	0.073938	0.004938	0.142939	0.0214988
NSA-NS15	0.157117	0.092433	0.221801	<0.001
NSA-NS16	0.159836	0.100715	0.218957	<0.001
NSB-GIRBZ40S	-0.16149	-0.26667	-0.05631	<0.001
NSB-GIRDG23S	-0.1276	-0.23278	-0.02242	0.003169
NSB-GIRDG24S	-0.14644	-0.25162	-0.04127	<0.001
NSB-GIRDG28S	-0.15589	-0.24164	-0.07014	<0.001
NSB-GIRDG29S	-0.1263	-0.23148	-0.02112	0.0037945
NSB-GIRPC54S	-0.21474	-0.26834	-0.16115	<0.001
NSB-GIRPC55S	-0.18596	-0.24646	-0.12545	<0.001
NSB-GIRPH01S	-0.16246	-0.21248	-0.11244	<0.001
NSB-GIRPH02S	-0.1307	-0.19478	-0.06661	<0.001
NSB-NS15	0.100047	0.050575	0.149519	<0.001
NSB-NS16	0.102766	0.060828	0.144703	<0.001
NSC-GIRBZ40S	-0.15796	-0.26623	-0.04969	<0.001

NSC-GIRDG23S	-0.12407	-0.23234	-0.0158	0.0081705
NSC-GIRDG24S	-0.14291	-0.25118	-0.03464	<0.001
NSC-GIRDG28S	-0.15235	-0.24186	-0.06284	<0.001
NSC-GIRDG29S	-0.12276	-0.23103	-0.0145	0.0096164
NSC-GIRPC54S	-0.21121	-0.27064	-0.15179	<0.001
NSC-GIRPC55S	-0.18242	-0.24815	-0.1167	<0.001
NSC-GIRPH01S	-0.15893	-0.21515	-0.1027	<0.001
NSC-GIRPH02S	-0.12716	-0.1962	-0.05813	<0.001
NSC-NS15	0.10358	0.047844	0.159316	<0.001
NSC-NS16	0.106299	0.057128	0.15547	<0.001

Table S8: TukeyHSD results for average core extension rate (cm/yr) in nearshore *S. siderea* corals.

Figures

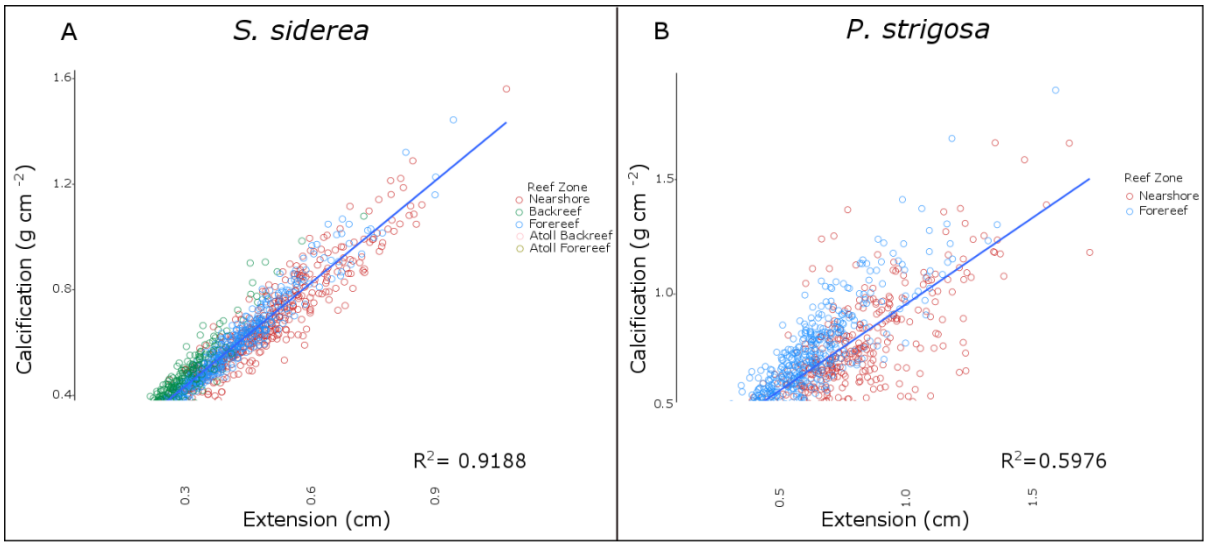

Fig S1: Property-property plots of extension vs calcification *S. siderea* (A) and *P. strigosa* (B). Points represent individual annual measurements from each core. Adjusted R^2 from linear regression is reported on each panel.

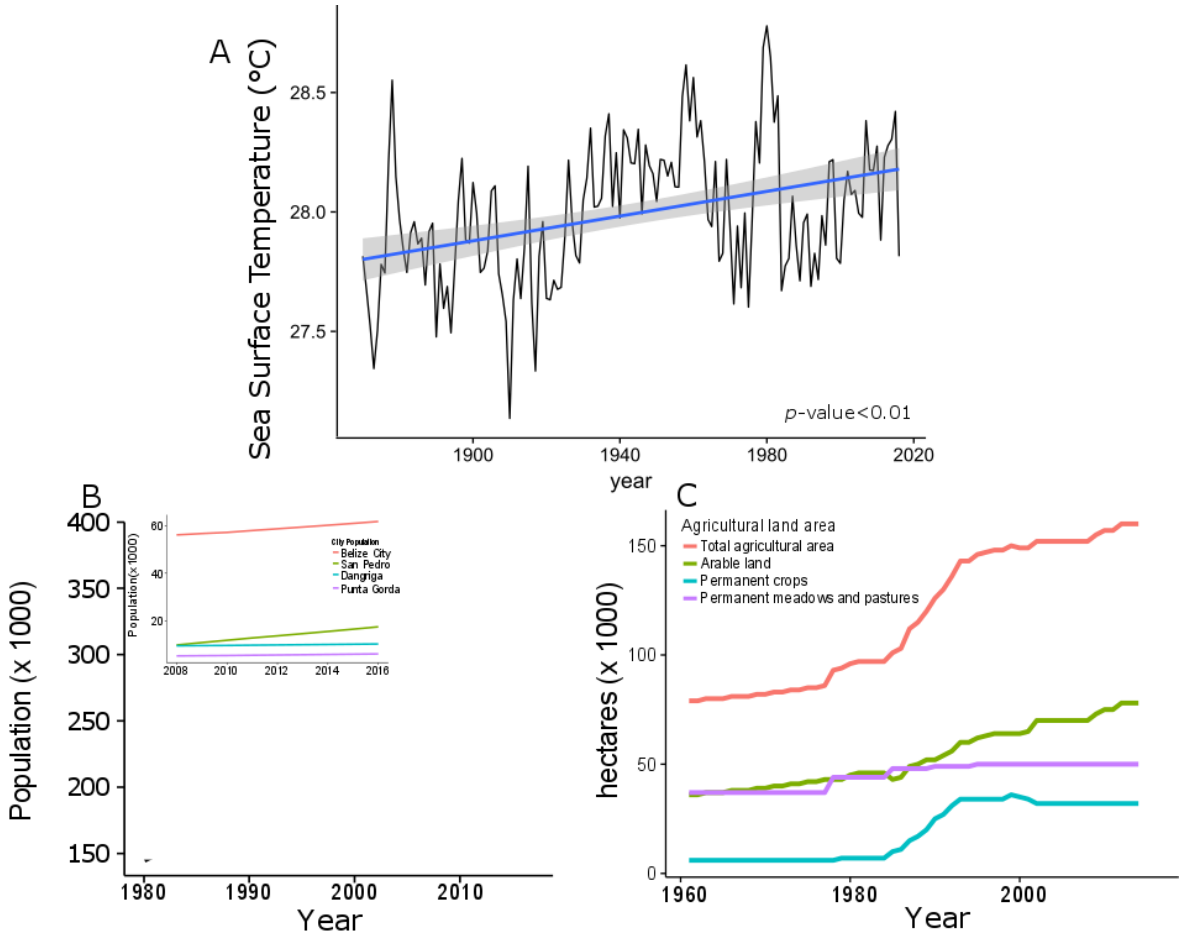

Fig S2: A.) Linear regression of HadiSST across the Belize MBRS from 1880-present. A significant *p*-value indicates a slope that is significantly different from zero (indicating increasing SST in the area). B.) population data for Belize (1980-present). Population data are from the Statistical Institute Belize (http://www.sib.org.bz/statistics/population) C.) Agricultural land use by thousand hectares. Data from the Food and Agricultural Organization of the United Nations (http://www.fao.org/faostat/)

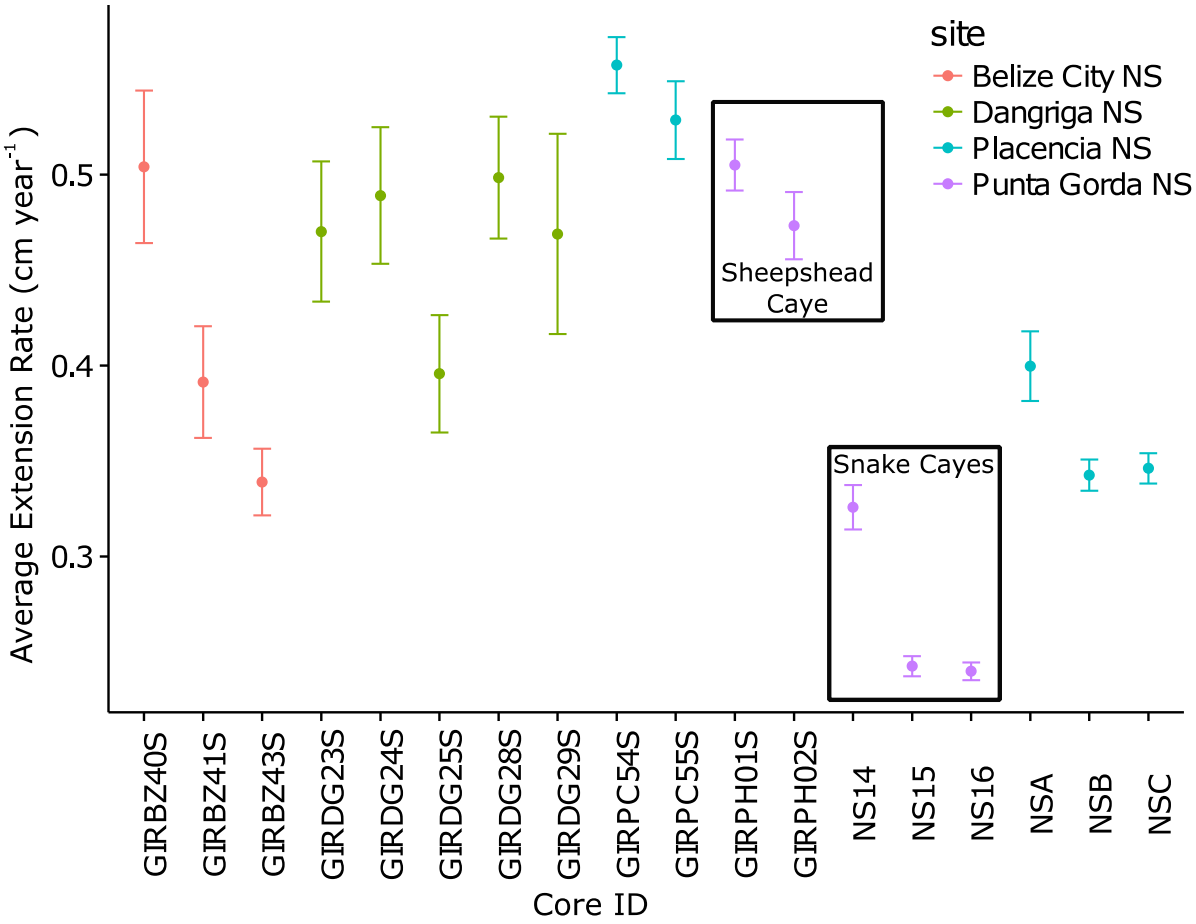

Fig S3: Core averaged extension rate (+/- 1 Standard Error) for all nearshore *S. siderea* cores. Results of ANOVA and TukeyHSD tests are available in tables S6 and S7.

Supplementary Methods

Coral core extraction

Cores were extracted by SCUBA divers using a pneumatic core drill (Castillo et al. 2011b) in 2009 or a hydraulic drill (Chicago Pneumatic COR 5 in 2012 or CS Unitec model 2 1335 0010, 3.8 HP) in 2015, both equipped with a 5 cm diameter diamond tipped core bit (Castillo et al. 2011b) Backreef *S. siderea* cores collected in 2015 were collected using a pneumatic drill with a 2.5 cm diameter diamond tipped core bit due to permitting restrictions. All cores were extracted from colonies that appeared healthy (i.e., no bleaching, abnormalities, scarring, or disease) near the center of each colony. Cores were extracted parallel to the

growth axis of each colony and spanned the entire height of the colony, with the exception of the backreef *S. siderea* cores collected in 2015 that ranged from 10-50 cm—spanning only the upper portion of the colony. Overall, core lengths ranged from 10 cm to > 1 m. After extracting each core, a concrete plug was inserted into the drilled hole and sealed with *Z-spar* underwater epoxy to prevent bioerosion. Epoxy was only placed on the skeleton and the concrete to avoid damage to the living tissue surrounding the hole. Cores were rinsed in ethanol, stored in PVC tubes for transport, and transported to the University of North Carolina at Chapel Hill for analysis. Collection permits were obtained from the Belize Fisheries Department and all cores were collected and transported pursuant to local, federal, and international regulations.

Coral CT Procedures

Coral cores collected in 2009 and 2012 were CT-scanned on a Siemens Somatom Definition AS (120 kV, 300 mAs, 0.6 mm slice thickness) (Saenger et al. 2009; Cantin et al. 2010; Carilli et al. 2012) at Wake Radiology Chapel Hill in 2013 using methods modified from Carilli et al. (Carilli et al. 2012) and De'ath et al. (De'ath et al. 2009). Briefly, whole (i.e., unslabbed) cores were CT scanned with the growth axis oriented perpendicular to the length of the CT table. The resulting CT scans were uploaded to the DICOM viewing program Osirix for further analysis following methods modified from Carilli et al. (Carilli et al. 2012). Transects were drawn parallel to the core growth axis using the "length" tool in Osirix. and within the exothecal space between corallite walls in order to standardize density measurements between transects and cores. Transects were performed in triplicate for each length of the core in order to establish an average, exported to XML, and read into the program RUNNINGCORALGUI, which identified the local density extrema (in Hounsfield

units) of the data in each XML file. The locations of these local extrema were then quantified via pixel counting, with halfway points between local extrema defining the boundaries of low and high density bands. The number of pixels between these halfway points and the average density in Hounsfield units was quantified for the set of pixels between the halfway points. The linear extension of each seasonal light and dark band was then quantified from the total length of the line tool data in pixels, which was then converted to cm.

Coral cores from 2015 were CT scanned on a Siemens Biograph mCT (120 kV, 250 mAs, 0.6 mm slice thickness) at UNC Biomedical Research Imaging Center (BRIC). CT images were reconstructed at 0.1 mm increments using the H70h "very sharp spine" window. All images were exported from the scanner as DICOM files, which were then read into the medical image viewer Horos v2.0.2 (open-source version of Osirix). Semiannual density bands were visualized using a 10-mm thick "Mean" projection oriented through the center of the core. In place of RUNNINGCORALGUI, all boundaries between high- and low-density bands were delineated manually and three sets of linear transects were drawn down the length of the cores using the ROI tool in Horos. Each set of transects was drawn within the exothecal space between corallite walls in order to standardize density measurements between cores and avoid abnormal density spikes in areas where the transect crossed a high-density corallite wall. By-pixel density measurements were then extracted from linear transects and average density was calculated for each semiannual density band. Linear extension (cm) was measured in Horos as the width of each density band, and calcification (g/cm^2) was calculated as the product of average density and linear extension.

Coral core density standardization

Nine coral standards were used for density calibration. These standards were pieces of various coral species from the Caribbean that had the same width as the coral cores. Volume and mass of these standards were calculated with calipers and a Mettler Toledo XPE205 analytical balance. Real world density for each standard was calculated as mass (determined by Mettler Toledo XPE205 analytical balance) divided by volume. The nine internal density standards were scanned along with the cores at least once per scanning session (3-4 scans were completed during each 1-2 hour scanning session). A standard curve was developed for each scanning session that related Houndsfield density (measured from CT scan) to actual coral density (g/cm^3), similar to DeCarlo et al. (DeCarlo et al. 2015).

Belize sea surface temperature, population, and agricultural data

Hadley Centre Sea Ice and Sea Surface Temperature (HadISST) data for Belize from 1880-present were obtained from the NOAA Environmental Research Division Data Access Program (ERDDAP) website (http://coastwatch.pfeg.noaa.gov/erddap/griddap/index.html). Population data for the country of Belize from 1980-present and for major coastal cities in Belize (Belize City, San Pedro, Dangriga, and Punta Gorda) from 2008-present were obtained from the Statistical Institute of Belize website (http://www.sib.org.bz/statistics/population). Agricultural land use statistics for Belize from 1960-present were obtained from the Food and Agricultural Organization of the United Nations (FAO) website (http://www.fao.org/faostat/).

Statistical Analysis

Model Selection

The central goal of the present study was to describe how annual skeletal extension of *S. siderea* and *P. strigosa* on the Belize Mesoamerican Barrier Reef System (MBRS) varied over for each species over the full extent of the data (1814-present for *S. siderea* and 1950-present for *P. strigosa*). A sequence of models was employed to determine how best to describe the structure of the data and to test the hypothesis of interest. Several models were tested, including (1) an ordinary regression model, (2) a random intercepts model that includes time as a predictor, (3) a random slopes and intercepts model with time as a predictor in which the intercept and coefficient of time (slope) were allowed to be random, and (4) versions of model 3 testing multiple correlation structure, including autoregressive moving average (ARMA) modeling. The variable year was 'centered' using a centering constant of 2013 for *S. siderea* (1814-present) and 2012 for *S. siderea* (1980-present) and *P. strigosa* (both time-scales) because this minimized correlation between the random slopes and intercepts. In general, centering enhances model interpretability and improves numerical stability by increasing the likelihood that the optimization algorithm converges on the correct solution. The estimate of the slope is unchanged by centering, but the intercept will estimate the mean value of the response variable in the year of centering (2013 or 2012)—rather than in year zero of an un-centered model (O'Connor et al. 2007). Model testing was performed for each species and timescale (Table S4). Akaike Information Criterion (AIC) was used to identify the best-fit model (Burnham and Anderson 2002) (Table S4). AIC provides a measure of the explanatory power of a model discounted by the number of parameters that contributed to its construction; a lower value indicates a better fitting model.

Statistical analyses were carried out using the nlme package (Pinheiro et al. 2017) of R (Team 2017). Slopes and the variance of slopes were extracted from each linear mixed effects model for all reef zones. 50% and 95% confidence intervals (CI) were calculated for all reef zones within each species, with 95% CI that do not overlap indicating significant differences between reef zones (Table S1, Figs 2, 3). T-tests were used to identify slopes that were significantly different from zero (Table S1, Figs 2, 3).

Sea surface temperature

Sea surface temperatures obtained from HadISST from 1880 to present obtained for 1° x 1° latitudinal-longitudinal grid cells were averaged across the coast of Belize. This average SST was plotted and regressed against time using a linear model to evaluate statistically significant changes in temperature over time (Fig 4).

Reef-zone averaged extension rates

Skeletal extension rates (cm/year) were averaged for all corals within a reef zone across five year time bins from 1950-2014 (e.g., 1950-1954, 1955-1959) in order to compare differences in recent extension rates between reef zones. A two-way analysis of variance (ANOVA) and a TUKEY HSD test were used to determine differences in average extension between reef zones within five-year time bins ($p<0.05$; Table S1; Fig 2C, Fig 3C).

Extension anomaly vs. mass-bleaching events

The lowest 10% of historical extension rates was identified for each core. The fraction of cores in each reef zone that registered an annual extension rate in the lowest 10%

of each core's historical extension rate was determined for each year in which the number of cores exceeded 5 for a given reef zone (1975-present in *P. strigosa* and 1920-present in *S. siderea*). The fraction of cores exhibiting low extension was time averaged for each species and reef zone. This time series of low-extension within each reef zone was then compared with the timing of historical mass-bleaching events in the Caribbean region: 1997-1998 (Podesta and Glynn 2001; Aronson et al. 2002b), 2005 (Donner et al. 2007a; LaJeunesse et al. 2009; Eakin et al. 2010), 2009-2010 (Alemu and Clement 2014; Kemp et al. 2014; Buglass et al. 2016) and 2014-2016 (Eakin et al. 2016). Least squares regression modeling was used to determine years containing significantly higher fractions of cores exhibiting low-extension within each reef zone. The fraction of cores exhibiting low extension was averaged for bleaching and non-bleaching years for each reef zone. Differences between bleaching and non-bleaching years were compared via two-way analysis of variance (ANOVA) and a TUKEY HSD test ($p<0.05$); Table S6).

APPENDIX 4: SUPPORTING INFORMATION FOR CHAPTER 5

Tables

	Df	Sum sq	Mean Sq	F	p-value
Species	1	$6.63*10^{14}$	$6.63*10^{14}$	339.542	**<0.001**
Transplant	3	$3.74*10^{13}$	$1.25*10^{13}$	6.383	**<0.001**
Time Point	1	$9.48*10^{12}$	$9.48*10^{12}$	4.857	**0.028**
Species: Transplant	3	$1.16*10^{13}$	$3.88*10^{12}$	1.985	0.116
Species: Time Point	1	$9.87*10^{13}$	$9.87*10^{13}$	50.545	**<0.001**
Transplant: Time Point	3	$4.25*10^{13}$	$1.42*10^{13}$	7.248	**<0.001**
Species: Transplant: Time Point	3	$1.70*10^{13}$	$5.66*10^{12}$	2.898	**0.035**
Residuals	386	$7.54*10^{14}$	$1.95*10^{12}$		

Tukey HSD Results	**Comparison**	***p*-value**
Species	SSID: PSTR	**<0.001**
Transplant	NS Transplant: NS Native	**<0.001**
	OS Native: NS Native	**0.001**
	OS Transplant: NS Native	**0.027**
Time Point	T0: T1	**0.029**
Species: Time Point	SSID T0: PSTR T0	**<0.001**
	PSTR T1: PSTR T0	**<0.001**
	SSID T1: PSTR T0	**<0.001**
	PSTR T1: SSID T0	**<0.001**
	SSID T1: SSID T0	**0.003**
	SSID T1: PSTR T1	**<0.001**
Transplant: Time Point	NS Native T1: NS Native T0	**<0.001**
	NS Native T1: NS Transplant T0	**<0.001**
	NS Native T1: OS Native T0	**<0.001**
	NS Transplant T1: NS Native T1	**<0.001**
	OS Native T1: NS Native T1	**<0.001**
	OS Transplant T1: NS Native T1	**<0.001**
Species: Transplant: Time Point	PS TR NS Native T1: PS TR NS Native T0	**<0.001**
	SSID NS Transplant T1: PS TR NS Native T0	**<0.001**
	SSID OS Native T1: PS TR NS Native T0	**<0.001**
	SSID OS Transplant T1: PS TR NS Native T0	**<0.001**
	PS TR NS Native T1: SSID NS Native T0	**<0.001**
	SSID NS Transplant T1: PS TR NS Transplant T0	**<0.001**
	SSID OS Native T1: PS TR NS Transplant T0	**<0.001**
	SSID OS Transplant T1: PS TR NS Transplant T0	**<0.001**

	PS TR NS Native T1: SSID NS Transplant T0	**<0.001**
	PS TR NS Transplant T1: SSID NS Transplant T0	**<0.001**
	PS TR OS Native T1: SSID NS Transplant T0	**<0.001**
	PS TR OS Transplant T1: SSID NS Transplant T0	**<0.001**
	SSID NS Transplant T1: PS TR OS Native T0	**<0.001**
	SSID OS Native T1: PS TR OS Native T0	**<0.001**
	SSID OS Transplant T1: PS TR OS Native T0	**<0.001**
	PS TR NS Native T1: SSID OS Native T0	**<0.001**
	PS TR NS Transplant T1: SSID OS Native T0	**<0.001**
	PS TR OS Native T1: SSID OS Native T0	**<0.001**
	PS TR OS Transplant T1: SSID OS Native T0	**<0.001**
	PS TR NS Native T1: PS TR OS Transplant T0	**<0.001**
	SSID NS Transplant T1: PS TR OS Transplant T0	**<0.001**
	SSID OS Native T1: PS TR OS Transplant T0	**<0.001**
	SSID OS Transplant T1: PS TR OS Transplant T0	**<0.001**
	PS TR NS Native T1: SSID OS Transplant T0	**<0.001**
	SSID NS Native T1: PS TR NS Native T1	**<0.001**
	SSID NS Transplant T1: PS TR NS Native T1	**<0.001**
	SSID OS Native T1: PS TR NS Native T1	**<0.001**
	SSID OS Transplant T1: PS TR NS Native T1	**<0.001**
	SSID NS Transplant T1: PS TR NS Transplant T1	**<0.001**
	SSID OS Native T1: PS TR NS Transplant T1	**<0.001**
	SSID OS Transplant T1: PS TR NS Transplant T1	**<0.001**
	PS TR OS Native T1: SSID NS Transplant T1	**<0.001**
	PS TR OS Transplant T1: SSID NS Transplant T1	**<0.001**
	SSID OS Native T1: PS TR OS Native T1	**<0.001**
	SSID OS Transplant T1: PS TR OS Native T1	**<0.001**
	PS TR OS Transplant T1: SSID OS Native T1	**<0.001**
	SSID OS Transplant T1: PS TR OS Transplant T1	**<0.001**
	PS TR OS Transplant T1: SSID NS Native T0	**<0.001**
	PS TR OS Transplant T1: SSID OS Transplant T0	**<0.001**
	SSID NS Transplant T0: PS TR NS Transplant T0	**<0.001**
	SSID OS Native T0: PS TR NS Transplant T0	**<0.001**
	PS TR OS Native T0: SSID NS Transplant T0	**<0.001**
	SSID OS Native T0: PS TR OS Native T0	**<0.001**

	PS TR NS Native T1: PS TR NS Transplant T0	**<0.001**
	PS TR NS Native T1: PS TR OS Native T0	**<0.001**
	PS TR OS Native T1: SSID NS Native T0	**<0.001**
	PS TR OS Native T1: SSID OS Transplant T0	**<0.001**
	SSID NS Transplant T0: PS TR NS Native T0	**<0.001**
	SSID OS Native T0: PS TR NS Native T0	**<0.001**
	PS TR OS Transplant T0: SSID NS Transplant T0	**<0.001**
	PS TR OS Transplant T0: SSID OS Native T0	**<0.001**
	PS TR OS Transplant T1: SSID NS Native T1	**<0.001**
	PS TR OS Native T1: SSID NS Native T1	**<0.001**
	PS TR NS Transplant T1: PS TR NS Native T1	**<0.001**
	PS TR NS Transplant T1: SSID NS Native T0	**<0.001**
	PS TR NS Transplant T1: SSID OS Transplant T0	**<0.001**
	PS TR NS Transplant T0: SSID NS Native T0	**0.002**
	PS TR OS Native T0: SSID NS Native T0	**0.002**
	SSID OS Transplant T0: PS TR NS Transplant T0	**0.002**
	SSID OS Transplant T0: PS TR OS Native T0	**0.002**
	PS TR NS Transplant T1: SSID NS Native T1	**0.003**
	PS TR OS Transplant T1: PS TR NS Native T1	**0.003**
	SSID OS Native T1: SSID NS Native T0	**0.004**
	SSID OS Native T1: SSID OS Transplant T0	**0.004**
	SSID NS Native T1: PS TR NS Transplant T0	**0.012**
	SSID NS Native T1: PS TR OS Native T0	**0.012**
	SSID NS Native T0: PS TR NS Native T0	**0.013**
	SSID OS Transplant T0: PS TR NS Native T0	**0.013**
	PS TR OS Transplant T0: SSID NS Native T0	**0.013**
	SSID OS Transplant T0: PS TR OS Transplant T0	**0.013**
	SSID OS Native T1: SSID NS Native T1	**0.040**
	SSID OS Transplant T1: SSID NS Native T0	**0.049**
	SSID OS Transplant T1: SSID OS Transplant T0	**0.049**

Table S1: Results of ANOVA and Tukey HSD tests comparing symbiont density (cells/ cm^2) within and between species, transplant treatments, and time points. Tukey results are only shown for significant factors in the ANOVA model. Only significant *p*-values are shown for Tukey tests (<0.05).

	Df	Sum sq	Mean sq	F value	*p*-value
Species	1	$1.08*10^9$	$1.08*10^9$	44.34	<0.001
Transplant	3	$1.68*10^8$	$5.59*10^7$	2.294	0.087
Time point	1	$4.09*10^6$	$4.09*10^6$	0.168	0.684
Species: Transplant	3	$9.91*10^7$	$3.30*10^7$	1.355	0.265
Species: Time point	1	$5.18*10^7$	$5.18*10^7$	2.125	0.150
Transplant: Time point	3	$1.53*100^8$	$5.11*10^7$	2.097	0.110
Species: Transplant: Time point	3	$7.16*10^7$	$2.39*10^7$	0.979	0.409
Residuals	62	$1.51*10^9$	$2.44*10^7$		
Tukey HSD Results	**Comparison**	***p*-value**			
Species	SSID-PSTR	**<0.001**			

Table S2: Results of ANOVA and Tukey HSD tests comparing chl*a* content (μg/cm^2) within and between species, transplant treatments, and time points. Tukey results are only shown for significant factors in the ANOVA model. Only significant *p*-values are shown for Tukey tests (<0.05).

	Df	sum sq	mean sq	F value	Pr (>F)
Species	1	0.006	0.006	0.714	0.401
Transplant	3	0.122	0.040	4.642	**0.005**
Time Point	1	0.040	0.040	4.573	**0.036**
Species: Transplant	3	0.017	0.006	0.653	0.584
Species: Time point	1	0.023	0.023	2.664	0.108
Transplant: Time point	3	0.027	0.009	1.038	0.382
Species: Transplant: Time point	3	0.007	0.002	0.271	0.846
Residuals	62	0.544	0.009		
Tukey HSD Results	**Comparison**	***p*-value**			
Transplant	OS Transplant: NS Native	0.998			
	NS Transplant: NS Native	0.239			
	OS Native: NS Native	**0.012**			
	NS Transplant: OS Transplant	0.305			
	OS Native: OS Transplant	0.016			
	OS Native: NS Transplant	0.562			
Time point	T1-T0	0.037			

Table S3: Results of ANOVA and Tukey HSD tests comparing total soluble protein content (g protein/g coral biomass) within and between species, transplant treatments, and time points. Tukey results are only shown for significant factors in the ANOVA model. Only significant *p*-values are shown for Tukey tests (<0.05).

REFERENCES

Abrego D, Van Oppen MJ, Willis BL (2009) Highly infectious symbiont dominates initial uptake in coral juveniles. Molecular Ecology 18:3518-3531

Alemu JB, Clement Y (2014) Mass coral bleaching in 2010 in the southern Caribbean. Plos ONE 9:e83829

Alvarez-Filip L, Carricart-Ganivet JP, Horta-Puga G, Iglesias-Prieto R (2013) Shifts in coral-assemblage composition do not ensure persistence of reef functionality. Scientific reports 3

Alvarez-Filip L, Dulvy NK, Gill JA, Côté IM, Watkinson AR (2009) Flattening of Caribbean coral reefs: region-wide declines in architectural complexity. Proceedings of the Royal Society of London B: Biological Sciences:rspb20090339

Alvarez-Filip L, Dulvy NK, Côté IM, Watkinson AR, Gill JA (2011) Coral identity underpins architectural complexity on Caribbean reefs. Ecological Applications 21:2223-2231

Andrefouet S, Mumby PJ, Mcfield M, Hu C, Muller-Karger RE (2002) Revisiting coral reef connectivity. Coral Reefs 21:43-48

Andréfouët S, Berkelmans R, Odriozola L, Done T, Oliver J, Müller-Karger F (2002) Choosing the appropriate spatial resolution for monitoring coral bleaching events using remote sensing. Coral Reefs 21:147-154

Anthony K (1999) Coral suspension feeding on fine particulate matter. Journal of Experimental Marine Biology and Ecology 232:85-106

Armoza-Zvuloni R, Segal R, Kramarsky-Winter E, Loya Y (2011) Repeated bleaching events may result in high tolerance and notable gametogenesis in stony corals: Oculina patagonica as a model. Mar Ecol-Prog Ser 426:149-159

Aronson R, Precht W, Toscano M, Koltes K (2002a) The 1998 bleaching event and its aftermath on a coral reef in Belize. Marine Biology 141:435-447

Aronson RB, Precht WF, Toscano MA, Koltes KH (2002b) The 1998 bleaching event and its aftermath on a coral reef in Belize. Marine Biology xxx

Aronson RB, Macintyre IG, Wapnick CM, O'Neill MW (2004) Phase shifts, alternative states, and the unprecedented convergence of two reef systems. Ecology 85:1876-1891

Arthur C, Baker J, Bamford H (2009) Proceedings of the International Research Workshop on the Occurrence, Effects, and Fate of Microplastic Marine Debris, September 9-11, 2008

Ateweberhan M, McClanahan TR (2010) Relationship between historical sea-surface temperature variability and climate change-induced coral mortality in the western Indian Ocean. Marine Pollution Bulletin 60:964-970

Azam F, Worden AZ (2004) Microbes, molecules, and marine ecosystems. Science 303:1622-1624

Baillon S, Hamel J-F, Wareham VE, Mercier A (2012) Deep cold-water corals as nurseries for fish larvae. Frontiers in Ecology and the Environment 10:351-356

Baird AH, Bhagooli R, Ralph PJ, Takahashi S (2009) Coral bleaching: the role of the host. Trends in Ecology & Evolution 24:16-20

Baker AC (2001) Reef corals bleach to survive change. Nature 411:765-766

Baker AC (2003) Flexibility and Specificity in Coral-Algal Symbiosis: Diversity, Ecology, and Biogeography of *Symbiodinium*. Annual Review of Ecology, Evolution, and Systematics 34:661-689

Baker AC, Rowan R, Knowlton N (1997) Symbiosis ecology of two Caribbean Acroporid corals. Proceedings of the 8th International Coral Reef Symposium 2:1296-1300

Baker AC, Starger CJ, McClanahan TR, Glynn PW (2004) Corals' adaptive response to climate change. Nature 430:741

Banks S, Foster K (2016) Baseline Levels of Siderastrea siderea Bleaching under Normal Environmental Conditions in Little Cayman. Open Journal of Marine Science 7:142

Barshis DJ (2015) Genomic Potential for Coral Survival of Climate Change Coral Reefs in the Anthropocene. Springer, pp133-146

Barshis DJ, Ladner JT, Oliver TA, Seneca FO, Traylor-Knowles N, Palumbi SR (2013) Genomic basis for coral resilience to climate change. Proceedings of the National Academy of Sciences 110:1387-1392

Baumann JH, Townsend JE, Courtney TA, Aichelman HE, Davies SW, Lima FP, Castillo KD (2016) Temperature Regimes Impact Coral Assemblages along Environmental Gradients on Lagoonal Reefs in Belize. Plos ONE 11:e0162098

Belkin IM (2009) Rapid warming of large marine ecosystems. Progress in Oceanography 81:207-213

Bell P (1992) Eutrophication and coral reefs—some examples in the Great Barrier Reef lagoon. Water Research 26:553-568

Bell PRF, Elmetri I, Lapointe BE (2014) Evidence of Large-Scale Chronic Eutrophication in the Great Barrier Reef: Quantification of Chlorophyll a Thresholds for Sustaining Coral Reef Communities. AMBIO 43:361-376

Berkelmans R, Van Oppen MJ (2006) The role of zooxanthellae in the thermal tolerance of corals: a 'nugget of hope'for coral reefs in an era of climate change. Proceedings of the Royal Society of London B: Biological Sciences 273:2305-2312

Bongaerts P, Riginos C, Ridgway T, Sampayo EM, van Oppen MJ, Englebert N, Vermeulen F, Hoegh-Guldberg O (2010) Genetic divergence across habitats in the widespread coral Seriatopora hystrix and its associated Symbiodinium. Plos ONE 5:e10871

Brosi GB, McCulley RL, Bush LP, Nelson JA, Classen AT, Norby RJ (2011) Effects of multiple climate change factors on the tall fescue–fungal endophyte symbiosis: infection frequency and tissue chemistry. New Phytologist 189:797-805

Brown BE (1997) Coral bleaching: causes and consequences. Coral Reefs 16 suppl:s129-s138

Buddemeier RW, Fautin DG (1993) Coral bleaching as an adaptive mechanism. BioScience 43:320-326

Buddemeier RW, Kleypas JA, Aronson RB (2004) Coral reefs and global climate change: potential contributions of climate change to stresses on coral reef ecosystems. Pew Center on Global Climate Change, Arlington, VA 56

Buglass S, Donner SD, Alemu JB (2016) A study on the recovery of Tobago's coral reefs following the 2010 mass bleaching event. Marine Pollution Bulletin 104:198-206

Burke LM, Maidens J, Spalding M, Kramer P, Green E (2004) Reefs at Risk in the Caribbean. World Resources Institute Washington, DC

Burnham KP, Anderson DR (2002) Model selection and multimodel inference: a practical information-theoretic approach. Springer Science & Business Media

Caldwell MC, Caldwell DK, Siebenaler JB (1965) Observations on captive and wild Atlantic bottlenosed dolphins, Tursiops Truncatus: In the northeastern Gulf of Mexico. Los Angeles County Museum

Camp EF, Smith DJ, Evenhuis C, Enochs I, Manzello D, Woodcock S, Suggett DJ (2016) Acclimatization to high-variance habitats does not enhance physiological tolerance of two key Caribbean corals to future temperature and pH. Proceedings of the Royal Society of London B: Biological Sciences 283

Cantin NE, van Oppen MJ, Willis BL, Mieog JC, Negri AP (2009) Juvenile corals can acquire more carbon from high-performance algal symbionts. Coral Reefs 28:405

Cantin NE, Cohen AL, Karnauskas KB, Tarrant AM, McCorkle DC (2010) Ocean warming slows coral growth in the central Red Sea. Science 329:322-325

Carilli J, Donner SD, Hartmann AC (2012) Historical temperature variability affects coral response to heat stress. Plos ONE 7:e34418

Carilli JE, Prouty NG, Hughen KA, Norris RD (2009a) Century-scale records of land-based activities recorded in Mesoamerican coral cores. Marine Pollution Bulletin 58:1835-1842

Carilli JE, Norris RD, Black BA, Walsh SM, McField M (2009b) Local Stressors Reduce Coral Resilience to Bleaching. PLoS One 4

Carilli JE, Norris RD, Black BA, Walsh SM, McField M (2009c) Local stressors reduce coral resilience to bleaching. Plos ONE 4:e6324

Carilli JE, Norris RD, Black B, Walsh SM, McFIELD M (2010) Century-scale records of coral growth rates indicate that local stressors reduce coral thermal tolerance threshold. Global Change Biology 16:1247-1257

Carilli JE, Hartmann AC, Heron SF, Pandolfi JM, Cobb K, Sayani H, Dunbar R, Sandin SA (2017) Porites coral response to an oceanographic and human impact gradient in the Line Islands. Limnology and Oceanography

Carpenter EJ, Anderson SJ, Harvey GR, Miklas HP, Peck BB (1972) Polystyrene spherules in coastal waters. Science 178:749-750

Carricart-Ganivet JP, Merino M (2001) Growth responses of the reef-building coral Montastraea annularis along a gradient of continental influence in the southern Gulf of Mexico. Bulletin of Marine Science 68:133-146

Carrillo L, Johns EM, Smith RH, Lamkin JT, Largier JL (2015) Pathways and Hydrography in the Mesoamerican Barrier Reef System Part 1: Circulation. Continental Shelf Research 109:164-176

Castillo K, Ries J, Weiss J (2011a) Declining coral skeletal extension for forereef colonies of *Siderastrea siderea* on the Mesoamerican Barrier Reef System, southern Belize. PLoS ONE 6:e14615

Castillo KD, Helmuth BST (2005) Influence of thermal history on the response of Montastraea annularis to short-term temperature exposure. Marine Biology 148:261 - 270

Castillo KD, Ries JB, Weiss JM (2011b) Declining coral skeletal extension for forereef colonies of Siderastrea siderea on the Mesoamerican Barrier Reef System, Southern Belize. Plos ONE 6:e14615

Castillo KD, Ries JB, Weiss JM, Lima FP (2012) Decline of forereef corals in response to recent warming linked to history of thermal exposure. Nature Climate Change 2:756-760

Castillo KD, Ries JB, Bruno JF, Westfield IT (2014) The reef-building coral Siderastrea siderea exhibits parabolic responses to ocean acidification and warming. Proceedings of the Royal Society of London B: Biological Sciences 281:20141856

Cesar H, Burke L, Pet-Soede L (2003) The economics of worldwide coral reef degradation. Cesar environmental economics consulting (CEEC)

Chérubin L, Kuchinke C, Paris C (2008) Ocean circulation and terrestrial runoff dynamics in the Mesoamerican region from spectral optimization of SeaWiFS data and a high resolution simulation. Coral Reefs 27:503-519

Chevenet F, Brun C, Bañuls A-L, Jacq B, Christen R (2006) TreeDyn: towards dynamic graphics and annotations for analyses of trees. BMC bioinformatics 7:439

Chiappone M, Dienes H, Swanson DW, Miller SL (2005) Impacts of lost fishing gear on coral reef sessile invertebrates in the Florida Keys National Marine Sanctuary. Biological conservation 121:221-230

Chin TM, Vazquez J, Armstrong E (2013) A multi-scale, high-resolution analysis of global sea surface temperature. Algorithm Theoretical Basis Document, Version 1:13

Chollett I, Mumby PJ, Müller-Karger FE, Hu C (2012a) Physical environments of the Caribbean Sea. Limnology and Oceanography 57:1233-1244

Chollett I, Mumby PJ, Muller-Karger FE, Hu CM (2012b) Physical environments of the Caribbean Sea. Limnol Oceanogr 57:1233-1244

Chollett I, Müller-Karger FE, Heron SF, Skirving W, Mumby PJ (2012c) Seasonal and spatial heterogeneity of recent sea surface temperature trends in the Caribbean Sea and southeast Gulf of Mexico. Marine Pollution Bulletin 64:956-965

Chomczynski P, Sacchi N (2006) The single-step method of RNA isolation by acid guanidinium thiocyanate–phenol–chloroform extraction: twenty-something years on. Nature protocols 1:581-585

Coffroth MA, Santos SR (2005) Genetic diversity of symbiotic dinoflagellates in the genus Symbiodinium. Protist 156:19-34

Cole M, Webb H, Lindeque PK, Fileman ES, Halsband C, Galloway TS (2014) Isolation of microplastics in biota-rich seawater samples and marine organisms. Scientific reports 4

Coles SL, Brown BE (2003) Coral Bleaching-Capacity for Acclimatization and Adaptation. Advances in Marine Biology 46:183-213

Connell SD, Russell BD (2010) The direct effects of increasing CO₂ and temperature on non-calcifying organisms: increasing the potential for phase shifts in kelp forests. Proceedings of the Royal Society B: Biological Sciences

Cooper TF, Uthicke S, Humphrey C, Fabricius KE (2007) Gradients in water column nutrients, sediment parameters, irradiance and coral reef development in the Whitsunday Region, central Great Barrier Reef. Estuarine, Coastal and Shelf Science 74:458-470

Correa AMS, McDonald MD, Baker AC (2009) Development of clade-specific Symbiodinium primers for quantitative PCR (qPCR) and their application to detecting clade D symbionts in Caribbean corals. Marine Biology 156:2403-2411

Cortés J (1990) The coral reefs of Golfo Dulce, Costa Rica: distribution and community structure. Citeseer

Cramer K (2010) Changes in coral communities and reef environments over the past few centuries in Caribbean Panama. Proceedings from the 2010 AGU Ocean Sciences Meeting

Cramer KL, Leonard-Pingel JS, Rodríguez F, Jackson JB (2015) Molluscan subfossil assemblages reveal the long-term deterioration of coral reef environments in Caribbean Panama. Marine Pollution Bulletin 96:176-187

Cramer KL, Jackson JB, Angioletti CV, Leonard-Pingel J, Guilderson TP (2012) Anthropogenic mortality on coral reefs in Caribbean Panama predates coral disease and bleaching. Ecology Letters 15:561-567

Cruz I, Kikuchi RK, Leão ZM (2008) Use of the video transect method for characterizing the Itacolomis reefs, eastern Brazil. Brazilian Journal of Oceanography 56:271-280

Cunning R, Gillette P, Capo T, Galvez K, Baker AC (2015) Growth tradeoffs associated with thermotolerant symbionts in the coral Pocillopora damicornis are lost in warmer oceans. Coral Reefs 34:155-160

D'Croz L, Mate JL, Oke JE (2001a) Responses to elevated sea water temperature and UV radiation in the coral Porites lobata from upwelling and non-upwelling environments on the Pacific coast of Panama. Bull Mar Sci 69:203-214

D'Croz L, Mate JL, Oke JE (2001b) Responses to elevated seawater temperature and UV radiation in the coral *Porites lobata* from upwelling and non-upwelling environments on the Pacific coast of Panama. Bulletin of Marine Science 69:203-214

D'Olivo J, McCulloch M, Judd K (2013) Long-term records of coral calcification across the central Great Barrier Reef: assessing the impacts of river runoff and climate change. Coral Reefs 32:999-1012

Dale MR, Fortin M-J (2002) Spatial autocorrelation and statistical tests in ecology. Ecoscience:162-167

Darling ES, McClanahan TR, Côté IM (2013) Life histories predict coral community disassembly under multiple stressors. Global Change Biology 19:1930-1940

Darling ES, Alvarez-Filip L, Oliver TA, McClanahan TR, Côté IM (2012) Evaluating life-history strategies of reef corals from species traits. Ecology Letters 15:1378-1386

Darriba D, Taboada GL, Doallo R, Posada D (2012) jModelTest 2: more models, new heuristics and parallel computing. Nature methods 9:772-772

Davies SW, Ries JB, Marchetti A, Granzotti R, Castillo KD (2017) *Symbiodinium* functional diversity and clade specificity under global change stressors. bioRxiv

Davies SW, Rahman M, Meyer E, Green EA, Buschiazzo E, Medina M, Matz MV (2013) Novel polymorphic microsatellite markers for population genetics of the endangered Caribbean star coral, Montastraea faveolata. Marine Biodiversity 43:167-172

Davy SK, Allemand D, Weis VM (2012) Cell biology of cnidarian-dinoflagellate symbiosis. Microbiology and Molecular Biology Reviews 76:229-261

De'ath G, Lough JM, Fabricius KE (2009) Declining Coral Calcification on the Great Barrier Reef. Science 323:116-119

DeCarlo TM, Cohen AL, Barkley HC, Cobban Q, Young C, Shamberger KE, Brainard RE, Golbuu Y (2015) Coral macrobioerosion is accelerated by ocean acidification and nutrients. Geology 43:7-10

Degnan PH, Lazarus AB, Brock CD, Wernegreen JJ (2004) Host–symbiont stability and fast evolutionary rates in an ant–bacterium association: Cospeciation of Camponotus species and their endosymbionts, Candidatus Blochmannia. Systematic Biology 53:95-110

Dereeper A, Audic S, Claverie J-M, Blanc G (2010) BLAST-EXPLORER helps you building datasets for phylogenetic analysis. BMC evolutionary biology 10:8

Dereeper A, Guignon V, Blanc G, Audic S, Buffet S, Chevenet F, Dufayard J-F, Guindon S, Lefort V, Lescot M (2008) Phylogeny. fr: robust phylogenetic analysis for the non-specialist. Nucleic acids research 36:W465-W469

DeSalvo MK, Sunagawa S, Fisher PL, Voolstra CR, IGLESIAS-PRIETO R, Medina M (2010) Coral host transcriptomic states are correlated with Symbiodinium genotypes. Molecular Ecology 19:1174-1186

Deser C, Phillips AS, Alexander MA (2010) Twentieth century tropical sea surface temperature trends revisited. Geophysical Research Letters 37

Diekmann O, Bak R, Tonk L, Stam W, Olsen J (2002) No habitat correlation of zooxanthellae in the coral genus Madracis on a Curacao reef. Marine Ecology Progress Series 227:221-232

Dixon GB, Davies SW, Aglyamova GV, Meyer E, Bay LK, Matz MV (2015) Genomic determinants of coral heat tolerance across latitudes. Science 348:1460-1462

Dodge RE, Aller RC, Thomson J (1974) Coral growth related to resuspension of bottom sediments. Nature 247:574-576

Done TJ (1982) Patterns in the distribution of coral communities across the central Great Barrier Reef. Coral Reefs 1:95-107

Donner SD, Knutson TR, Oppenheimer M (2007a) Model-based assessment of the role of human-induced climate change in the 2005 Caribbean coral bleaching event. Proceedings of the National Academy of Science 104:5483-5488

Donner SD, Knutson TR, Oppenheimer M (2007b) Model-based assessment of the role of human-induced climate change in the 2005 Caribbean coral bleaching event. Proceedings of the National Academy of Sciences of the United States of America 104:5483-5488

Donner SD, Knutson TR, Oppenheimer M (2007c) Model-based assessment of the role of human-induced climate change in the 2005 Caribbean coral bleaching event. Proceedings of the National Academy of Sciences 104:5483-5488

Donner SD, Skirving WJ, Little CM, Oppenheimer M, Hoegh-Guldberg O (2005a) Global assessment of coral bleaching and required rates of adaptation under climate change. Glob Change Biol 11:2251-2265

Donner SD, Skirving WJ, Little CM, Oppenheimer M, Hoegh-Guldberg O (2005b) Global assessment of coral bleaching and required rates of adaptation under climate change. Global Change Biology 11:2251-2265

Dustan P, Doherty O, Pardede S (2013) Digital reef rugosity estimates coral reef habitat complexity. Plos ONE 8:e57386

Eakin C, Liu G, Gomez A, De la Cour J, Heron S, Skirving W, Geiger E, Tirak K, Strong A (2016) Global coral bleaching 2014–2017: status and an appeal for observations. Reef Encounter 31:20-26

Eakin CM, Morgan JA, Heron SF, Smith TB, Liu G, Alvarez-Filip L, Baca B, Bartels E, Bastidas C, Bouchon C (2010) Caribbean corals in crisis: record thermal stress, bleaching, and mortality in 2005. Plos ONE 5:e13969

Elmhagen B, Kindberg J, Hellström P, Angerbjörn A (2015) A boreal invasion in response to climate change? Range shifts and community effects in the borderland between forest and tundra. AMBIO 44:39-50

Eyre BD, Andersson AJ, Cyronak T (2014) Benthic coral reef calcium carbonate dissolution in an acidifying ocean. Nature Climate Change 4:969

Eyre BD, Cyronak T, Drupp P, De Carlo EH, Sachs JP, Andersson AJ (2018) Coral reefs will transition to net dissolving before end of century. Science 359:908-911

Ezzat L, Towle E, Irisson JO, Langdon C, Ferrier-Pagès C (2015) The relationship between heterotrophic feeding and inorganic nutrient availability in the scleractinian coral T. reniformis under a short-term temperature increase. Limnology and Oceanography

Fabricius K, Mieog J, Colin P, Idip D, H VAN OPPEN M (2004) Identity and diversity of coral endosymbionts (zooxanthellae) from three Palauan reefs with contrasting bleaching, temperature and shading histories. Molecular Ecology 13:2445-2458

Fabricius KE (2005) Effects of terrestrial runoff on the ecology of corals and coral reefs: review and synthesis. Marine Pollution Bulletin 50:125-146

Farrell P, Nelson K (2013) Trophic level transfer of microplastic: Mytilus edulis (L.) to Carcinus maenas (L.). Environmental Pollution 177:1-3

Fine M, Gildor H, Genin A (2013) A coral reef refuge in the Red Sea. Glob Change Biol 19:3640-3647

Finney JC, Pettay, D.T., Sampayo, E.M., Warner, M.E., Oxenford, H.A. and T.C. LaJeunesse (2010) On the relative significance of host-habitat, irradiance, and dispersal in the ecological distribution and speciation of coral endosymbionts. Microbial Ecology In Press

Fitt WK, Spero HJ, Halas J, White MW, Porter JW (1993) Recovery of the coral *Montastrea annularis* in the Florida Keys after the 1987 Caribbean "bleaching event". Coral Reefs 12:57-64

Frade P, Englebert N, Faria J, Visser P, Bak R (2008) Distribution and photobiology of Symbiodinium types in different light environments for three colour morphs of the coral Madracis pharensis: is there more to it than total irradiance? Coral Reefs 27:913-925

Frias J, Sobral P, Ferreira A (2010) Organic pollutants in microplastics from two beaches of the Portuguese coast. Marine Pollution Bulletin 60:1988-1992

Frieler K, Meinshausen M, Golly A, Mengel M, Lebek K, Donner S, Hoegh-Guldberg O (2013a) Limiting global warming to 2 [thinsp][deg] C is unlikely to save most coral reefs. Nature Climate Change 3:165-170

Frieler K, Meinshausen M, Golly A, Mengel M, Lebek K, Donner SD, Hoegh-Guldberg O (2013b) Limiting global warming to 2 °C is unlikely to save most coral reefs. Nature Climate Change 3:165-170

Game ET, McDonald-Madden E, Puotinen ML, Possingham HP (2008) Should we protect the strong or the weak? Risk, resilience, and the selection of marine protected areas. Conservation Biology 22:1619-1629

Gardner TA, Cote IM, Gill JA, Grant A, Watkinson AR (2003) Long-term region-wide declines in Caribbean corals. Science 301:958-960

Garren M, Walsh SM, Caccone A, Knowlton N (2006) Patterns of association between Symbiodinium and members of the Montastraea annularis species complex on spatial scales ranging from within colonies to between geographic regions. Coral Reefs 25:503-512

Ginsburg R, Lang J (2003) Status of coral reefs in the western Atlantic: Results of initial surveys, Atlantic and Gulf Rapid Reef Assessment(AGRRA) program. Atoll Research Bulletin 496

Gittleman JL, Kot M (1990) Adaptation: statistics and a null model for estimating phylogenetic effects. Systematic Biology 39:227-241

Gleeson M, Strong A (1995) Applying MCSST to coral reef bleaching. Advances in Space Research 16:151-154

Glynn PW (1993) Coral reef bleaching: ecological perspectives. Coral Reefs 12:1-17

Glynn PW (1996) Coral reef bleaching: Facts, hypotheses and implications. Glob Change Biol 2:495-509

Glynn PW, Mate JL, Baker AC, Calderon MO (2001) Coral bleaching and mortality in Panama and Ecuador during the 1997-1998 El Nino Southern Oscillation event: spatial/temporal patterns and comparisons with the 1982-1983 event. Bulletin of Marine Science 69:79-109

Gordon HR (1989) Can the Lambert-Beer law be applied to the diffuse attenuation coefficient of ocean water? Limnology and Oceanography 34:1389-1409

Graham NAJ, Cinner JE, Norström AV, Nyström M (2014) Coral reefs as novel ecosystems: embracing new futures. Current Opinion in Environmental Sustainability 7:9-14

Green D, Edmunds P, Carpenter R (2008) Increasing relative abundance of Porites astreoides on Caribbean reefs mediated by an overall decline in coral cover. Marine Ecology Progress Series 359:1-10

Green EA, Davies SW, Matz MV, Medina M (2014) Quantifying cryptic Symbiodinium diversity within Orbicella faveolata and Orbicella franksi at the Flower Garden Banks, Gulf of Mexico. PeerJ 2:e386

Greenstein B, Curran H, Pandolfi J (1998) Shifting ecological baselines and the demise of Acropora cervicornis in the western North Atlantic and Caribbean Province: a Pleistocene perspective. Coral Reefs 17:249-261

Gregory MR (2009) Environmental implications of plastic debris in marine settings—entanglement, ingestion, smothering, hangers-on, hitch-hiking and alien invasions. Philosophical Transactions of the Royal Society of London B: Biological Sciences 364:2013-2025

Grime JP, Pierce S (2012) The evolutionary strategies that shape ecosystems. John Wiley & Sons

Grottoli AG, Rodrigues LJ, Palardy JE (2006) Heterotrophic plasticity and resilience in bleached corals. Nature 440:1186-1189

Guindon S, Gascuel O (2003) A simple, fast, and accurate algorithm to estimate large phylogenies by maximum likelihood. Systematic Biology 52:696-704

Guindon S, Dufayard J-F, Lefort V, Anisimova M, Hordijk W, Gascuel O (2010) New algorithms and methods to estimate maximum-likelihood phylogenies: assessing the performance of PhyML 3.0. Systematic Biology 59:307-321

Guzman HM, Tudhope AW (1998) Seasonal variation in skeletal extension rate and stable isotopic ($^{13}C/^{12}C$ and $^{18}O/^{16}O$) composition in response to several environmental

variables in the Caribbean reef coral *Siderastrea siderea*. Marine Ecology Progress Series 166:109-118

Hall N, Berry K, Rintoul L, Hoogenboom M (2015) Microplastic ingestion by scleractinian corals. Marine Biology 162:725-732

Helmle KP, Dodge RE, Ketcham R (2000) Skeletal architecture and density banding in Diploria strigosa by X-ray computed tomography

Hennige SJ, Smith DJ, Walsh S-J, McGinley MP, Warner ME, Suggett DJ (2010) Acclimation and adaptation of scleractinian coral communities along environmental gradients within an Indonesian reef system. Journal of Experimental Marine Biology and Ecology 391:143-152

Heron SF, Maynard JA, Ruben van Hooidonk C (2016) Warming Trends and Bleaching Stress of the World's Coral Reefs 1985–2012. Scientific reports 6

Heyman WD, Kjerfve B (1999) Hydrological and oceanographic considerations for integrated coastal zone management in southern Belize. Environmental Management 24:229-245

Hoegh-Guldberg O (1999) Climate change, coral bleaching and the future of the world's coral reefs. Marine Freshwater Research 50:839-866

Hoegh-Guldberg O, Bruno JF (2010) The Impact of Climate Change on the World's Marine Ecosystems. Science 328:1523-1528

Hoegh-Guldberg O, Mumby PJ, Hooten AJ, Steneck RS, Greenfield P, Gomez E, Harvell CD, Sale PF, Edwards AJ, Caldeira K, Knowlton N, Eakin CM, Iglesias-Prieto R, Muthiga N, Bradbury RH, Dubi A, Hatziolos ME (2007) Coral Reefs under Rapid Climate Change and Ocean Acidification. Science 318:1737-1742

Honegger R (1991) Functional aspects of the lichen symbiosis. Annual review of plant biology 42:553-578

Howells E, Beltran V, Larsen N, Bay L, Willis B, Van Oppen M (2012) Coral thermal tolerance shaped by local adaptation of photosymbionts. Nature Climate Change 2:116-120

Howells EJ, Berkelmans R, van Oppen MJ, Willis BL, Bay LK (2013) Historical thermal regimes define limits to coral acclimatization. Ecology 94:1078-1088

Hughes TP, Tanner JE (2000) Recruitment failure, life histories, and long-term decline of Caribbean corals. Ecology 81:2250-2263

Hughes TP, Kerry JT, Álvarez-Noriega M, Álvarez-Romero JG, Anderson KD, Baird AH, Babcock RC, Beger M, Bellwood DR, Berkelmans R (2017a) Global warming and recurrent mass bleaching of corals. Nature 543:373-377

Hughes TP, Barnes ML, Bellwood DR, Cinner JE, Cumming GS, Jackson JBC, Kleypas J, van de Leemput IA, Lough JM, Morrison TH, Palumbi SR, van Nes EH, Scheffer M (2017b) Coral reefs in the Anthropocene. Nature 546:82-90

Hughes TP, Baird AH, Bellwood DR, Card M, Connolly SR, Folke C, Grosberg R, Hoegh-Guldberg O, Jackson JBC, Kleypas J, Lough JM, Marshall P, Nystrom M, Palumbi SR, Pandolfi JM, Rosen B, Roughgarden J (2003) Climate change, human impacts, and the resilience of coral reefs. Science 301:929-933

Hume BC, D'Angelo C, Smith EG, Stevens JR, Burt J, Wiedenmann J (2015) Symbiodinium thermophilum sp. nov., a thermotolerant symbiotic alga prevalent in corals of the world's hottest sea, the Persian/Arabian Gulf. Scientific reports 5:8562

Hume BC, Voolstra CR, Arif C, D'Angelo C, Burt JA, Eyal G, Loya Y, Wiedenmann J (2016) Ancestral genetic diversity associated with the rapid spread of stress-tolerant coral symbionts in response to Holocene climate change. Proceedings of the National Academy of Sciences 113:4416-4421

Hunte W, Wittenberg M (1992) Effects of eutrophication and sedimentation on juvenile corals. Marine Biology 114:625-631

Jackson JB, Kirby MX, Berger WH, Bjorndal KA, Botsford LW, Bourque BJ, Bradbury RH, Cooke R, Erlandson J, Estes JA (2001) Historical overfishing and the recent collapse of coastal ecosystems. Science 293:629-637

Jambeck JR, Geyer R, Wilcox C, Siegler TR, Perryman M, Andrady A, Narayan R, Law KL (2015) Plastic waste inputs from land into the ocean. Science 347:768-771

Jokiel PL, Coles SL (1990) Response of Hawaiian and other Indo-Pacific reef corals to elevated temperature. Coral Reefs 8:155-162

Jokiel PL, Maragos JE, Franzisket L (1978) Coral growth: buoyant weight technique. In: Stoddart DR, Johannes RE (eds) Coral Reefs: Research Methods. UNESCO, Paris, France, pp529-541

Jones A, Berkelmans R (2010) Potential Costs of Acclimatization to a Warmer Climate: Growth of a Reef Coral with Heat Tolerant vs. Sensitive Symbiont Types. Plos ONE 5:e10437

Jones AM, Berkelmans R (2011) Tradeoffs to thermal acclimation: energetics and reproduction of a reef coral with heat tolerant Symbiodinium type-D. Journal of Marine Biology 2011

Jones AM, Berkelmans R, van Oppen MJ, Mieog JC, Sinclair W (2008) A community change in the algal endosymbionts of a scleractinian coral following a natural bleaching event: field evidence of acclimatization. Proceedings of the Royal Society of London B: Biological Sciences 275:1359-1365

Kearse M, Moir R, Wilson A, Stones-Havas S, Cheung M, Sturrock S, Buxton S, Cooper A, Markowitz S, Duran C (2012) Geneious Basic: an integrated and extendable desktop software platform for the organization and analysis of sequence data. Bioinformatics 28:1647-1649

Kemp DW, Hernandez-Pech X, Iglesias-Prieto R, Fitt WK, Schmidt GW (2014) Community dynamics and physiology of Symbiodinium spp. before, during, and after a coral bleaching event. Limnology and Oceanography 59:788-797

Kemp DW, Thornhill DJ, Rotjan RD, Iglesias-Prieto R, Fitt WK, Schmidt GW (2015) Spatially distinct and regionally endemic Symbiodinium assemblages in the threatened Caribbean reef-building coral Orbicella faveolata. Coral Reefs 34:535-547

Kenkel C, Meyer E, Matz M (2013a) Gene expression under chronic heat stress in populations of the mustard hill coral (Porites astreoides) from different thermal environments. Molecular Ecology 22:4322-4334

Kenkel C, Goodbody-Gringley G, Caillaud D, Davies S, Bartels E, Matz M (2013b) Evidence for a host role in thermotolerance divergence between populations of the

mustard hill coral (Porites astreoides) from different reef environments. Molecular Ecology 22:4335-4348

Kenkel CD, Almanza AT, Matz MV (2015) Fine-scale environmental specialization of reef-building corals might be limiting reef recovery in the Florida Keys. Ecology 96:3197-3212

Kennedy EV, Foster NL, Mumby PJ, Stevens JR (2015) Widespread prevalence of cryptic Symbiodinium D in the key Caribbean reef builder, Orbicella annularis. Coral Reefs 34:519-531

Kennedy EV, Tonk L, Foster NL, Chollett I, Ortiz J-C, Dove S, Hoegh-Guldberg O, Mumby PJ, Stevens JR (2016) Symbiodinium biogeography tracks environmental patterns rather than host genetics in a key Caribbean reef-builder, Orbicella annularis. Proc R Soc B 283:20161938

Kirstein IV, Kirmizi S, Wichels A, Garin-Fernandez A, Erler R, Löder M, Gerdts G (2016) Dangerous hitchhikers? Evidence for potentially pathogenic Vibrio spp. on microplastic particles. Marine environmental research 120:1-8

Klepac CN, Beal J, Kenkel CD, Sproles A, Polinski JM, Williams MA, Matz MV, Voss JD (2015) Seasonal stability of coral-Symbiodinium associations in the subtropical coral habitat of St. Lucie Reef, Florida. Marine Ecology Progress Series 532:137-151

Knowlton N (2001) The future of coral reefs. Proceedings of the National Academy of Sciences 98:5419-5425

Kurz WA, Dymond CC, Stinson G, Rampley GJ, Neilson ET, Carroll AL, Ebata T, Safranyik L (2008) Mountain pine beetle and forest carbon feedback to climate change. Nature 452:987-990

LaJeunesse T, Trench R (2000) Biogeography of two species of Symbiodinium (Freudenthal) inhabiting the intertidal sea anemone Anthopleura elegantissima (Brandt). The Biological Bulletin 199:126-134

LaJeunesse TC (2001) Investigating biodiversity, ecology, and phylogeny of endosymbiotic dinoflagellates in the genus *Symbiodinium* using the ITS region: In search of a 'species' level marker. Journal of Phycology 37:866-880

LaJeunesse TC, Lee S, Bush S, Bruno JF (2005) Persistence of non-Caribbean algal symbionts in Indo-Pacific mushroom corals released to Jamaica 35 years ago. Coral Reefs 24:157-159

LaJeunesse TC, Smith RT, Finney J, Oxenford H (2009) Outbreak and persistence of opportunistic symbiotic dinoflagellates during the 2005 Caribbean mass coral 'bleaching'event. Proceedings of the Royal Society of London B: Biological Sciences 276:4139-4148

LaJeunesse TC, Loh WK, Van Woesik R, Hoegh-Guldberg O, Schmidt GW, Fitt WK (2003) Low symbiont diversity in southern Great Barrier Reef corals, relative to those of the Caribbean. Limnology and Oceanography 48:2046-2054

LaJeunesse TC, Wham DC, Pettay DT, Parkinson JE, Keshavmurthy S, Chen CA (2014) Ecologically differentiated stress-tolerant endosymbionts in the dinoflagellate genus Symbiodinium (Dinophyceae) Clade D are different species. Phycologia 53:305-319

LaJeunesse TC, Pettay DT, Sampayo EM, Phongsuwan N, Brown B, Obura DO, Hoegh-Guldberg O, Fitt WK (2010) Long-standing environmental conditions, geographic isolation and host–symbiont specificity influence the relative ecological dominance and genetic diversification of coral endosymbionts in the genus Symbiodinium. Journal of Biogeography 37:785-800

LaJeunesse TC, Smith, R., Walther, M., Pinzon, J., Pettay, D.T., McGinley, M., Aschaffenfurg, M., Medina-Rosas, P., Cupul-Magana, A.L., Perez, A.L., Reyes-Bonilla, H., and M.E. Warner (2010) Host-symbiont reconbination vs. natural selection in response of coral-dinoflagellate symbioses to environmental disturbance. . Proceedings of the Royal Society B

Lee MJ, Jeong HJ, Jang SH, Lee SY, Kang NS, Lee KH, Kim HS, Wham DC, LaJeunesse TC (2016) Most Low-Abundance "Background" Symbiodinium spp. Are Transitory and Have Minimal Functional Significance for Symbiotic Corals. Microbial Ecology:1-13

Li W, Fu L, Niu B, Wu S, Wooley J (2012) Ultrafast clustering algorithms for metagenomic sequence analysis. Briefings in bioinformatics:bbs035

Lirman D, Fong P (2007) Is proximity to land-based sources of coral stressors an appropriate measure of risk to coral reefs? An example from the Florida Reef Tract. Marine Pollution Bulletin 54:779-791

Lirman D, Manzello D (2009) Patterns of resistance and resilience of the stress-tolerant coral Siderastrea radians (Pallas) to sub-optimal salinity and sediment burial. Journal of Experimental Marine Biology and Ecology 369:72-77

Lirman D, Manzello D, Maciá S (2002) Back from the dead: the resilience of Siderastrea radians to severe stress. Coral Reefs 21:291-292

Lirman D, Gracias N, Gintert B, Gleason A, Reid R, Negahdaripour S, Kramer P (2007) Development and application of a video-mosaic survey technology to document the status of coral reef communities. Environmental monitoring and assessment 125:59-73

Little AF, Van Oppen MJ, Willis BL (2004) Flexibility in algal endosymbioses shapes growth in reef corals. Science 304:1492-1494

Lönnstedt OM, Eklöv P (2016) Environmentally relevant concentrations of microplastic particles influence larval fish ecology. Science 352:1213-1216

Lough J, Barnes D (1997) Several centuries of variation in skeletal extension, density and calcification in massive Porites colonies from the Great Barrier Reef: A proxy for seawater temperature and a background of variability against which to identify unnatural change. Journal of Experimental Marine Biology and Ecology 211:29-67

Lough J, Barnes D (2000) Environmental controls on growth of the massive coral Porites. Journal of Experimental Marine Biology and Ecology 245:225-243

Lough J, Barnes D, Devereux M, Tobin B, Tobin S (1999) Variability in growth characteristics of massive Porites on the Great Barrier Reef. CRC Reef Research Centre Technical Report:95

Lough JM, Cantin NE (2014) Perspectives on massive coral growth rates in a changing ocean. The Biological Bulletin 226:187-202

Loya Y, Sakai K, Yamazato K, Nakano Y, Sambali H, van Woesik R (2001) Coral bleaching: the winners and the losers. Ecology Letters 4:122-131

Marubini F, Atkinson MJ (1999) Effects of lowered pH and elevated nitrate on coral calcification. Marine Ecology Progress Series 188:117-121

Matz MV, Wright RM, Scott JG (2013) No control genes required: Bayesian analysis of qRT-PCR data. Plos ONE 8:e71448

McClanahan T, Maina J (2003) Response of coral assemblages to the interaction between natural temperature variation and rare warm-water events. Ecosystems 6:551-563

McClanahan TR, Ateweberhan M, Omukoto J (2008) Long-term changes in coral colony size distributions on Kenyan reefs under different management regimes and across the 1998 bleaching event Marine Biology 153:755-768

McClanahan TR, Graham NA, Darling ES (2014) Coral reefs in a crystal ball: predicting the future from the vulnerability of corals and reef fishes to multiple stressors. Current Opinion in Environmental Sustainability 7:59-64

McCormick A, Hoellein TJ, Mason SA, Schluep J, Kelly JJ (2014) Microplastic is an abundant and distinct microbial habitat in an urban river. Environmental science & technology 48:11863-11871

McWilliams JP, Cote IM, Gill JA, Sutherland WJ, Watkinson AR (2005) Accelerating impacts of temperature-induced coral bleaching in teh Caribbean. Ecology 86:2055-2060

Meyer FH (1966) Mycorrhiza and other plant symbioses. Symbiosis 1:171-255

Middlebrook R, Hoegh-Guldberg O, Leggat W (2008) The effect of thermal history on the susceptibility of reef-building corals to thermal stress. Journal of Experimental Biology 211:1050-1056

Miller J, Muller E, Rogers C, Waara R, Atkinson A, Whelan K, Patterson M, Witcher B (2009) Coral disease following massive bleaching in 2005 causes 60% decline in coral cover on reefs in the US Virgin Islands. Coral Reefs 28:925

Mills MM, Sebens KP (2004) Ingestion and assimilation of nitrogen from benthic sediments by three species of coral. Marine Biology 145:1097-1106

Mills MM, Lipschultz F, Sebens KP (2004) Particulate matter ingestion and associated nitrogen uptake by four species of scleractinian corals. Coral Reefs 23:311-323

Moberg F, Folke C (1999) Ecological goods and services of coral reef ecosystems. Ecological Economics 29:2151-2233

Moore CJ (2008) Synthetic polymers in the marine environment: a rapidly increasing, long-term threat. Environmental research 108:131-139

Muscatine L (1990) The role of symbiotic algae in carbon and energy flux in reef corals. In: Dubinsky Z (ed) Ecosystems of the World 25: Coral Reefs. Elsevier, New York, pp75-87

Nadal M, Alomar C, Deudero S (2016) High levels of microplastic ingestion by the semipelagic fish bogue Boops boops (L.) around the Balearic Islands. Environmental Pollution 214:517-523

Nybakken JW, Bertness MD (2005) Marine biology : an ecological approach. Pearson/Benjamin Cummings, San Francisco

O'Connor MI, Bruno JF, Gaines SD, Halpern BS, Lester SE, Kinlan BP, Weiss JM (2007) Temperature control of larval dispersal and the implications for marine ecology, evolution, and conservation. Proceedings of the National Academy of Sciences 104:1266-1271

O'Reilly CM, Alin SR, Plisnier P-D, Cohen AS, McKee BA (2003) Climate change decreases aquatic ecosystem productivity of Lake Tanganyika, Africa. Nature 424:766-768

Oksanen J, Blanchet FG, Kindt R, Legendre P, Minchin PR, O'Hara R, Simpson GL, Solymos P, Stevens M, Wagner H (2013) Package 'vegan'. R Packag ver 254:20-28

Oliver T, Palumbi S (2011a) Do fluctuating temperature environments elevate coral thermal tolerance? Coral Reefs 30:429-440

Oliver TA, Palumbi SR (2011b) Do fluctuating temperature environments elevate coral thermal tolerance? Coral Reefs 30:429-440

Palumbi SR, Barshis DJ, Traylor-Knowles N, Bay RA (2014) Mechanisms of reef coral resistance to future climate change. Science 344:895-898

Pandolfi JM, Bradbury RH, Sala E, Hughes TP, Bjorndal KA, Cooke RG, McArdle D, Mcclenachan L, Newman MJH, Paredes G, Warner RR, Jackson JBC (2003) Global trajectories of the long-term decline of coral reef ecosystems. Science 301:955-957

Paris CB, Cherubin LM (2008) River-reef connectivity in the Meso-American Region. Coral Reefs 27:773-781

Paris CB, Chérubin LM, Cowen RK (2007) Surfing, spinning, or diving from reef to reef: effects on population connectivity. Marine Ecology Progress Series 347:285-300

Parsons TR, Maita Y, Lalli CM (1984) 4.3 - Fluorometric Determination of Chlorophylls A Manual of Chemical & Biological Methods for Seawater Analysis. Pergamon, Amsterdam, pp107-109

Perry C, Larcombe P (2003) Marginal and non-reef-building coral environments. Coral Reefs 22:427-432

Pettay DT, Wham DC, Smith RT, Iglesias-Prieto R, LaJeunesse TC (2015) Microbial invasion of the Caribbean by an Indo-Pacific coral zooxanthella. Proceedings of the National Academy of Sciences 112:7513-7518

Pineda J, Starczak V, Tarrant A, Blythe J, Davis K, Farrar T, Berumen M, da Silva JC (2013a) Two spatial scales in a bleaching event: Corals from the mildest and the most extreme thermal environments escape mortality. Limnology and Oceanography 58:1531-1545

Pineda J, Starczak V, Tarrant A, Blythe J, Davis K, Farrar T, Berumen M, da Silva JCB (2013b) Two spatial scales in a bleaching event: Corals from the mildest and the most extreme thermal environments escape mortality. Limnol Oceanogr 58:1531-1545

Pinheiro J, Bates D, DebRoy S, Sarkar D, Heisterkamp S, Van Willigen B, Maintainer R (2017) Package 'nlme'. Linear and nonlinear mixed effects models:3-1

Pochon X, Pawlowski J, Zaninetti L, Rowan R (2001) High genetic diversity and relative specificity among Symbiodinium-like endosymbiotic dinoflagellates in soritid foraminiferans. Marine Biology 139:1069-1078

Podesta GP, Glynn PW (2001) The 1997-98 El Nino event in Panama and Galapagos: an update of thermal stress indices relative to coral bleaching. Bulletin of Marine Science 69:43-59

Polónia ARM, Cleary DFR, de Voogd NJ, Renema W, Hoeksema BW, Martins A, Gomes NCM (2015) Habitat and water quality variables as predictors of community composition in an Indonesian coral reef: a multi-taxon study in the Spermonde Archipelago. Science of The Total Environment 537:139-151

Pratchett MS, Anderson KD, Hoogenboom MO, Widman E, Baird AH, Pandolfi JM, Edmunds PJ, Lough JM (2015) Spatial, temporal and taxonomic variation in coral growth—implications for the structure and function of coral reef ecosystems. Oceanography and Marine Biology: An Annual Review 53:215-296

Prouty N, Hughen K, Carilli J (2008) Geochemical signature of land-based activities in Caribbean coral surface samples. Coral Reefs 27:727-742

Quigley KM, Davies SW, Kenkel CD, Willis BL, Matz MV, Bay LK (2014) Deep-sequencing method for quantifying background abundances of Symbiodinium types: exploring the rare Symbiodinium biosphere in reef-building corals. Plos ONE 9:e94297

Ries JB, Ghazaleh MN, Connolly B, Westfield I, Castillo KD (2016) Impacts of seawater saturation state (ΩA=0.4–4.6) and temperature (10, 25°C) on the dissolution kinetics of whole-shell biogenic carbonates. Geochimica et Cosmochimica Acta 192:318-337

Roark EB, Guilderson TP, Dunbar RB, Fallon SJ, Mucciarone DA (2009) Extreme longevity in proteinaceous deep-sea corals. Proceedings of the National Academy of Sciences 106:5204-5208

Roberts JM, Wheeler AJ, Freiwald A (2006) Reefs of the deep: the biology and geology of cold-water coral ecosystems. Science 312:543-547

Rochman CM (2015) The complex mixture, fate and toxicity of chemicals associated with plastic debris in the marine environment Marine anthropogenic litter. Springer, pp117-140

Rochman CM, Kurobe T, Flores I, Teh SJ (2014) Early warning signs of endocrine disruption in adult fish from the ingestion of polyethylene with and without sorbed

chemical pollutants from the marine environment. Science of The Total Environment 493:656-661

Rochman CM, Browne MA, Halpern BS, Hentschel BT, Hoh E, Karapanagioti HK, Rios-Mendoza LM, Takada H, Teh S, Thompson RC (2013) Policy: Classify plastic waste as hazardous. Nature 494:169-171

Rodrigues LJ, Grottoli AG (2007) Energy reserves and metabolism as indicators of coral recovery from bleaching. Limnology and Oceanography 52:1874-1882

Rosset S, Wiedenmann J, Reed AJ, D'Angelo C (2017) Phosphate deficiency promotes coral bleaching and is reflected by the ultrastructure of symbiotic dinoflagellates. Marine Pollution Bulletin 118:180-187

Rowan R (2004) Thermal adaptation in reef coral symbionts. Nature 430:742

Rowan R, Knowlton N, Baker A, Jara J (1997) Landscape ecology of algal symbionts creates variation in episodes of coral bleaching. Nature 388:265-269

Saenger C, Cohen AL, Oppo DW, Halley RB, Carilli JE (2009) Surface-temperature trends and variability in the low-latitude North Atlantic since 1552. Nature Geoscience 2:492-495

Sampayo EM, Ridgway T, Bongaerts P, Hoegh-Guldberg O (2008) Bleaching susceptibility and mortality of corals are determined by fine-scale differences in symbiont type. Proceedings of the National Academy of Sciences of the United States of America 105:10444-10449

Santos S, Shearer T, Hannes A, Coffroth M (2004) Fine-scale diversity and specificity in the most prevalent lineage of symbiotic dinoflagellates (Symbiodinium, Dinophyceae) of the Caribbean. Molecular Ecology 13:459-469

Setälä O, Fleming-Lehtinen V, Lehtiniemi M (2014) Ingestion and transfer of microplastics in the planktonic food web. Environmental Pollution 185:77-83

Setälä O, Norkko J, Lehtiniemi M (2016) Feeding type affects microplastic ingestion in a coastal invertebrate community. Marine Pollution Bulletin 102:95-101

Sheng J, Tang L (2003) A numerical study of circulation in the western Caribbean Sea. Journal of Physical Oceanography 33:2049-2069

Sheng J, Tang L (2004) A two-way nested-grid ocean-circulation model for the Meso-American Barrier Reef System. Ocean Dynamics 54:232-242

Silverstein RN, Correa AMS, Baker AC (2012) Specificity is rarely absolute in coral–algal symbiosis: implications for coral response to climate change. Proceedings of the Royal Society B: Biological Sciences 279:2609-2618

Silverstein RN, Cunning R, Baker AC (2015) Change in algal symbiont communities after bleaching, not prior heat exposure, increases heat tolerance of reef corals. Global Change Biology 21:236-249

Silverstein RN, Cunning R, Baker AC (2017) Tenacious D: Symbiodinium in clade D remain in reef corals at both high and low temperature extremes despite impairment. The Journal of Experimental Biology

Simons R (2011a) ERDDAP–The Environmental Research Division's Data Access Program.'. Pacific Grove CA: NOAA/NMFS/SWFSC/ERD

Simons R (2011b) ERDDAP- The Envionmental Research Division's Data Access Program.

Smale DA, Wernberg T (2013) Extreme climatic event drives range contraction of a habitat-forming species. Proceedings of the Royal Society B: Biological Sciences 280

Soto I, Muller Karger F, Hallock P, Hu C (2011a) Sea surface temperature variability in the Florida Keys and its relationship to coral cover. Journal of Marine Biology 2011

Soto IM, Muller Karger FE, Hallock P, Hu C (2011b) Sea Surface Temperature Variability in the Florida Keys and Its Relationship to Coral Cover. Journal of Marine Biology 2011:10

Stat M, Yost DM, Gates RD (2015) Geographic structure and host specificity shape the community composition of symbiotic dinoflagellates in corals from the Northwestern Hawaiian Islands. Coral Reefs 34:1075-1086

Stat M, Loh WKH, Hoegh-Guldberg O, Carter DA (2009) Stability of coral–endosymbiont associations during and after

a thermal stress event in the southern Great Barrier Reef. Coral Reefs 28:709-713

Stone L, Huppert A, Rajagopalan B, Bhasin H, Loya Y (1999) Mass coral reef bleaching: A recent outcome of increased El Nino activity? Ecol Lett 2:325-330

Szmant AM (2002) Nutrient enrichment on coral reefs: is it a major cause of coral reef decline? Estuaries 25:743-766

Tang L, Sheng J, Hatcher BG, Sale PF (2006) Numerical study of circulation, dispersion, and hydrodynamic connectivity of surface waters on the Belize shelf. Journal of Geophysical Research: Oceans 111

Taylor M, Gwinnett C, Robinson L, Woodall L (2016) Plastic microfibre ingestion by deep-sea organisms. Scientific reports 6

Tchernov D, Gorbunov MY, de Vargas C, Yadav SN, Milligan AJ, Haggblom M, Falkowski PG (2004) Membrane lipids of symbiotic algae are diagnostic of sensitivity to thermal bleaching in corals. Proceedings of the National Academy of Sciences of the United States of America 101:13531-13535

Team RC (2014) R: A language and environment for statistical computing. R Foundation for Statistical Computing, Vienna, Austria, 2012. ISBN 3-900051-07-0

Team RC (2017) R: A language and environment for statistical computing. R Foundation for Statistical Computing Vienna, Austria

Thattai D, Kjerfve B, Heyman W (2003) Hydrometeorology and variability of water discharge and sediment load in the inner Gulf of Honduras, western Caribbean. Journal of Hydrometeorology 4:985-995

Thompson D, Van Woesik R (2009) Corals escape bleaching in regions that recently and historically experienced frequent thermal stress. Proceedings of the Royal Society of London B: Biological Sciences 276:2893-2901

Thornhill D, Howells E, Wham D, Steury T, Santos S (2017) Population genetics of reef coral endosymbionts (Symbiodinium, Dinophyceae). Molecular Ecology

Thornhill DJ, LaJeunesse TC, Santos SR (2007) Measuring rDNA diversity in eukaryotic microbial systems: how intragenomic variation, pseudogenes, and PCR artifacts confound biodiversity estimates. Molecular Ecology 16:5326-5340

Thornhill DJ, Xiang Y, Fitt WK, Santos SR (2009) Reef endemism, host specificity and temporal stability in populations of symbiotic dinoflagellates from two ecologically dominant Caribbean corals. Plos ONE 4:e6262

Thornhill DJ, LaJeunesse TC, Kemp DW, Fitt WK, Schmidt GW (2006) Multi-year, seasonal genotypic surveys of coral-algal symbioses reveal prevalent stability or post-bleaching reversion Marine Biology 148:711-722

Thornhill DJ, Kemp DW, Bruns BU, Fitt WK, Schmidt GW (2008) Correspondence between Cold Tolerance and Temperate Biogeography in a Western Atlantic Symbiodinium (Dinophyta) Lineage1. Journal of Phycology 44:1126-1135

Toller WW, Rowan R, Knowlton N (2001) Repopulation of zooxanthellae in the Caribbean corals *Montastraea annularis* and *M. faveolata* following experimental and disease-associated bleaching. Biological Bulletin 201:360-373

Tomascik T (1990) Growth rates of two morphotypes of Montastrea annularis along a eutrophication gradient, Barbados, WI. Marine Pollution Bulletin 21:376-381

Tong H, Cai L, Zhou G, Yuan T, Zhang W, Tian R, Huang H, Qian P-Y (2017) Temperature shapes coral-algal symbiosis in the South China Sea. Scientific reports 7:40118

Torres JL, Morelock J (2002) Effect of terrigenous sediment influx on coral cover and linear extension rates of three Caribbean massive coral species. Caribbean Journal of Science 38:222-229

Turner JA, Polunin NV, Field SN, Wilson SK (2015) Measuring coral size-frequency distribution using stereo video technology, a comparison with in situ measurements. Environmental monitoring and assessment 187:1-10

Ulstrup KE, Van Oppen M (2003) Geographic and habitat partitioning of genetically distinct zooxanthellae (Symbiodinium) in Acropora corals on the Great Barrier Reef. Molecular Ecology 12:3477-3484

Ulstrup KE, Ralph PJ, Larkum AWD, Kuhl M (2006) Intra-colonial variability in light acclimation of zooxanthellae in coral tissues of Pocillopora damicornis. Marine Biology 149:1325 - 1335

van Hooidonk R, Maynard JA, Liu Y, Lee S-K (2015a) Downscaled projections of Caribbean coral bleaching that can inform conservation planning. Global Change Biology:n/a-n/a

Van Hooidonk R, Maynard JA, Liu Y, Lee SK (2015b) Downscaled projections of Caribbean coral bleaching that can inform conservation planning. Global Change Biology

Van Oppen M, Mieog J, Sanchez C, Fabricius K (2005) Diversity of algal endosymbionts (zooxanthellae) in octocorals: the roles of geography and host relationships. Molecular Ecology 14:2403-2417

Van Woesik R, Tomascik T, Blake S (1999) Coral assemblages and physico-chemical characteristics of the Whitsunday Islands: evidence of recent community changes. Marine and Freshwater Research 50:427-440

Van Woesik R, Sakai K, Ganase A, Loya Y (2011) Revisiting the winners and the losers a decade after coral bleaching. Mar Ecol Prog Ser 434:67-76

van Woesik R, Houk P, Isechal AL, Idechong JW, Victor S, Golbuu Y (2012) Climate-change refugia in the sheltered bays of Palau: analogs of future reefs. Ecol Evol 2:2474-2484

Veal CJ, Holmes G, Nunez M, Hoegh-Guldberg O, Osborn J (2010) A comparative study of methods for surface area and threedimensional

shape measurement of coral skeletons. LIMNOLOGY

and

OCEANOGRAPHY: METHODS 8:241-253

Vega Thurber RL, Burkepile DE, Fuchs C, Shantz AA, McMinds R, Zaneveld JR (2014) Chronic nutrient enrichment increases prevalence and severity of coral disease and bleaching. Global Change Biology 20:544-554

Veron JEN, Hoeg-Guldberg O, Lenton TM, Lough JM, Obura DO, Pearce-Kelly P, Sheppard CRC, Spalding M, Stafford-Smith MG, Rogers AD (2009) The coral reef crisis: The critical importance of <350 ppm CO2. Marine Pollution Bulletin 58:1428-1436

Walther G-R, Post E, Convey P, Menzel A, Parmesan C, Beebee TJC, Fromentin J-M, Hoegh-Guldberg O, Bairlein F (2002) Ecological responses to recent climate change. Nature 416

Warner ME, Fitt WK, Schmidt GW (1996) The effects of elevated temperature on the photosynthetic efficiency of zooxanthellae in hospite from four different species of reef coral: a novel approach. Plan, Cell and Environment 19:291-299

Warner ME, LaJeunesse TC, Robison JD, Thur RM (2006) The ecological distribution and comparative photobiology of symbiotic dinoflagellates from reef corals in Belize: Potential implications for coral bleaching. Limnology and Oceanography 51:1887-1897

West K, Van Woesik R (2001) Spatial and temporal variance of river discharge on Okinawa (Japan): inferring the temporal impact on adjacent coral reefs. Marine Pollution Bulletin 42:864-872

Wiedenmann J, D'Angelo C, Smith EG, Hunt AN, Legiret F-E, Postle AD, Achterberg EP (2013) Nutrient enrichment can increase the susceptibility of reef corals to bleaching. Nature Climate Change 3:160-164

Wild C, Hoegh-Guldberg O, Naumann MS, Colombo-Pallotta MF, Ateweberhan M, Fitt WK, Iglesias-Prieto R, Palmer C, Bythell JC, Ortiz J-C, Loya Y, van Woesik R (2011) Climate change impedes scleractinian corals as primary reef ecosystem engineers. Marine and Freshwater Research 62:205-215

Wilkinson C (2000) Status of Coral Reefs of the World: 2000. Australian Institute for Marine Science, Townsville

Woesik R, Houk P, Isechal AL, Idechong JW, Victor S, Golbuu Y (2012) Climate-change refugia in the sheltered bays of Palau: analogs of future reefs. Ecology and evolution 2:2474-2484

Wooldridge S (2009a) A new conceptual model for the enhanced release of mucus in symbiotic reef corals during 'bleaching' conditions. Marine Ecology Progress Series 396:145-152

Wooldridge S, Done T, Berkelmans R, Jones R, Marshall P (2005) Precursors for resilience in coral communities in a warming climate: a belief network approach. Marine Ecology Progress Series 295:157-169

Wooldridge SA (2009b) Water quality and coral bleaching thresholds: Formalising the linkage for the inshore reefs of the Great Barrier Reef, Australia. Marine Pollution Bulletin 58:745-751

Wright SL, Rowe D, Thompson RC, Galloway TS (2013) Microplastic ingestion decreases energy reserves in marine worms. Current Biology 23:R1031-R1033

Zaneveld JR, Burkepile DE, Shantz AA, Pritchard CE, McMinds R, Payet JP, Welsh R, Correa AM, Lemoine NP, Rosales S (2016) Overfishing and nutrient pollution interact with temperature to disrupt coral reefs down to microbial scales. Nature communications 7

Ziegler M, Seneca FO, Yum LK, Palumbi SR, Voolstra CR (2017) Bacterial community dynamics are linked to patterns of coral heat tolerance. Nature communications 8:14213